공학박사학위논문

Enhancing Gas-Liquid Mass Transfer and (Bio) Chemical Reactivity using ultrafine/Nanobubble in Water and Wastewater Treatments

초미세/나노버블을이용한물및상수및폐수처리에서의
기체액체 물질 전달 및 (생)화학적 반응 강화

August 2017

서울대학교 대학원
건설환경공학부

Tatek Temesgen Terfasa

Enhancing Gas-Liquid Mass Transfer and (Bio) Chemical Reactivity Using Ultrafine/Nanobubble in Water and Wastewater Treatments

초미세/나노 버블을 이용한 물 및 폐수 처리에서의 기체-액체 물질 전달 및 (생)화학적 반응 강화

지도교수 한 무 영

이 논문을 공학박사학위논문으로 제출함
2017 년 8 월

서울대학교 대학원
건설환경공학부
TATEK TEMESGEN TERFASA

TATEK TEMESGEN TERFASA의 박사학위논문을 인준함
2017 년 6 월

위 원 장 김 재 영 (인)

부 위 원 장 한 무 영 (인)

위 원 독 고 석 (인)

위 원 최 용 주 (인)

위 원 최 정 권 (인)

Enhancing Gas-Liquid Mass Transfer and (Bio) Chemical Reactivity using ultrafine/Nanobubble in Water and Wastewater Treatments

By

Tatek Temesgen Terfasa

Advisor: Professor Mooyoung Han

A dissertation submitted in partial fulfillment of the requirements for the degree of

Doctor of Philosophy

Department of Civil and Environmental Engineering

Seoul National University

August 2017

Abstract

Enhancing Gas-Liquid Mass Transfer and (Bio) Chemical Reactivity using ultrafine/Nanobubble in Water and Wastewater Treatments

Tatek Temesgen Terfasa

Department of Civil and Environmental Engineering

College of Engineering

Seoul National University

In the four major environmental spheres, phase involving processes are mostly responsible for the mass transfer of a given matter. The interaction between different phases mostly detect the outcome of a given natural or artificial process. Among the phase-related processes, gas–liquid phase interactions are often encountered in many environmental processes industries, water and wastewater treatment plants, gas absorption systems, aquatic system restoration techniques, aqua farming, surface cleaning and other chemical as well as petrochemical industries. In most of this processes the gas-liquid mass transfer efficiency is the process limiting factor.

In this research, the possibility of intensifying mass transfer efficiency by applying ultrafine/nano bubbles is investigated giving a prior emphasis to

its application in water and wastewater treatment techniques. To achieve this target, aeration, O_3 based advanced oxidation and aerobic MBR water treatment techniques all having different gas-liquid mass transfer interaction theories are selected. Through studying the application of nanobubbles in these three different processes, the influence of ultrafine bubbles in:

1- systems with pure gas liquid mass transfer (no reaction),

2- systems with fast reaction in the liquid film and,

3- systems involving slow reactions in the bulk liquid are studied in different sections of the research.

The influence of nanobubbles on the improvement of each system is addressed by comparing the final outcomes of applying ultrafine bubbles with that of the bubble types currently in use for the respective technologies.

In the first chapter of the thesis, general information about the existing knowledge gap in the area of nanobubbles application in water technologies is discussed giving due emphasis on mass transfer. A brief summary of works relating bubble and the selected water treatment technologies is covered. Clear objectives and specific targets are described and presented in detail.

Theoretical framework relating both bubble technology and mass transfer are summarized in the second chapter of the dissertation. In this section, clear definition on the size range of the different bubble categories is

proposed. The proposal was necessary considering the lack of clear size range definition or overlapping of currently existing representations of the different bubble types. This definition is proposed from an intensive review work based on the agreement of most researchers on the properties shared by the range of bubble sizes. It is believed that at least it will help to clearly communicate among the chapters of this thesis if not used beyond to clarify the current existing overlapping definitions. Relevant bubble properties related to bubble mass transfer properties and that will be used in successive chapters of this dissertation are discussed briefly. Basic mass transfer theories and assumptions, for the selection of the two film theory for this research is also justified.

The effect of nanobubbles in pure gas-liquid mass transfer is studied in chapter three. In this section, hydrodynamic splitting technique was applied for bubble generation. The influence of the design and operation parameters of the bubble generation unit on the bubble size reduction is studied. By determining the effect of design and operation parameters on the mass transfer indicators, an indirect analysis of the bubble size effect on mass transfer was induced. Furthermore, a regression model is developed to relate the design parameters of the bubble splitter with the volumetric mass transfer coefficient to better express the contributions of the major design and operational parameters. By the regression model, it was confirmed that bubble splitter

flow path length, flow area and recycled water flow rate are the dominant contributors for bubble size change using hydrodynamic splitting. An increase in flow path length and gas-liquid mixture flow rate as well as reduction in flow area decrease the bubble size to nano scale. This in turn improved the volumetric mass transfer coefficient of a nanobubbled system up to 600% more compared to the conventional bubbled and/or 100-200 % compared to microbubbled systems.

Process improvement possibilities for mass transfer involving fast reactions in ozone based advanced oxidation processes is covered in chapter four. For the semibatch system tested, nano bubbles show the tendency of suppressing the negative effects of temperature and pH on ozonation efficiency. The effect of increasing process temperature on reduction in solubility of ozone gas was reduced by application of nanobubbles. Similarly, ozone nanobubbles show high tendency of generating hydroxyl radical in acidic environment with higher concentration than microbubbles. This was not possible in previous studies using big bubbles, without addition of other hydroxyl radical formation reaction initiators. This indicates nanobubble's potential in initiating radical formation reactions which improve advanced oxidation processes in low pH medium. Moreover, mathematical model was developed based on the two-film theory to predict the volumetric mass transfer coefficient. The values of mass transfer coefficients showed a relative higher

value for nanobubbles compared to microbubbles. Similarly, the ozone consumption rate was too high for nanobubbles even at low pH value. Based on this outcome, the concentration of hydroxyl radicals was checked and the result confirmed that the application of nanobubbles generate high concentration of hydroxyl radicals in all pH zones tested. This proofs that application of nanobubbles could improve advanced oxidation process.

Finally, the benefit of nanobubbles over conventional was tested for aerobic wastewater treatment which involves a slow biological reaction process in the liquid phase. Theoretical floc models were adopted and modified to express the process of mass transfer in gas-liquid-solid phases. These models are supported by the results from different experiments on comparison of the rate of mass transfer, biological waste degradation rate, biomass growth rate and membrane filteration. In the nanobubble supported aerobic digester, the volumetric mass transfer coefficient was found to be 0.13 which is double to that of the conventional bubble supported system with the value of 0.07. Similarly, the oxygen uptake rate was also double to that of conventional bubble system. This improvement in mass transfer boosted the supply of oxygen to the biological reaction, reducing the limiting effect of oxygen shortage in the conventional aerobic digesters. Finally, because of the influence of nanobubbles, better efficiency of biomass growth, biological

waste degradation, reduction in excess sludge production and reduction in membrane fouling possibility was achieved.

Keywords: Nanobubble, ultrafine bubbles, mass transfer, water treatment, wastewater treatment, modeling

Student Number: 2014-30862

Contents

List of Figures

List of Tables

Chapter 1

Introduction

1.1 Background

Processes involving different phase interaction are largely applicable in environmental, agricultural, healthcare, chemical or industrial and energy fields. Among the phase-related processes, gas–liquid phase interactions are often encountered in wastewater and water treatment technologies, aquatic system restoration, food processing industries, aqua farming, and chemical as well as petrochemical industries (Kulkarni and Joshi 2005).

In water and wastewater treatment plants gas-liquid phase involving operations include aeration, dissolved air flotation (DAF) as well as disinfection and advanced oxidation (AOP). In all these operations application of bubbles as a delivery of the gaseous phase is common. Based on the application and purpose of bubbles the types in use differ.

Application of Microbubbles (MBs) and Nanobubbles (NBs) in water-treatment technology has been recently gaining attention (Kim and Han 2010). It has been reported that MBs and NBs can detoxify contaminated water by catalyzing the reactions of chemicals, thereby improving the efficiency of the chemical treatment process (Takahashi 2009, Agarwal, Ng et al. 2011). According to several studies, bubbles generated from air and nitrogen could

enhance the activities of microorganisms and/or bacteria in both anaerobic and aerobic conditions as well as in defouling solid surface and membranes (Yamasaki, Uda et al. 2009, Agarwal, Ng et al. 2011, Ghadimkhani, Zhang et al. 2016). In different literatures, MB have been tried in typical treatment processes (Tasaki, Wada et al. 2009, Yamasaki, Uda et al. 2009, Yamasaki, Sakata et al. 2010), flotation, and disinfection (Jyoti and Pandit 2001, Jyoti and Pandit 2003, Sumikura, Hidaka et al. 2007, Mezule, Tsyfansky et al. 2009, Kim and Han 2010). In most of researches done on MB and NB, the main objectives were focused on the generation, characterization and modeling of their behaviors. Except few trial works, researches on their application is not yet done extensively. To help the premises of the objectives of this research, background of previous limited works on the application of M-N bubbles in aeration, disinfection and AOP are selectively summarized hereunder to show the current research status of NBs.

Aeration: Application bubbles in natural water restoration and water treatment for aeration plays a major role in delivering oxygen, which is an important life-sustaining component for aquatic lives and biochemical reaction substrate in aerobic treatment. In addition, fluid therapy is one of the most common intervention areas in cell biology and healthcare (Matsuki, Ishikawa et al. 2014). Many studies have been conducted on the effect of aeration processes in biological water and wastewater treatment, ground water

remediation as well as agriculture. The main target objectives of most studies are improving the aeration efficiency to improve biological matter degradation, microbial growth rate, seed germination, and growth rates. In the studies, the main concern is optimizing the efficiency of the mass-transfer rate-limiting factor. In the conventional aerobic systems, dissolved oxygen is a critical factor to consider in efficiency (Tang, Zuo et al. 2016). In these conventional systems, the mass-transfer rate of oxygen is very important because most equipment utilize the mechanical aerators or diffusers, which require high electrical input and mechanical part maintenance resulting in high operating costs (El-Zahaby and El-Gendy 2016).

Recently application of MBs and NBs received attention in the applications stated earlier to improve mass transfer in the aeration research. (Li, Li et al. 2016) studied the dispersion and gas–liquid mass-transfer characteristics of the MBs for aeration in stirred-tank reactors and concluded that a higher impeller speed does not always mean a greater k_la, and proposed that the MB aeration was more suitable for bioreactors. (Weber and Agblevor 2005) investigated the impact of the MB aeration on the fermentation of Trichoderma reesei, which is highly affected by the limited mass-transfer rate of oxygen. Their study concluded that, by applying the MB aeration, the dissolved oxygen concentration was above the critical concentration at low agitation rates and the cell mass concentration increases very rapidly during

the fast growth stage with the mass productivity increment from 0.1 to 0.18 g/lh in comparison to the conventional bubbling. (Liu, Oshita et al. 2016) studied the oxidative capacity of the NB aeration of seeds and its effects on germination. Their result concluded that the seed germination improved by using the NB aerated water in comparison to those submerged in distilled water. Similarly, (Park and Kurata 2009) investigated the effect of the MB aeration on the growth of leaf lettuce (Lactuca sativa) and found that fresh and dry weights of the MB aerated lettuce are 2.1 and 1.7 times greater than the macro bubble aerated lettuce, respectively. In both studies above, the researchers speculated that the resulted germination and growth improvement was because of the high specific-surface area of Micro-NBs and the ability of attracting positive ions owing to their high negative electronic charges. However, in such studies the effect of MBs and NBs on nitrifying bacteria and other useful bacteria growth was overlooked. (Li, Hu et al. 2014) studied the aeration possibility of ground water by micro-NBs and found that the hydraulic conductivity of the sand was not affected by the micro-NBs inside the pore water. Moreover, the dissolved mass transfer rate of oxygen in the water was found to be 125 times faster than the macro bubbled water with 16 times less dissolved oxygen enhancement durability compared to micro-nano bubbled water. Based on the outcome of the study, they forcasted that the

applications of MBs and NBs can predictably facilitate the aerobic biodegradation process for ground-water contaminant removal.

Disinfection and AOP: Oxidation of pollutants and disinfection of pathogens using ozone is a promising method for treatment of drinking water and wastewater (Zhang, Xi et al. 2013, Khuntia, Majumder et al. 2015). Ozone gas bubbles have been applied for water treatment because of its powerful disinfection ability under low concentration and short contact time. Its disinfection efficiency increased its preference for the disinfection application of chemical resistance spore forming bacteria like Bacillus subtilis and Cryptosporidium parvum (Larson and Mariñas 2003, kim, Von et al. 2004, Kim, Elovitz et al. 2007, Aydogan and Gurol 2012, Zhang, Xi et al. 2013). Further improvement of its efficiency was achieved by applying MB. The observation of disinfection kinetic for E. Coli by illustrated a faster reduction rate (approximately 99.99% of inactivation), a smaller tank size, and a lower ozone requirement for application of MBs in comparison to the conventional ozonation disinfection process (Sumikura, Hidaka et al. 2007). Another study on stopping multiplication of E. Coli by cavitation of MB resulted in 75% reduction within 3 min at an energy input of 490 W/L (Mezule, Tsyfansky et al. 2009). Similar results of the hydrodynamic cavitation reported in several studies convincingly prove the effectiveness of a non-reagent technique, such as MB application technologies, for water disinfection (Jyoti and Pandit 2001,

Jyoti and Pandit 2003). The generation of $OH^{\cdot}$ and shock waves from collapsing MBs are discussed as the main cause of E. Coli inactivation; however, the deactivation level of each influence factor still requires further research.

Inlet ozone concentration for the generation of MBs was taken as a main factor affecting the removal of Bacillus subtilis spores, at a greater log reduction rate for higher ozone concentration (Zhang, Xi et al. 2013). Studies like this concludes that high inlet-ozone concentration would enhance the log reduction of persistent bacteria because the dissolved zone rises during the disinfection. Which does not show the impact of MB application rather than the obvious effect of increasing O_3 concentration on bacteria. In another study analysis on deactivation of bacteria using oxygen MB in a continuous test indicated the effect of bursting force of the bubble on the disinfection efficiency (Kim and Han 2010). This investigation revealed that E. Coli was not detected (Han, Kim et al. 2001, Han, Kim et al. 2001, Han, Kim et al. 2006) after 30 min of MB generation. Moreover, the disinfection level of other bacteria was also very high (Kim and Han 2010). In the application of NBs for bathing pools, (K 2009) observed a high prevention of pathogen growth. In this study, two circulation systems are applied to connect the bathing pool with a reservoir, and the range of the sizes of the NBs were 10–20 nm. It has been found that subsequent burst of the NBs would provide a greater disinfection

and cleaning in both the bath and reservoir pools compared to that of the traditional ultrasonic vibrator. The application of ozone MB is not only limited to disinfection as mentioned earlier. Recent researches revealed that reduction MB also improved the oxidation of different pollutants by improving the formation of hydroxyl radical for advanced oxidation (Khuntia, Majumder et al. 2015).

The limited and inconsistent research output existing currently and the lack to address the ambiguities between researchers about the actual effect of NBs on different parameters affecting aeration, and AOP, shows the need of an in-depth research in the area. Of the gaps existing argument of scientists over the effect of mass transfer by NBs is the major one. Some researchers debate that the possibility of mass transfer improvement by using NBs is still a question to answer despite the theoretical prediction of NBs ability to improve surface area to volume ratio. These group of researchers argue from the point of view that the stability of NBs is a result of the "organic skin" or "contamination" of bubble surfaces which has a resistance effect to mass transfer (Wu, Nesset et al. 2012). These facts would be a concern, more during the idea of applying NBs in water and wastewater treatment operations like aerobic digestion and AOP. In these systems the water contaminants could facilitate the formation of thick NB interfaces as a result of "organic skin" or "contamination". Therefore, in the latter chapters (Chapter 4 and 5) of this

research the outcome of an in-depth experimental investigation on the effect of bubble size reduction to nano size on different parameters will be covered, giving foremost emphasis to mass transfer. For the experiments in this chapters a laboratory scale bubble column simulating the two treatment systems, AOP and aerobic digestion, was applied. Moreover, in gas-liquid phase processes, mass transfer controls the rates (Bouaifi, Hebrard et al. 2001, Linek, Kordač et al. 2005, Gourich, Azher et al. 2007). Studies on gas–liquid mass transfer focus on the effect of design parameters of contacting equipment, operating parameters and properties of contacting fluids. In the classical theoretical of phase mass-transfer, an increase in the interfacial area of exposure between the two phases, and nature and degree of dispersion of fluids in one another are the major factors that contribute towards an improvement in the process performance (E. 1968). To improve these factors different researchers have been studying the effect of various design and operating parameters over the years. Mixer design, packing column materials, tray and baffle type structures, reactor dimensions, injection nozzles, and sparger-type are major design parameters that play an important role (Pinilla, DÍaz et al. 1984, Javed, Mahmud et al. 2006, Wu, Nesset et al. 2012) in enhancing the mass transfer between the contacting phases. Similarly, gas and liquid superficial velocities, pressure, temperature, mixing or agitation speed and contacting method are those frequently studied operating factors that have

influence on bubble size and mass transfer (Bouaifi, Hebrard et al. 2001, Han and Al-Dahhan 2007, Dhaouadi, Poncin et al. 2008, Wu, Nesset et al. 2012). Considering;

1- The experience of previous studies on the effect of design and operating parameters and

2- The new design of bubble splitting generator used for this research, the effect of the design and operating parameters of the bubble generator on bubble size reduction and its effect on mass transfer without an influence of any reaction in the bulk liquid will be addressed and modeled in chapter 3.

1.2 Objectives and Scope

Bubbles exhibits different characteristics based on the variation of their size. Theoretically the rate of mass transfer is one of the characteristics affected by the change in bubble size. For a given mass of gas a reduction in bubble size increases the interfacial area to volume ratio. This leads to an increase in the rate of mass transfer from the gas phase in the bubble to the bulk liquid surrounding it. But in the other hand, previous researches claim that nanobubbles are very stable and have a hard shell of film as a result of contaminated surface which could develop resistance to the rate of mass transfer. Water and wastewater treatment technologies are the ideal environments for contamination of bubble surfaces by “organic skin” or contaminants in case of nanobubble application. Therefore, the general

objective of this research is to investigate the effect of bubble size reduction on the rate of mass transfer improvement of three different process types in water and wastewater treatment. The three processes investigated in this research are pure aeration (no reaction in the bulk liquid), O_3 driven AOP (fast reaction in the liquid film) and aerobic wastewater treatment (slow reaction in the bulk liquid).

The specific objectives of this research are categorized based on the investigations focus areas as:

1) Investigate mass transfer performance improvement on non-reactive aeration process via reduction of microbubbles to nano size applying hydrodynamic splitter, through studying:
   a. the effect of bubble splitter design parameters on trend of bubble size change
   b. the relationship between the splitter design parameters and mass transfer indicators
   c. the difference between mass transfer parameter (kla) and bubble persistence time for micro-bubbled and nano-bubbled water and
   d. and developing regression model for the volumetric mass transfer coefficient (kla) with respect to design parameters
2) Investigate effect of ultrafine/ nanobubble utilization on ozone based advanced oxidation process of wastewater treatment by studying:

a. the impact of O_3 bubble size reduction to nano size in affecting the influence of operating parameters (pH and T) on residual O_3 concentration
b. the improvement possibility of mass transfer
c. the effect of bubble size reduction to nano size on reaction mechanism and improvement possibility towards AO

3) Examine the influence of ultrafine bubble on the performance improvement possibility of biological wastewater treatment by checking:
    a. the effect of nanobubble application on the improvement of mass transfer rate in biological wastewater treatment.
    b. the improvement of microorganism cultivation rate by the application of nanobubbles compared to conventional systems
    c. the improvement of organic waste degradation efficiency by the application of nanobubbles compared to conventional system
    d. the effect of ultrafine bubble utilization on membrane filtration operation in comparison to conventional bubbles

1.3 Dissertation structure

This dissertation is composed of six chapters. In chapter one, the background of the research is contained in to three parts as introduction,

objectives and scope as well as the dissertation structure. Chapter two summarized the theoretical framework for the rest of the chapters. It is not a complete literature review, rather it is the basic chapter where a fundamental terms and theories that are going to be used in the rest of the chapters is compiled. For the following three independent chapters, Chapter 3-5, enough literature survey is included at the respective chapters. In chapter three, the bubble splitter is tested for its nanobubble production tendency. The effect of its design and operating parameters on the rate of non-reactive aeration process mass transfer is investigated and modeled. Chapter 4 covers the overall theoretical background, experimental method and result discussion of the effect of nanobubble utilization on AOP of wastewater treatment using O_3. The suppressing power of nanobubbles on other parameters affecting AOP was also assessed in addition of studying its effect on treatment mechanisms. Chapter five, also focus on the outcomes of applying nanobubbles for aerobic wastewater treatment and its tendency on improving mass transfer, treatment efficiency and microbial growth rate in comparison to currently applied conventional systems. Finally, in chapter six, the conclusions drawn from the researches done are compiled and summarized.

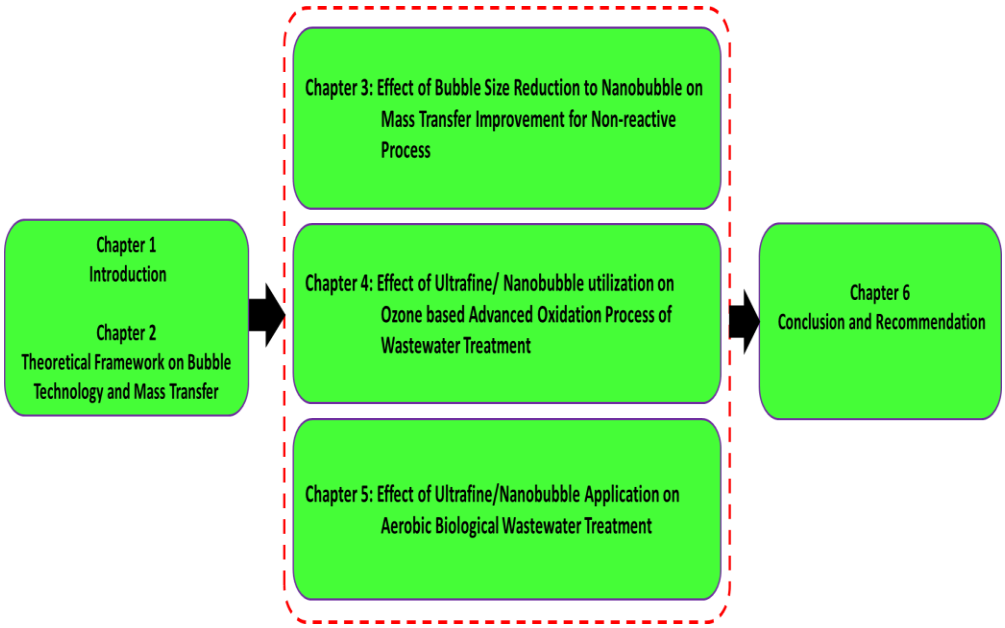

Figure 1.1 Structure of the dissertation

1.4 Reference

Agarwal, A., W. J. Ng and Y. Liu (2011). "Principle and applications of microbubble and nanobubble technology for water treatment." Chemosphere 84(9): 1175-1180.

Aydogan, A. and M. D. Gurol (2012). "Application of Gaseous Ozone for Inactivation of Bacillus subtilis Spores." Journal of the Air & Waste Management Association 56(2): 179-185.

Bouaifi, M., G. Hebrard, D. Bastoul and M. Roustan (2001). "A comparative study of gas hold-up, bubble size, interfacial area and mass transfer coefficients in stirred gas–liquid reactors and bubble columns."

Chemical Engineering and Processing: Process Intensification 40(2): 97-111.

Dhaouadi, H., S. Poncin, J. M. Hornut and N. Midoux (2008). "Gas–liquid mass transfer in bubble column reactor: Analytical solution and experimental confirmation." Chemical Engineering and Processing: Process Intensification 47(4): 548-556.

E., T. R. (1968). Mass-transfer Operations, Mcgraw-Hill Kogakusha.

El-Zahaby, A. M. and A. S. El-Gendy (2016). "Passive aeration of wastewater treated by an anaerobic process—A design approach." Journal of Environmental Chemical Engineering 4(4, Part A): 4565-4573.

Ghadimkhani, A., W. Zhang and T. Marhaba (2016). "Ceramic membrane defouling (cleaning) by air Nano Bubbles." Chemosphere 146: 379-384.

Gourich, B., N. E. Azher, C. Vial, M. B. Soulami, M. Ziyad and A. Zoulalian (2007). "Influence of operating conditions and design parameters on hydrodynamics and mass transfer in an emulsion loop–venturi reactor." Chemical Engineering and Processing: Process Intensification 46(2): 139-149.

Han, L. and M. H. Al-Dahhan (2007). "Gas–liquid mass transfer in a high pressure bubble column reactor with different sparger designs." Chemical Engineering Science 62(1–2): 131-139.

Han, M., W. Kim and S. Dockko (2001). "Collision efficiency factor of bubble and particle (abp) in DAF: theory and experimental verification." Water Science and Technology 43(8): 139-144.

Han, M., W. Kim and S. Dockko (2001). "Collision efficiency factor of bubble and particle (alpha bp) in DAF: theory and experimental verification." Water Sci Technol 43(8): 139-144.

Han, M. Y., M. K. Kim and H. J. Ahn (2006). "Effects of surface charge, micro-bubble size and particle size on removal efficiency of electro-flotation." Water Science and Technology 53(7): 127-132.

Javed, K. H., T. Mahmud and E. Purba (2006). "Enhancement of Mass Transfer in a Spray Tower Using Swirling Gas Flow." Chemical Engineering Research and Design 84(6): 465-477.

Jyoti, K. K. and A. B. Pandit (2001). "Water disinfection by acoustic and hydrodynamic cavitation." Biochemical Engineering Journal 7(3): 201-212.

Jyoti, K. K. and A. B. Pandit (2003). "Hybrid cavitation methods for water disinfection: simultaneous use of chemicals with cavitation." Ultrasonics Sonochemistry 10(4–5): 255-264.

K, C. K. (2009). Bathing Pool Assembly with Water Full of Nano-Scale Ozone Bubbles for Rehabilitation. U. S. Patent. USA.

Khuntia, S., S. K. Majumder and P. Ghosh (2015). "Quantitative prediction of generation of hydroxyl radicals from ozone microbubbles." Chemical Engineering Research and Design 98: 231-239.

Kim, J.-H., M. S. Elovitz, U. von Gunten, H. M. Shukairy and B. J. Mariñas (2007). "Modeling Cryptosporidium parvum oocyst inactivation and bromate in a flow-through ozone contactor treating natural water." Water Research 41(2): 467-475.

kim, J.-H., G. U. Von and B. J.Martin (2004). "Simultaneous Prediction of Cryptosporidium parvum Oocyst Inactivation and Bromate Formation during Ozonation of Synthetic Waters." Environmental Science and Technology 38: 2232-2241.

Kim, T.-i. and M. Han (2010). Analysis of bubble potential energy and its disinfection application and oil washing. PhD degree, Seoul National University.

Kulkarni, A. A. and J. B. Joshi (2005). "Bubble Formation and Bubble Rise Velocity in Gas−Liquid Systems: A Review." Industrial & Engineering Chemistry Research 44(16): 5873-5931.

Larson, M. A. and B. J. Mariñas (2003). "Inactivation of Bacillus subtilis spores with ozone and monochloramine." Water Research 37(4): 833-844.

Li, H., L. Hu, D. Song and A. Al-Tabbaa (2014). "Subsurface Transport Behavior of Micro-Nano Bubbles and Potential Applications for Groundwater Remediation." International Journal of Environmental Research and Public Health 11(1): 473.

Li, X., P. Li, L. Zu and C. Yang (2016). "Gas-Liquid Mass Transfer Characteristics with Microbubble Aeration – I. Standard Stirred Tank." Chemical Engineering & Technology 39(5): 945-952.

Linek, V., M. Kordač and T. Moucha (2005). "Mechanism of mass transfer from bubbles in dispersions: Part II: Mass transfer coefficients in stirred gas–liquid reactor and bubble column." Chemical Engineering and Processing: Process Intensification 44(1): 121-130.

Liu, S., S. Oshita, Y. Makino, Q. Wang, Y. Kawagoe and T. Uchida (2016). "Oxidative Capacity of Nanobubbles and Its Effect on Seed Germination." ACS Sustainable Chemistry & Engineering 4(3): 1347-1353.

Matsuki, N., T. Ishikawa, S. Ichiba, N. Shiba, Y. Ujike and T. Yamaguchi (2014). "Oxygen supersaturated fluid using fine micro/nanobubbles." International Journal of Nanomedicine 9: 4495-4505.

Mezule, L., S. Tsyfansky, V. Yakushevich and T. Juhna (2009). "A simple technique for water disinfection with hydrodynamic cavitation: Effect on survival of Escherichia coli." Desalination 248(1–3): 152-159.

Park, J.-S. and K. Kurata (2009). "Application of microbubbles to hydroponics solution promotes lettuce growth." HortTechnology 19(1): 212-215.

Pinilla, E. A., J. M. DÍaz and J. Coca (1984). "Mass transfer and axial dispersion in a spray tower for gas-liquid contacting." The Canadian Journal of Chemical Engineering 62(5): 617-622.

Sumikura, M., M. Hidaka, H. Murakami, Y. Nobutomo and T. Murakami (2007). "Ozone micro-bubble disinfection method for wastewater reuse system." Water Science and Technology 56(5): 53-61.

Takahashi, M. (2009). "Base and technological application of micro-bubble and nanobubble." Material Integration 22: 2-19.

Tang, C.-C., W. Zuo, Y. Tian, N. Sun, Z.-W. Wang and J. Zhang (2016). "Effect of aeration rate on performance and stability of algal-bacterial symbiosis system to treat domestic wastewater in sequencing batch reactors." Bioresource Technology 222: 156-164.

Tasaki, T., T. Wada, K. Fujimoto, S. Kai, K. Ohe, T. Oshima, Y. Baba and M. Kukizaki (2009). "Degradation of methyl orange using short-wavelength UV irradiation with oxygen microbubbles." Journal of Hazardous Materials 162(2–3): 1103-1110.

Weber, J. and F. Agblevor (2005). "Microbubble fermentation of Trichoderma reesei for cellulase production." Process Biochemistry 40(2): 669-676.

Wu, C., K. Nesset, J. Masliyah and Z. Xu (2012). "Generation and characterization of submicron size bubbles." Advances in Colloid and Interface Science 179–182: 123-132.

Yamasaki, K., K. Sakata and K. Chuhjoh (2010). Wastewater Treatment Method and WaterTreatment System. U. patent, Editor. USA.

Yamasaki, K., K. Uda and K. Chuhjoh (2009). Wastewater Treatment Equipment and Method of Wastewater Treatment. U. patent, Editor. USA.

Zhang, F., J. Xi, J.-J. Huang and H.-Y. Hu (2013). "Effect of inlet ozone concentration on the performance of a micro-bubble ozonation system for inactivation of Bacillus subtilis spores." Separation and Purification Technology 114: 126-133.

Chapter 2

Theoretical Framework on Bubble Technology and Mass Transfer

2.1 Definition and classification of bubbles

Studies pertaining to bubbles in bulk-liquid mediums have been conducted for more than half a century. However, the types and classifications of bubbles were hardly defined in a clear, comprehensive manner. Researchers attempted to classify bubbles based on different bubble characteristics. The most frequently studied factors are bubble scale, surface nature, and the reservation/persistence time of the bubbles (Shu, Qunhui et al. 2010). (Ushikubo, Furukawa et al. 2010) found that most of these factors depend on the size distribution of the bubbles. Hence, many researchers frequently employed the bubble sizes as a basis for categorization.

In previous studies bubbles were categorized as macro bubbles, MBs, and sub-micro or NBs for conventional or big bubbles, fine bubbles, and ultrafine bubbles, respectively (Wu, Chen et al. 2008, Xu, Nakajima et al. 2008, Edzwald 2010, Ohgaki, Khanh et al. 2010, Agarwal, Ng et al. 2011, Terasaka, Hirabayashi et al. 2011, Pérez-Garibay, Martínez-Ramos et al. 2012, Wu, Nesset et al. 2012). However, the researchers defined the range of sizes for these categories differently. (Pérez-Garibay, Martínez-Ramos et al. 2012) employed the term conventional bubbles to describe the bubbles with sizes

ranging between 600–2500 μm, whereas (Xu, Nakajima et al. 2008) categorized them vaguely as large bubbles in comparison to MBs. In another study, (Khuntia, Majumder Subrata et al. 2012) labeled the conventional bubbles with diameters in the range of 2–5 mm as "macrobubbles," representing those commonly used in fermenters, gas–liquid reactors, and ore-flotation equipment. In another study, (Edzwald 2010) grouped the spherical-shaped conventional bubbles with diameters in the range 1–10 mm as "large bubbles". Similarly, (Krishna and Van Baten 2001) considered conventional industrially applicable bubbles to be in the range of 1–7 mm, for their research on scale-up of bubble column reactors. Based on these studies, Most of the researchers grouped the conventional bubbles size range between 0.6–10 mm, and the bubbles with diameters greater than 10 mm are assumed to have different shapes. (Edzwald 2010) showed that these conventional bubbles exhibit a change in their shape from spherical to elliptical with an increase in their sizes. For the bubbles with diameters greater than 10 mm, the individual bubbles take the shape of a spherical cup, and the flow regime changes to churn flow rather than bubbly flow.

MBs or fine bubbles are defined by (Agarwal, Ng et al. 2011) as tiny bubbles having sizes in the range of 10–50 μm, whereas (Takahashi, Chiba et al. 2007) categorized these types of bubbles as having diameters less than 50 μm. In another study, (Terasaka, Hirabayashi et al. 2011) classified these

bubble types as small bubbles with sizes in the range of 10–60 μm based on their field of application in a study of physiological activity. Similarly, (Edzwald 2010) categorized the bubbles under the size of several 100 μm and less, as small bubbles having a rigid spherical shape. (Pérez-Garibay, Martínez-Ramos et al. 2012) classified MBs in the range of 30–100 μm. Likewise, (Ebina, Shi et al. 2013) considered MBs as bubbles in the range of 10-50 μm. Although the researchers disagree on the size boundaries of the MBs, most of them suggested a minimum size of approximately 10 μm, while the maximum size suggested was 100 μm.

The presence and stability of NBs has been a controversial issue since the proposal of their contribution to the attraction between hydrophobic surfaces in water (Parker, Claesson et al. 1994, Berkelaar, Zandvliet et al. 2013, Walczyk and Schönherr 2014). Since then, many researchers investigated their presence using different techniques (Ushikubo, Furukawa et al. 2010, Walczyk and Schönherr 2014). Similar to the case of the MBs, the researchers did not arrive at a consensus regarding the definition of the NBs sizes; moreover, some of the definitions exclude a range of bubble sizes that is not between the minimum size proposed for the MBs and the maximum for the NBs. (Agarwal, Ng et al. 2011) did not classify the bubbles that fall in the range between 200 nm and 10 μm. Based on their definition, the diameters below 200 nm represent the NBs. To define this range, (Agarwal, Ng et al.

2011) presented the names 'micro-nano bubbles' (MNBs) based on the suggestion from (Tsuge 2010), which shows the confusion and lack of a clear category for ultrafine bubbles. In addition, (Wu, Nesset et al. 2012) defined the NBs or sub-micron bubbles as bubbles having sizes less than a micron and categorized the bubbles they generated with a size less than 500 nm as sub-MBs or NBs. Moreover, recently, (Parmar and Majumder 2013) defined the NBs as bubbles having a diameter less than few hundreds of a nanometer, which is vague and controversial. By summarizing the upper limit of the bubbles that different researchers considered for NBs, bubbles less than a micron was found reasonable to categorize them under ultrafine bubbles/NBs based on their measured size and shared similarity of properties.

The bubble categorization proposed in the previous studies do not only depend on size but also on the shared characteristics and behaviors of the bubbles in a bulk-liquid medium. Fig. 1 shows the summary of the size category based on the most agreed size ranges for the different bubbles with their major properties. For the bubbles ranging in between 1–10 μm, the name "sub-MBs" is proposed because the properties of these bubbles falls in between the MBs and NBs.

Although the researchers agree on the characteristics of the MBs, the agreement on clear size boundary for the different bubble types is not yet standardized. Given this fact and the above justifications for the ambiguity in

bubble size catagorization, for the purpose of this research it is proposed to follow the following definition for the different bubble categories, as shown in Fig. 1. It can also be adopted as a basis for standardization process based on the perspectives of the reviewed articles as well as the common properties shared by the bubbles with sizes categorized under the respective groups.

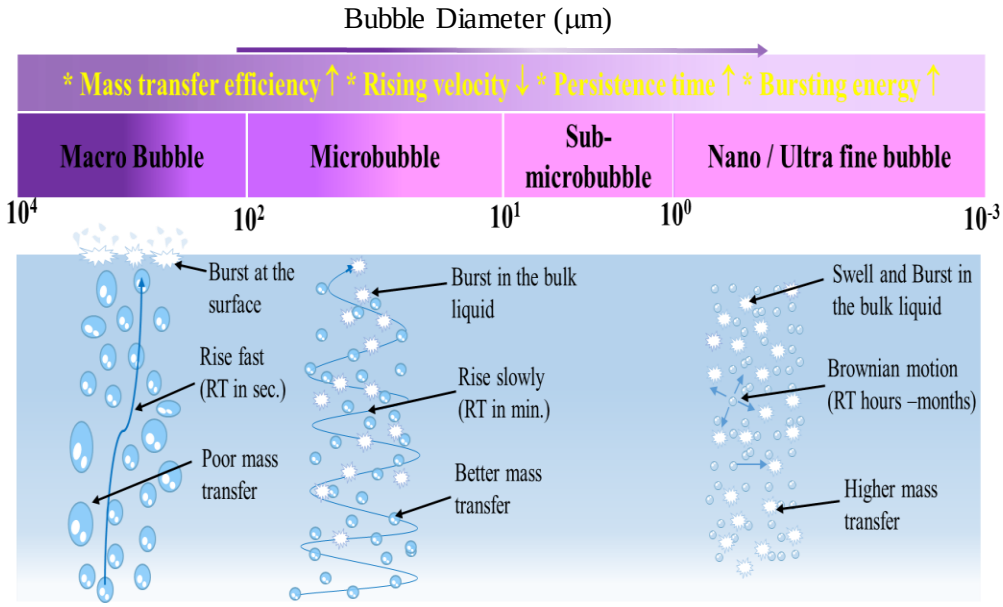

Figure 2.1 Proposed range of the bubble sizes and major properties

2.2 Bubble generation techniques

Bubble formation is considered as a static or quasi-static process. It is followed by the dynamic processes, namely, coalescence and break up. (Agarwal, Ng et al. 2011) defined these overall process of bubble formation, growth, and collapse process of bubbles as cavitation. In bubble formation coalescence and break up are two opposite states of the fine bubbles. In the

case of coalescence, fine bubbles combine to form bigger bubbles, whereas the possibility of further breakup favors the formation of ultrafine bubble generation and/or collapse. Different studies applied different techniques of fine and ultrafine generation: hydrodynamic cavitation and particle cavitation (Agarwal, Ng et al. 2011), acoustic or sonication (Xu, Nakajima et al. 2008, Kim and Han 2010, Agarwal, Ng et al. 2011), electrochemical cavitation (Wu, Chen et al. 2008), and mechanical agitation (Xu, Nakajima et al. 2008). The hydrodynamic cavitation is the most frequently applied system in water-treatment technologies and it can be achieved by pressurized saturation, bubble shearing, splitting, and mechanical agitation (AWWA 1999, Kim and Han 2010, Ohgaki, Khanh et al. 2010, Shu, Qunhui et al. 2010, Ushikubo, Furukawa et al. 2010, Terasaka, Hirabayashi et al. 2011, Ebina, Shi et al. 2013, Kim and Han 2014, Li, Li et al. 2016). (Terasaka, Hirabayashi et al. 2011) Discussed some of the MB generators in detail including the spiral liquid-flow type, Venturi type, ejector type, and pressure dissolution type, which use hydrodynamic-cavitation mechanism based on the liquid and gas flow. The mechanical cavitation is a technique that employs high speed agitation by using mechanical mixers to a given volume of bulk liquid with a limited amount of gas (Wu, Nesset et al. 2012). On the other hand, Hydrodynamic bubble splitter system apply a plug flow big bubble shearing technique to reduce bubble sizes (Kim and Han 2014). In this research this method is

applied for the generation of MB and NB generation. Its generation technique and parts of the bubble generating system is explained in detail in chapter three. The acoustic or sonication system employs the ultrasonic waves either by using an ultrasonic probe (Xu, Nakajima et al. 2008) inside the bulk liquid or external ultrasonic wave generator (Kim and Han 2010). The electrochemical systems employ an electrical current on a given surface, which is immersed into a given solution to generate surface nucleated bubbles (Wu, Chen et al. 2008).

2.3 Bubble size distribution and measurement

Several techniques have been used for measuring the size and size distribution of the MBs and NBs. Among the measurement methods applied, the laser-diffraction particle-size analyzer (Yoshida, Masuda et al. 2001, Yoshida, Masuda et al. 2003, Cho, Kim et al. 2005, Kukizaki and Goto 2006, Takahashi, Chiba et al. 2007, Han, Kim et al. 2009, Tasaki, Wada et al. 2009, Agarwal, Ng et al. 2011, Xiong and Peng 2015) atomic force microscope (Binnig, Quate et al. 1986), and image analysis (Kim and Han 2010, Kim, Kim et al. 2012, Kim and Han 2014) are considered as the most typical tools. Each measurement method has its own merits and limitations. For example, the image analysis and atomic force microscope methods could report the average diameter with a visible image; however, these methods require considerable time for provision of a meaningful size because of lack of obtaining enough

focused bubble images in few snapshots for meaningful size determination. Studies show that Image analysis can be used for bubble sizes of the minimum size of 0.8 μm, which is relatively higher compared to the other measuring techniques (Kim and Han 2014). Moreover atomic force microscopy technique has shortcomings in the case of measuring homogeneous bubbles surrounded by only the bulk fluid. Laser-diffraction particle-size analyzer is a simple tool that can be used to obtain the average size of a large number of bubbles without a visible image. It employs bubble size measurement technique based on their light-scattering properties. It is applicable to measure sizes ranging from approximately 0.1μm to 3 mm. (Kobayashi, Maeda et al. 2014) proposed another technique for determination of ultrafine bubbles using resonant mass measurement method. It is assumed to solve the drawbacks of other conventional techniques in differentiating particles from NBs with the size range of 100-200 nm. It is capable of distinguishing positively buoyant particles (bubbles) from negatively buoyant particles. Since one of the objectives in this research is to confirm the trend observed by (Kim and Han 2014), which is the change of bubble size with design and operating conditions of the bubble splitter, image analysis is applied.

Several studies show the effects of design and operation conditions on the size and/or distribution of the MBs and NBs. For instance, it was demonstrated for a nozzle system that the size and fraction of the MBs mainly

depend on the pressure differences across the nozzle system. Higher pressure would produce smaller bubbles because of an increase in air density and at pressures above approximately 3.5 atm, the sizes of the MBs were almost constant (de Rijk, Jaap H.J.M. aivan der et al. 1994, Han 2002, Kim, Kim et al. 2012, Bui and Han 2015). For the case of the NBs, the pressure (de Rijk, Jaap H.J.M. aivan der et al. 1994, Kim, Kim et al. 2012, Kim and Han 2014), sonic power (Cho, Kim et al. 2005), and other operation conditions, such as the length, diameter, and type of hose (Kim and Han 2014) are introduced as relatively major factors affecting the size. (Ushikubo, Furukawa et al. 2010) indicated that different types of gases used in bubble creation; such as oxygen and air, resulted in NBs with similar, common average sizes (measured using particle analyzer) of 137 nm and 140 nm, respectively. But for macro size and relatively bigger size MBs using higher molecular weight gas increases the density leading to smaller bubble generation (Kulkarni and Joshi 2005). Because of the above reason, the oxygen, O_3 and air MBs and NBs generated in this research under the same operating and design conditions of the generator are assumed to be of similar size. Table 2.1 summarize some of the studies on the size dependency of the MBs and NBs on the aforementioned factors.

Table 2.1 MBs and NBs – sized dependence of design and operation parameters

Affecting parameters		Size range	Average size	References
Pressures (atm)	2	20 – 130 µm*	71 µm*	(de Rijk, Jaap H.J.M. aivan der et al. 1994, Han, Park et al. 2002)
	3			
	≥ 3.5	10 – 110 µm*	41 µm *	(Han, Park et al. 2002, Kim, Kim et al. 2012, Bui and Han 2015)
		15 - 85 µm*	30 µm *	(Han, Park et al. 2002, Bui and Han 2015)
Sonic power (W)	50	-	750 nm	(Cho, Kim et al. 2005)
	100	-	935 nm	
	150	-	921 nm	
	200	-	965 nm	
Hose diameter (mm)	8	-	2.65 µm	(Kim and Han 2014)
	10	-	3.61 µm	
Hose length (m)	10	-	3.19 µm	(Kim and Han 2014)
	20	-	2.90 µm	
	30	-	2.56 µm	
	40	-	2.61 µm	
	50	-	2.61 µm	

Hose type	Braid	-	3.26 μm	(Kim and Han 2014)
	Teflon	-	2.93 μm	
	Wrinkle pipe	-	2.49 μm	

* Bubble size is measured using laser-diffraction particle-size analyzer method;

Other results: bubble size is measured using image analysis method.

2.4 Mass transfer and Bubble properties

Gas absorption is one of the mass transfer operations representing the movement of gaseous molecules to the liquid phase. Bubble columns, tray columns, spray towers, packed columns and mixing tanks are some of the reactor types used in gas-liquid mass transfer. In many applications involving gas–liquid phase operations bubble columns reactors are commonly used as contacting process units because of easy design and construction cost (Han and Al-Dahhan 2007, Hecht, Bey et al. 2015). But the mass transfer efficiency for the bubble column is relatively the lowest. Therefore, the rate of gas-to-liquid phase mass transfer often controls the process efficiency; hence, it is a critical design criterion (Prince and Blanch 1990, Bouaifi, Hebrard et al. 2001, Weiguo, Jinfu et al. 2001, Wongsuchoto, Charinpanitkul et al. 2003, Linek, Kordač et al. 2005). In this research, because of its ease of production and the crucial need of investigating the possibility of improving its mass transfer efficiency applying nanobubbles, bubble column was applied as a processing unit operation.

2.4.1 Mass transfer theories

There are many developed theories used to express the gas-liquid mass transfer. Film theory, Penetration theory and surface renewal theory are the basic and fundamental theories. The film theory is the oldest theory compared to all. It works under the assumptions of:

1) Stagnant film between gas and liquid,
2) Steady state at equilibrium
3) Amount of gas in the film is very small compared to that passes through it
4) Laminar flow at the film surface (No turbulence)(E. 1968, Garcia-Ochoa and Gomez 2009)

All these assumptions are a gross approximations of the real operations in conventional bubble columns, where macro bubbles are the main actors in mass transfer in addition to manifested effect of turbulence at the surface of bubbles. It works where local steady state conditions are fulfilled especially for slow rising bubbles in relatively stagnant fluid. Therefore, the other models stated earlier were developed to replace the film theory for a better approximation with an assumptions of:

1) The velocity of the fluid at the surface of the bubble is not zero
2) The contact time between bubble and liquid is instantaneous and not enough to establish steady state assumption

3) Bubbles are under the influence of turbulent motion

4) Constant renewal of contacting phases at the surface of contact

5) thickness of the liquid is infinite in depth (E. 1968)

These assumptions more express the cases of conventional bubble systems where there is high local mixing and fast rising bubbles.

In this research, considering very nature of fine and ultrafine bubbles having longer resident time and low or negligible rising velocity, the contact time between bubble and liquid is not instantaneous and it is assumed to be enough to establish steady state assumption of the film theory. The low flowrates applied in the experiments are assumed to reduce the effect of turbulence and to be considered negligible. Therefore, considering this assumptions and the simplicity of the film theory model, it is taken as the main theory to follow for this research to approximate the mass transfer.

Two-film theory

The two film theory is proposed by (W.K and W.G 1924) (Whitman 1962) with an assuming two existing stationary films at each sides of the gas-liquid interface between the two phases. For the fundamental assumptions stated earlier the following diagram is set to represent the theory for the case of no reaction inside the phases (or pure mass transfer case). This schematics and derivation will be followed for chapter 3 of this thesis.

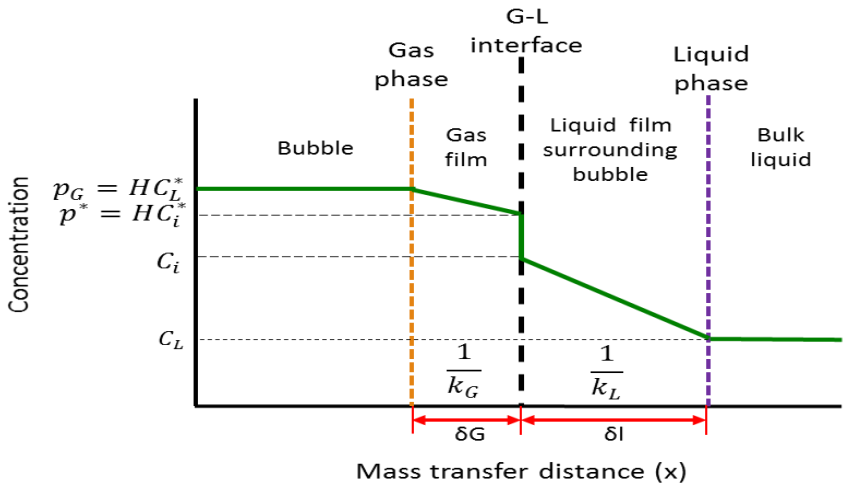

Figure 2.2 Schematic representation of the gas liquid interface for the two film theory

where p_G is the partial pressure of specific gas in the bulk gas, k_G and k_L are local mass transfer coefficients, p_G is gas phase pressure, P^* is interface partial pressure, C_i is interface concentration and, C_i^* equilibrium concentration at the liquid film, C_L is concentration in the bulk liquid, H Henry's constant, $\delta_G$thickness of the gas film and $\delta_l$thickness of the liquid film

The flux through each film is assumed to be constant and it is expressed as a product of the driving force by the mass transfer coefficient as it is given by:

$$J = k_G * (p_G - p_i) = k_L * (C_i - C_L) \qquad 2.1$$

where, J is the max flux, k_G and k_L are local mass transfer coefficients p_G is gas phase pressure, p_i is interface partial pressure, C_i is interface concentration and C_i is concentration of the liquid phase.

But p_i and C_i cannot be measured directly, therefore using the overall mass transfer coefficient the mass flux is adjusted using the equilibrium gas pressures and concentration as:

$$J = K_G * (p_G - p^*) = K_L * (C^* - C_L) \quad 2.2$$

where, K_G and K_L are overall mass transfer coefficients in the gas and liquid phases, P^* is gas phase equilibrium partial pressure, C^* is equilibrium concentration in the liquid phase given by the relationship

$p^* = H * C^*$; Where, H is Henry's constant and the overall mass transfer coefficient is given by:

$$\frac{1}{K_L} = \frac{1}{Hk_G} + \frac{1}{k_L} \quad 2.3$$

From equation 2.2 the gas phase mass transfer rate per unit reactor volume to the bulk liquid (GTR) is given by multiplying the overall mass flux, J, by the gas-liquid interfacial area per unit liquid volume, *a*.

$$GTR = \frac{dC}{dt} = J * a = k_L a * (C^* - C_L) \quad 2.4$$

where $\frac{dC}{dt}$, rate of mass transfer of a specific component, K_L overall mass transfer coefficient, a interfacial area of mass transfer, C^* equilibrium

concentration of the specific component in the bulk liquid and C_L concentration of the specific component in the bulk liquid at any time t.

But the profile in fig. 3 changes as the process type changes or when there is a reaction inside the liquid film or bulk liquid. Since in chapter 4 and 5 of this thesis we are going to deal with the process of O_3 reaction taking place in the bulk liquid and very slow reaction of biological waste degradation taking place in the bacteria floc present in the bulk liquid figure 3 is modified as shown in figure 4 for each process.

The net mass transfer rate equation for these reaction involving processes is given by considering the dissolved mass balance in the bulk liquid phase. It is described as:

$$\frac{dC}{dt} = GTR - GCR \qquad 2.5$$

Where, GTR is the gas transfer rate given by equation 2.4 and GCR is the gas consumption rate in the bulk liquid by any reaction type. In chapter 3 equation 2.4 is used as a governing model for the determination of the volumetric mass transfer coefficient ($k_L a$) whereas, in chapters 4 and 5 governing models are developed by using equation 2.5. The critical concept of $k_L a$ is covered separately in the next section.

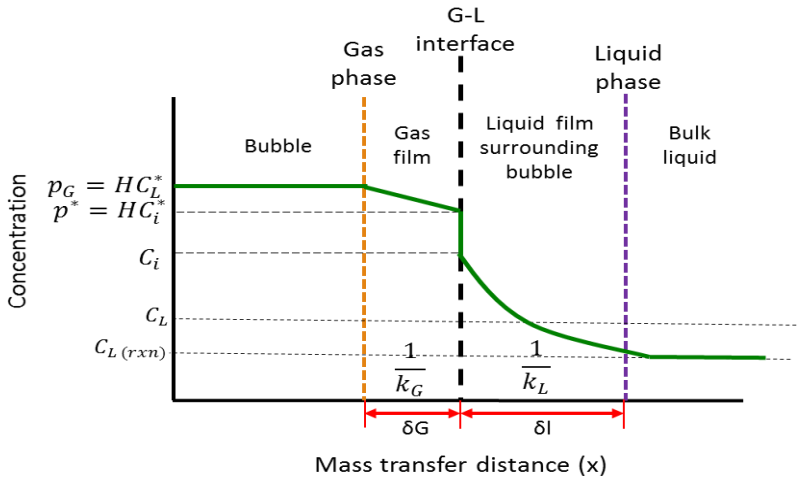

(a)

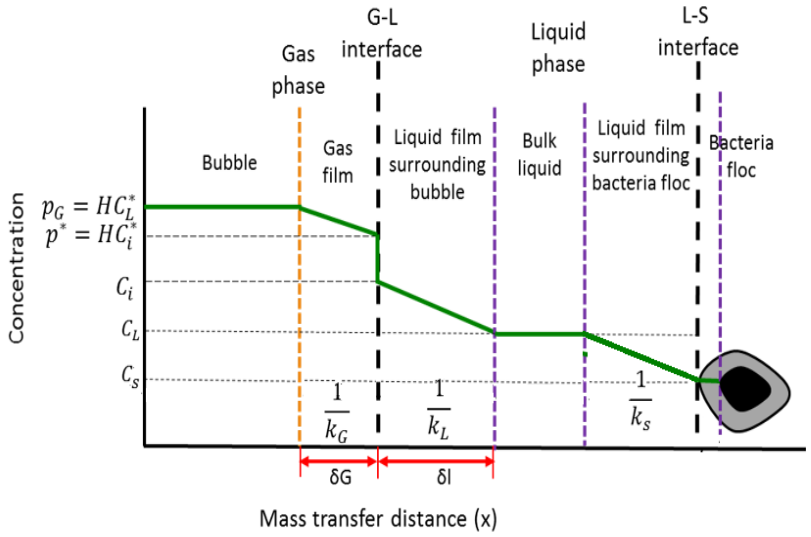

(b)

Figure 2.3 Schematic representation of the gas liquid mass transfer step for reactions in (a) bulk liquid (case of O_3 reaction) and (b) in bacteria floc in the bulk liquid where *ks* is the mass transfer coefficients in the film surrounding the bacteria

The mass-transfer efficiency of the bubble columns depends on the size distribution of the bubbles, rising velocity of the bubbles, surface area to volume ratio, coalescence and breakup, gas–liquid hydrodynamics, phase mixing, and physical properties (Wilkinson and v. Dierendonck 1990, Bouaifi, Hebrard et al. 2001, Camacho Rubio, Sánchez Mirón et al. 2004). This is readily can be explained by the influence of each factor on the parameters of equation 2.4. According to the classical two-film theory of gas absorption, the rate of mass transfer between two phases depends on the change of the following three factors; the gas and liquid phase mass-transfer coefficient, mass-transfer surface area to volume ratio, and the concentration gradient between the two phases (Whitman 1962, Bouaifi, Hebrard et al. 2001). Those parameters influencing these three factors are categorized in to four as; process types, fluid properties, operational parameters, and design parameters. The interrelation between the parameters and the factors is shown by figure 4. The arrow directions show which parameters influence the corresponding factor at the next end of the arrow. In most researches rate of mass transfer is evaluated by the volumetric mass transfer and gas hold up as a proxy parameters. Similarly in this research since some parameters are used in different sections, their meanings and components are discussed hereunder.

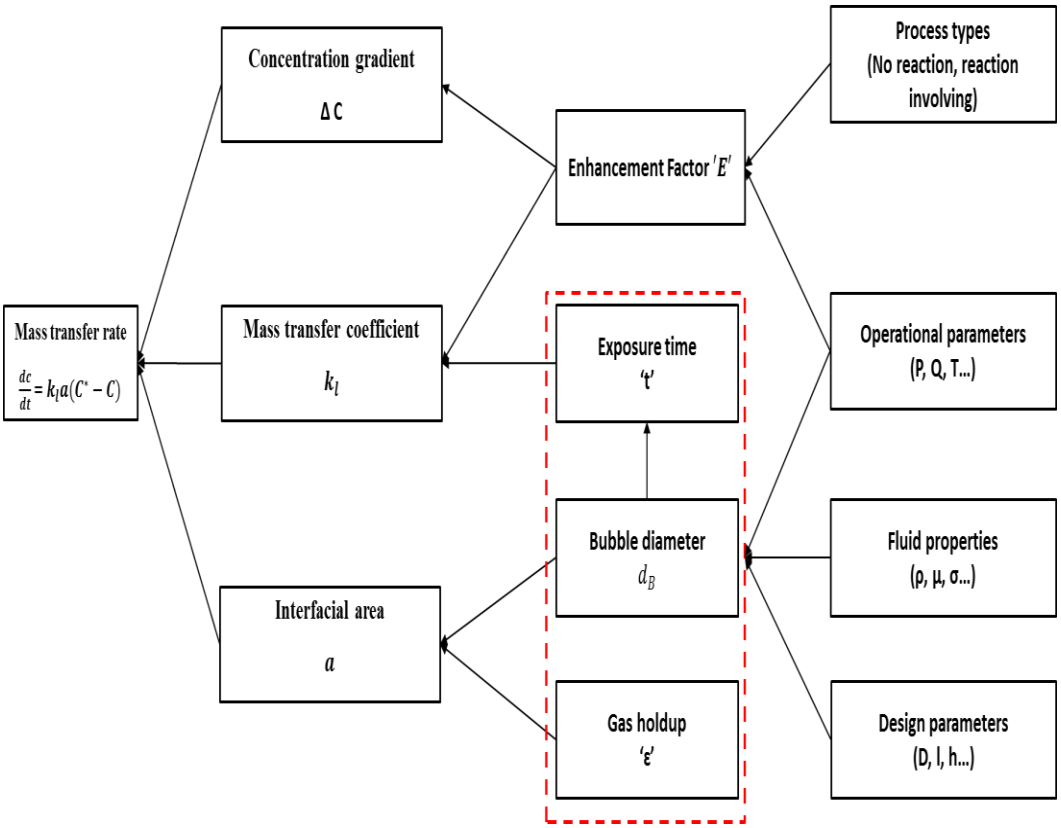

Figure 2.4 Interrelations between parameters and factors affecting rate of mass transfer.

2.4.2 Bubble rising velocity

Rising velocity is a key parameter affecting the behavior of the bubbles in water and liquid solution (Liu, Oshita et al. 2016). Several studies mention the theoretical approach for determining the terminal velocity of a single, sphere bubble that could be expressed with Stoke's law and/or Hadmard–Rybczynski's equation (H–R equation) at a Reynolds number of zero (Parkinson, Sedev et al. 2008). Based on these principles, the diameter of the bubble and liquid viscosity are concluded as factors affecting the rising

velocity. These equations give an approximately zero value for nanobubbles. Moreover, different researchers confirmed the longer persistence time of microbubbles (in minutes) and nanobubbles (in days to months) compared to the shortest stay of macro bubbles (in seconds) in the bulk liquid.

2.4.3 Volumetric mass transfer coefficient

In the gas–liquid reactors, mass transfer can be characterized by measuring the volumetric mass transfer coefficient, as it is an important parameter for evaluating the performance of the reactor (Bouaifi and Roustan 1998). It is the product of the liquid mass-transfer coefficient "k_l" and the interfacial surface area"a". The liquid mass-transfer coefficient is a function of the turbulence and liquid parameters affecting the liquid film renewal. The interfacial area depends on the size distribution of the bubbles, which is a function of the gas flow rate, sparger and nozzle design, shear rate, fluid properties like (liquid viscosity and gas density) and other design and operating parameters. Different correlations have been proposed for estimation of the mass transfer coefficient for conventional and MBs with respect to different factors based on mathematical modeling and experimental studies. One of the major problems of the experimental studies is the divergence of the proposed correlations mainly because of the difference in the system size and the measuring methods (Bouaifi and Roustan 1998). The models developed so far have different approaches based on the system,

application, and modeling methods followed. So far, studies on the mass transfer using the ultrafine bubbles are limited. In most of previously done researches dynamic method, CO_2 absorption method and Sodium sulfite oxidation method are applied for determination of k_la for fine bubble processes (Worden and Bredwell 1998, Garcia-Ochoa and Gomez 2009, Ying, Al-Mashhadani et al. 2013, Li, Li et al. 2016).

2.4.4 Surface area to volume ratio

The other key parameter in determining the rate of mass transfer in a gas–liquid system is the interfacial area to volume ratio "a". In most of the developed mass-transfer models in the aforementioned studies, the rate of mass transfer is related to the bubble size through the interfacial area using the relation given in equation 2.6 based on the common assumption that bubbles have a simple, spherical shape with one representative diameter and the dependence of gas holdup on the size of the bubble (Akita and Yoshida 1974, Ruen-ngam, Wongsuchoto et al. 2008, Agarwal, Ng et al. 2011, Ying, Al-Mashhadani et al. 2013).

$$a = \frac{6\varepsilon_g}{d_b(1-\varepsilon_g)} \qquad 2.6$$

Where, ε_g is the gas holdup and d_b is bubble diameter

2.4.5 Gas holdup

Gas holdup (ε) is defined as the volume fraction occupied by the bubble or gas in the entire gas–liquid dispersion, usually given by equation (4) (Bouaifi, Hebrard et al. 2001, Wongsuchoto, Charinpanitkul et al. 2003, Agarwal, Ng et al. 2011). It is determined by the volume expansion method (Wongsuchoto, Charinpanitkul et al. 2003) and calculated by measuring either the bulk liquid table depth/pressure change or volume change before and after aeration/de-aeration.

$$\varepsilon = \frac{V_g}{V_S} = \frac{V_f - V_i}{V_f} = \frac{H_D - H_L}{H_D} \qquad 2.7$$

where V_g is the volume of the gas, $V_s = V_f$ is the final volume of the gas–liquid solution, V_i is the initial volume of the liquid before bubbling, H_D is the final water table head of the gas–liquid solution, and H_L is the initial water table head of the bulk liquid.

2.4.6 Enhancement factor

Enhancement factor expresses the effect of any reaction taking place in a given phase (usually in the liquid phase) in to consideration while computing the overall mass transfer coefficient. It represents the enhancement of the mass transfer rate due to the presence of a reaction in the given phase over a pure mass transfer without reaction (Levenspiel 1972, Garcia-Ochoa

and Gomez 2009). It is given by the ratio of the mass transfer flux with the presence of reaction to that of the mass transfer flux without reaction as:

$$E = \frac{\text{Rate of mass transfer with reaction}}{\text{Rate of mass transfer without reaction}} = \frac{K_{lr}a}{k_l a} \qquad 2.8$$

Where, E is enhancement factor, $K_{lr}a$ is volumetric mass transfer with reaction, and $k_l a$ is a volumetric mass transfer without reaction. If there is a reaction in the liquid phase the overall mass transfer coefficient expressed by equation 2.3 will change its format to the one in equation 2.9:

$$\frac{1}{K_{lr}} = \frac{1}{HK_G} + \frac{1}{EK_L} \qquad 2.9$$

2.5 Reference

Agarwal, A., W. J. Ng and Y. Liu (2011). "Principle and applications of microbubble and nanobubble technology for water treatment." Chemosphere 84(9): 1175-1180.

Akita, K. and F. Yoshida (1974). "Bubble Size, Interfacial Area, and Liquid-Phase Mass Transfer Coefficient in Bubble Columns." Industrial & Engineering Chemistry Process Design and Development 13(1): 84-91.

AWWA, A. W. W. A. (1999). Water quality and Treatment. United States of America, McGraw-Hill.

Berkelaar, R. P., H. J. W. Zandvliet and D. Lohse (2013). "Covering Surface Nanobubbles with a NaCl Nanoblanket." Langmuir 29(36): 11337-11343.

Binnig, G., C. F. Quate and C. Gerber (1986). "Atomic Force Microscope." Physical Review Letters 56(9): 930-933.

Bouaifi, M., G. Hebrard, D. Bastoul and M. Roustan (2001). "A comparative study of gas hold-up, bubble size, interfacial area and mass transfer coefficients in stirred gas–liquid reactors and bubble columns." Chemical Engineering and Processing: Process Intensification 40(2): 97-111.

Bouaifi, M. and M. Roustan (1998). "Bubble size and mass transfer coefficients in dual-impeller agitated reactors." The Canadian Journal of Chemical Engineering 76(3): 390-397.

Bui, T. T. and M. Han (2015). "Removal of Phormidium sp. by positively charged bubble flotation." Minerals Engineering 72: 108-114.

Bui, T. T. and M. Han (2015). "Removal of Phormidium sp. by positively charged bubble flotation." Minerals Engineering 72(Complete): 108-114.

Camacho Rubio, F., A. Sánchez Mirón, M. C. Cerón García, F. García Camacho, E. Molina Grima and Y. Chisti (2004). "Mixing in bubble

columns: a new approach for characterizing dispersion coefficients." Chemical Engineering Science 59(20): 4369-4376.

Cho, S.-H., J.-Y. Kim, J.-H. Chun and J.-D. Kim (2005). "Ultrasonic formation of nanobubbles and their zeta-potentials in aqueous electrolyte and surfactant solutions." Colloids and Surfaces A: Physicochemical and Engineering Aspects 269(1–3): 28-34.

de Rijk, S. E., G. Jaap H.J.M. aivan der and J. G. den Blanken (1994). "Bubble size in flotation thickening." Water Research 28(2): 465-473.

E., T. R. (1968). Mass-transfer Operations, Mcgraw-Hill Kogakusha.

Ebina, K., K. Shi, M. Hirao, J. Hashimoto, Y. Kawato, S. Kaneshiro, T. Morimoto, K. Koizumi and H. Yoshikawa (2013). "Oxygen and Air Nanobubble Water Solution Promote the Growth of Plants, Fishes, and Mice." PLoS ONE 8(6): e65339.

Edzwald, J. K. (2010). "Dissolved air flotation and me." Water Research 44(7): 2077-2106.

Garcia-Ochoa, F. and E. Gomez (2009). "Bioreactor scale-up and oxygen transfer rate in microbial processes: An overview." Biotechnology Advances 27(2): 153-176.

Han, L. and M. H. Al-Dahhan (2007). "Gas–liquid mass transfer in a high pressure bubble column reactor with different sparger designs." Chemical Engineering Science 62(1–2): 131-139.

Han, M., T.-i. Kim and D. Kwak (2009). "Measurement of bubble bed depth in dissolved air flotation using a particle counter." Journal of Water Supply: Research and Technology - Aqua 58(1): 57-63.

Han, M., Y. Park, J. Lee and J. Shim (2002). "Effect of pressure on bubble size in dissolved air flotation." Water Science and Technology: Water Supply 2(5-6): 41-46.

Han, M. Y. (2002). "Modeling of DAF: the effect of particle and bubble characteristics." Journal of Water Supply: Research and Technology - Aqua 51(1): 27-34.

Hecht, K., O. Bey, J. Ettmüller, P. Graefen, R. Friehmelt and M. Nilles (2015). "Effect of Gas Density on Gas Holdup in Bubble Columns." Chemie Ingenieur Technik 87(6): 762-772.

Khuntia, S., K. Majumder Subrata and P. Ghosh (2012). Microbubble-aided water and wastewater purification: a review. 28: 191.

Kim, H. and M. Han (2014). A study on the development of sub-micron bubble generator and characterization of sub-micron bubble. PhD degree, Seoul National University

Kim, T.-i. and M. Han (2010). Analysis of bubble potential energy and its application to disinfection and oil washing. Doctorate, Seoul National University.

Kim, T.-i. and M. Han (2010). Analysis of bubble potential energy and its disinfection application and oil washing. PhD degree, Seoul National University.

Kim, T.-i., Y.-h. Kim and M. Han (2012). "Development of novel oil washing process using bubble potential energy." Marine Pollution Bulletin 64(11): 2325-2332.

Kim, T. I., Y. H. Kim and M. Han (2012). "Development of novel oil washing process using bubble potential energy." Marine Pollution Bulletin 64(11): 2325-2332.

Kobayashi, H., S. Maeda, M. Kashiwa and T. Fujita (2014). Measurement and identification of ultrafine bubbles by resonant mass measurement method.

Krishna, R. and J. M. Van Baten (2001). "Scaling up Bubble Column Reactors with the Aid of CFD." Chemical Engineering Research and Design 79(3): 283-309.

Kukizaki, M. and M. Goto (2006). "Size control of nanobubbles generated from Shirasu-porous-glass (SPG) membranes." Journal of Membrane Science 281(1–2): 386-396.

Kulkarni, A. A. and J. B. Joshi (2005). "Bubble Formation and Bubble Rise Velocity in Gas−Liquid Systems: A Review." Industrial & Engineering Chemistry Research 44(16): 5873-5931.

Levenspiel, O. (1972). Chemical reaction engineering, Wiley.

Li, X., P. Li, L. Zu and C. Yang (2016). "Gas-Liquid Mass Transfer Characteristics with Microbubble Aeration – I. Standard Stirred Tank." Chemical Engineering & Technology 39(5): 945-952.

Linek, V., M. Kordač and T. Moucha (2005). "Mechanism of mass transfer from bubbles in dispersions: Part II: Mass transfer coefficients in stirred gas–liquid reactor and bubble column." Chemical Engineering and Processing: Process Intensification 44(1): 121-130.

Liu, S., S. Oshita, Y. Makino, Q. Wang, Y. Kawagoe and T. Uchida (2016). "Oxidative Capacity of Nanobubbles and Its Effect on Seed Germination." ACS Sustainable Chemistry & Engineering 4(3): 1347-1353.

Ohgaki, K., N. Q. Khanh, Y. Joden, A. Tsuji and T. Nakagawa (2010). "Physicochemical approach to nanobubble solutions." Chemical Engineering Science 65(3): 1296-1300.

Parker, J. L., P. M. Claesson and P. Attard (1994). "Bubbles, cavities, and the long-ranged attraction between hydrophobic surfaces." The Journal of Physical Chemistry 98(34): 8468-8480.

Parkinson, L., R. Sedev, D. Fornasiero and J. Ralston (2008). "The terminal rise velocity of 10–100 μm diameter bubbles in water." Journal of Colloid and Interface Science 322(1): 168-172.

Parmar, R. and S. K. Majumder (2013). "Microbubble generation and microbubble-aided transport process intensification—A state-of-the-art report." Chemical Engineering and Processing: Process Intensification 64: 79-97.

Pérez-Garibay, R., E. Martínez-Ramos and J. Rubio (2012). "Gas dispersion measurements in microbubble flotation systems." Minerals Engineering 26: 34-40.

Prince, M. J. and H. W. Blanch (1990). "Bubble coalescence and break-up in air-sparged bubble columns." AIChE Journal 36(10): 1485-1499.

Ruen-ngam, D., P. Wongsuchoto, A. Limpanuphap, T. Charinpanitkul and P. Pavasant (2008). "Influence of salinity on bubble size distribution and gas-liquid mass transfer in airlift contactors." Chemical Engineering Journal 141(1-3): 222-232.

Shu, L., W. Qunhui, M. Hongzhi, H. Peikun, L. Jun and K. Takashige (2010). "Effect of micro-bubbles on coagulation flotation process of dyeing wastewater." Separation and Purification Technology 71(3): 337-346.

Takahashi, M., K. Chiba and P. Li (2007). "Free-Radical Generation from Collapsing Microbubbles in the Absence of a Dynamic Stimulus." The Journal of Physical Chemistry B 111(6): 1343-1347.

Tasaki, T., T. Wada, K. Fujimoto, S. Kai, K. Ohe, T. Oshima, Y. Baba and M. Kukizaki (2009). "Degradation of methyl orange using short-

wavelength UV irradiation with oxygen microbubbles." Journal of Hazardous Materials 162(2–3): 1103-1110.

Terasaka, K., A. Hirabayashi, T. Nishino, S. Fujioka and D. Kobayashi (2011). "Development of microbubble aerator for waste water treatment using aerobic activated sludge." Chemical Engineering Science 66(14): 3172-3179.

Tsuge, H. (2010). "Fundamentals of microbubbles and nanobubbles." Bulletin of the society of sea water science 64: 4-10.

Ushikubo, F. Y., T. Furukawa, R. Nakagawa, M. Enari, Y. Makino, Y. Kawagoe, T. Shiina and S. Oshita (2010). "Evidence of the existence and the stability of nano-bubbles in water." Colloids and Surfaces A: Physicochemical and Engineering Aspects 361(1–3): 31-37.

W.K, L. and W. W.G (1924). Industrial Engineering Chem. 16.

Walczyk, W. and H. Schönherr (2014). "Characterization of the Interaction between AFM Tips and Surface Nanobubbles." Langmuir 30(24): 7112-7126.

Weiguo, Y., W. Jinfu and J. Yong (2001). "Gas-liquid mass transfer in a slurry bubble column reactor under high temperature and high pressure." Chinese Journal of Chemical Engineering 9(3): 253-257.

Whitman, W. G. (1962). "The two film theory of gas absorption." International Journal of Heat and Mass Transfer 5(5): 429-433.

Wilkinson, P. M. and L. L. v. Dierendonck (1990). "Pressure and gas density effects on bubble break-up and gas hold-up in bubble columns." Chemical Engineering Science 45(8): 2309-2315.

Wongsuchoto, P., T. Charinpanitkul and P. Pavasant (2003). "Bubble size distribution and gas–liquid mass transfer in airlift contactors." Chemical Engineering Journal 92(1–3): 81-90.

Worden, R. M. and M. D. Bredwell (1998). "Mass-Transfer Properties of Microbubbles. 2. Analysis Using a Dynamic Model." Biotechnology Progress 14(1): 39-46.

Wu, C., K. Nesset, J. Masliyah and Z. Xu (2012). "Generation and characterization of submicron size bubbles." Advances in Colloid and Interface Science 179–182: 123-132.

Wu, Z., H. Chen, Y. Dong, H. Mao, J. Sun, S. Chen, V. S. J. Craig and J. Hu (2008). "Cleaning using nanobubbles: Defouling by electrochemical generation of bubbles." Journal of Colloid and Interface Science 328(1): 10-14.

Xiong, Y. and F. Peng (2015). "Optimization of cavitation venturi tube design for pico and nano bubbles generation." International Journal of Mining Science and Technology 25(4): 523-529.

Xu, Q., M. Nakajima, S. Ichikawa, N. Nakamura and T. Shiina (2008). "A comparative study of microbubble generation by mechanical agitation

and sonication." Innovative Food Science & Emerging Technologies 9(4): 489-494.

Ying, K., M. Al-Mashhadani, J. Hanotu, D. Gilmour and W. Zimmerman (2013). "Enhanced Mass Transfer in Microbubble Driven Airlift Bioreactor for Microalgal Culture." Engineering 5(9).

Ying, K., M. K. H. Al-Mashhadani, J. O. Hanotu, D. J. Gilmour and W. B. Zimmerman (2013). "Enhanced Mass Transfer in Microbubble Driven Airlift Bioreactor for Microalgal Culture " Engineering 5: 735-743.

Yoshida, H., H. Masuda, K. Fukui and Y. Tokunaga (2001). "Particle size measurement with an improved sedimentation balance method and microscopic method together with computer simulation of necessary sample size." Advanced Powder Technology 12(1): 79-94.

Yoshida, H., H. Masuda, K. Fukui, Y. Tokunaga, K. Takarada, T. Sakurai and H. Matsumoto (2003). "Particle size measurement of standard reference particle candidates with improved size measurement devices." Advanced Powder Technology 14(1): 17-31.

Chapter 3

Effect of Bubble Size Reduction to Nanobubble on Mass Transfer Improvement for Non-reactive Aeration Process

3.1 Introduction

Mass transfer via bubble dispersion in bulk fluid occurs widely in biological, chemical, and environmental applications. In these processes, gas-liquid mass transfer controls the rates (Bouaifi, Hebrard et al. 2001, Linek, Kordač et al. 2005). In most of these processes, bubble column reactors are widely employed owing to their advantages of simple design and construction as well as low energy requirement (Bartrand, Farouk et al. 2009).

In bubble column, mass transfer performance is usually expressed by the volumetric mass transfer coefficient (k_la) and gas hold-up (ε). These performance indicators are highly affected by different design and operational parameters including bubble size.

Many research studies have been conducted to improve bubble column performance by changing the design and operating parameters inside the bubble column. (Lau, Peng et al. 2004) investigated the effects of column pressure, temperature, and superficial gas and liquid velocities as well as column dimensions on gas-liquid mass transfer. They concluded that these are the major factors affecting the mass transfer in a bubble column. Similarly,

(Dhaouadi, Poncin et al. 2008) emphasized that the effect of pressure on gas solubility is highly important especially for tall columns. The effects of these operating conditions on different gases were examined by (Weiguo, Jinfu et al. 2001) for slurry bubble columns, and the same conclusion was reached. Despite many efforts to address factors affecting gas-liquid mass transfer of bubble columns, reports relating effect of bubble size with mass transfer efficiency have been limited. (Han and Al-Dahhan 2007) investigated the effect of three sparger designs with different hole numbers and sizes on $k_l a$ and ε by indirectly affecting bubble size. (Terasaka, Hirabayashi et al. 2011) also evaluated the efficiencies of three types of microbubble generators based on oxygen transfer rate. Their results showed that the microbubbles generated had an improved oxygen dissolving rate compared to those from typical industrial aerators. Similarly, (Shu, Qunhui et al. 2010) investigated the effect of microbubbles on the coagulation process and showed the possibility of increasing dissolved oxygen in the bulk liquid in comparison to using conventional macrobubbles. They also reported an increased persistence time of microbubbles in the bulk liquid for a relatively longer minutes in comparison to that of the macrobubbles. These studies showed that reduction to micro-sized bubbles increased the interfacial area between the gas and liquid phases. It also increased the persistence time of bubbles in the bulk liquid which intuitively tend to increase contact time for mass transfer.

However, there has been debates on the contribution of nanobubbles' stability to mass transfer improvement. Theoretically, the bubble size reduction to Nano-size is expected to improve gas-liquid mass transfer by increasing the surface area to volume ratio. But, a group of researches (Wu, Nesset et al. 2012) argue that the stability of nanobubbles is a result of the "organic skin" or "contamination" of bubble surfaces which has a resistance effect to mass transfer. Besides such kind of arguments, there is no profound study that shows the effect of bubble size on intensification gas-liquid mass transfer using bubble size reduction, this is also witnessed by (Parmar and Majumder 2013). On top of the fact that there is no study on the effect of ultrafine bubble on mass transfer, all of the studies that have been conducted on mass transfer focused mainly on the influence of operating parameters in the bubble columns.

In this research, the effect of bubble size reduction from the micro to the nano level (ultrafine bubbles), using a hydrodynamic bubble splitter and its impact on the mass transfer improvement was investigated. Ultrafine bubbles were generated externally in a bubble splitter (unlike previous studies) and injected into the bulk fluid in the bubble column. In the bubble splitter, factors that could affect the bubble size reduction are categorized as design and operating parameters. The effects of purposely selected design and operating parameters on mass transfer and gas hold-up inside the bubble

column were studied. Finally, a regression model was developed based on experimental data to predict the effect of operating and design parameters of the bubble generator on"kla".

3.2 Experimental Setup

The gas-liquid mass transfer experiments were conducted in a semi-batch system composed of a Plexiglas column with an internal diameter of 0.152 m, height of 0.7 m, and working volume of 10 L. The experimental setup is shown in Fig. 3.1. For microbubble generation, an air-water mixing variable speed pump with an outlet saturator pipe of 8 mm diameter and length of 2 m was fitted with an interchangeable exit nozzles having diameters of Dn_1 = 2 mm and Dn_2 = 3 mm. For nanobubble generation, a hydrodynamic microbubble splitter with an interchangeable flow path length "l" and flow area was installed between the air-water mixing pump and the bubble column as shown in Fig. 3.1. The flow channel in the splitter is designed to simulate a plug flow (PF) scheme. It is made to have a rough wall to further reduce the size of the milli- and microbubbles created by the mixing pump and saturation pipe. Four different flow areas (with nominal diameters "d" of d_1 = 2 mm, d_2 = 3, d_3 = 4 mm, and d_4 = 6 mm), three bubble flow path lengths (l_1 = 2 m, l_2= 6 m, and l_3= 15 m) and four air-liquid mixture flow rates "Q" (0.6, 0.8, 1 and 1.2 L/min) inside the bubble splitter were used for the experiments to

understand the influence of"l", "d" and “Q”on "kla". Nitrogen (N_2, 99.99%) gas was used to purge air from the system before oxygen (O_2, 99%) is injected to the bulk liquid for the purpose of kla determination using the dynamic system. N_2 and O_2 gases were measured and maintained at a constant flow rate of 200 mL/min for all experiments. The column pressure was maintained at 1 atm. A microscope camera (Camscope) and computer with Image-J software were employed for bubble size characterization.

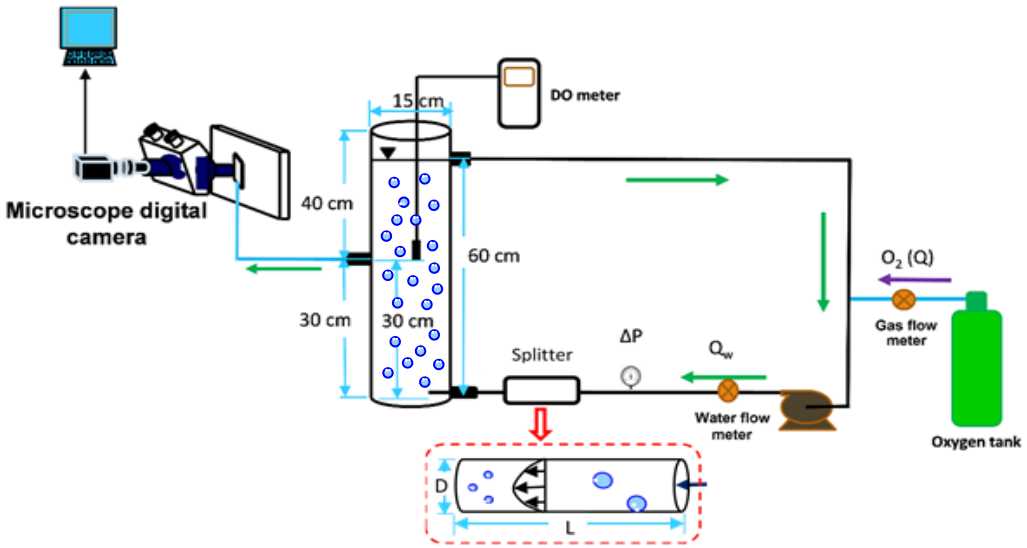

Figure 3.1 Schematic diagram for nanobubble generation system

3.3 Materials and Methods

Tracer test determination

Tracer response test is applied for determination of the flow in the bubble column. Sodium chloride (NaCl) is used for both the pulse input and

step input tests. The NaCl solution is assumed to simulate the flow of the nanobubbled water inside the bubble column. The concentration of NaCl in the solution is measured by the change in conductivity of the solution. A conductivity meter [made: ThermoOrion (U.S.A), model: 550A] was used to measure the conductivity. The conductivity reading is calibrated by a known concentrations of NaCl solution. The dispersion number or the inverse of Peclet number ($P_e^- = \frac{D}{uL}$) is determined from the pulse input test using the concentration versus time data collected at the outlet of the recycled water point of the bubble column by using equation 3.1. The step test was applied to compare the F-Curve response of the system with that of the ideal plug flow and mixed flow systems.

$$\delta_\theta^2 = \frac{\delta^2}{t^2} = 2Pe^- + 8pe^{-2} \qquad 3.1$$

Dissolved oxygen concentration measurement

An optical dissolved oxygen (DO) meter [made: YSI (U.S.A), model: ProODO] with a response time of approximately 25 s was used to measure the DO in the column. To check the accuracy of the instrument in the presence of ultrafine bubbles, a random test for the O_2 ranges between 0–50 mg/L was performed in the presence and after removal of bubbles from the bulk liquid via ultrasonic coalescence. The result showed slight difference in accuracy of approximately ± 10% and ± 15% for ultrafine bubbled water of DO ranges less than 25 mg/l and greater than 25 mg/l respectively. It is assumed that for higher concentrations of ultrafine bubbles, the error of measurement slightly

increased due to too much bubbles attachment on the DO meter tip. To reduce this effect, the attached bubbles are cleaned by gently moving the DO meter back and forth for few millimeters during the measurement period.

Characterization of bubbles

Bubbled water was characterized according to its bubble size and persistence time in the bulk liquid. Bubble size was measured using a microscope photographic system, as shown in Fig. 1. The system consisted of a microscope with a magnification of up to 2400× and a charged coupled device (CCD) camera. A computer installed with I-solution and Image-J software were applied for image capturing and processing respectively. A sample of bubbled water was diverted to a transparent $8 \times 8 \times 65$ mm^3 plexiglas cuboid cell, simulating a one-directional flow to reduce eddy formation in the cell and minimize the effect of coalescence. The impact of pumping on the bubble size was minimized through utilizing very low flow rate of sample transport from the column to the measuring cell by using gravity as a driving force. More than 250 images were taken and analyzed after it is calibrated. A three-step image analysis technique was applied to obtain images of focused bubbles with clear edges Fig S1. The Sauter mean diameter, D_{32} (Shu, Qunhui et al. 2010), was calculated using equation 3.2:

$$D_{32} = \frac{\sum_i^n n_i d_i^3}{\sum_i^n n_i d_i^2} \qquad 3.2$$

where ‘n’ is the total number of focused bubbles used for the calculation of the mean diameter and ‘n_i’ is the number of bubbles with a diameter of ‘d_i’ (μm).

Additionally, the type of bubble generated was characterized by visual inspection and photographic image analysis. Microbubbled water exhibit a milky color due to the light diffraction tendency of microbubbles while nanobubbled water exhibit colorless nature (Tschun-Il and Han 2007, Xu, Nakajima et al. 2008).

Bubble persistence in the bulk liquid is determined indirectly by measuring the desorption rate of oxygen gas using a DO meter after the bubble generation is stopped.

Measurement of volumetric oxygen transfer coefficient

There are different kla determinations techniques. Chemical methods, dynamic method and carbon dioxide adsorption method have been used in previous studies (Garcia-Ochoa and Gomez 2009). The chemical and carbon dioxide methods are relatively time consuming and measure gas concentration based on reactions. Since reactions are affected by different process parameters these methods are prone to higher error. Dynamic method is the most popular and frequently applied technique in kla determination of O_2 gas. This is true because of the convenience and direct measuring capability of

oxygen gas developed through continually advancing technology of oxygen sensors. Considering these advantages dynamic technique was used for this research. In this method, the $k_l a$ was determined from the DO concentration measurements of dynamic unsteady state processes using an optical DO meter. Deaeration and absorption of O_2 gas are the two dynamic unsteady state processes occurring consecutively Fig. 3.2a. At the first stage air in the water is removed or forced out of the bulk liquid by bubbling N_2 gas. In the next stage the bubbled nitrogen gas is replaced by O_2 gas bubbles with a discontinuous switch for the oxygen absorption process to take place (Garcia-Ochoa and Gomez 2009). Taking the small diameter of the column into consideration, perfect mixing was assumed in the radial direction. this assumption was tested by performing a tracer test. For an oxygen absorption experimental data of a kind given by Fig. 3.2b the *kla* was evaluated by curve fitting the right sides of equation 3.3 with the normalized data values in the left side.

$$\ln\left(\frac{C^* - C_L}{C^* - C_0}\right) = k_l a * t_A \qquad 3.3$$

where 't_A' is the aeration time, 'C_L' is the DO concentration at any time 't_A', 'C^*' is the equilibrium DO concentration in the liquid phase, and 'C_0' is the DO concentration at the nitrogen equilibrium point.

According to Darcy-Weisbach relation, since the flow in the splitter is assumed to be plug flow in all the experiments, the changes in design and operating parameters of the splitter highly affect the friction inside the bubble splitter. The heat loss by friction in the splitter channel result in the variation of the water temperature at each experiment. Therefore, during comparison of the effects of each parameter on mass transfer, measured 'kla' for each experiment must be corrected to the same temperature T = 20 °C using equation 3.4(Stenstrom and Gilbert 1981, Al-Ahmady 2006).

$$kla_{20} = \frac{kla_{(T)}}{1.024^{(T-20)}} \qquad 3.4$$

where: 'kla_{20}' is the value of 'kla' at 20 °C, '$kla_{(T)}$' is 'kla' value at test water temperature and 'T' is the test water temperature in °C.

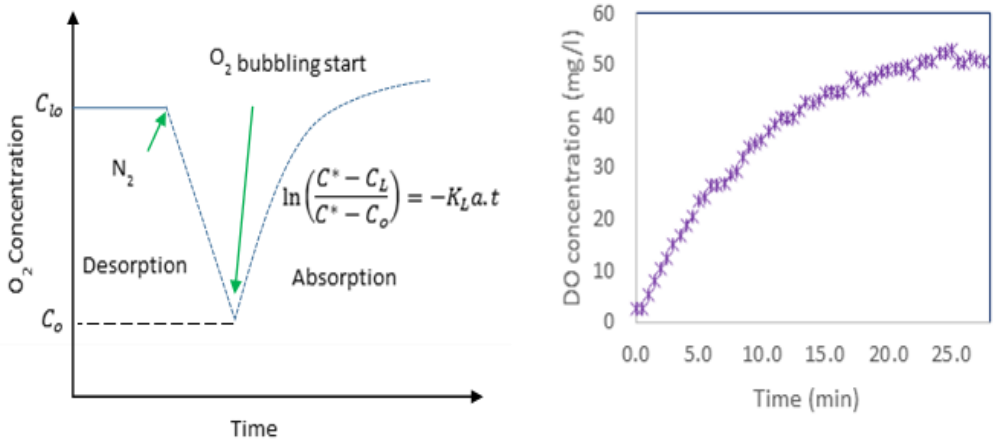

(a) (b)

Figure 3.2. a) Graphical demonstration for the consecutive processes in the dynamic method, b) typical DO concentration Vs time graph during O2 bubbling for Q= 1 L/min, l = 3m and d= 4mm

Measurement of gas hold-up

Gas hold-up is of a given system is highly related with interfacial area '*a*' of the mass transfer. It is measured from the liquid volume difference before and after de-aeration of saturated water by oxygen ultrafine bubbles. De-aeration is achieved by applying ultrasonic coalescence after nanobubble generation. To evaluate the effect of design parameters on ε, a constant gas liquid flow rate of 1.2 l/min was applied. The ε values for each experiment is calculated by equation 3.5.

$$\varepsilon = \frac{\Delta V}{V+\Delta V} \qquad 3.5$$

Where 'ΔV' (mL) is the water volume change between the time of saturation and the completion of ultrasonic coalescence of O_2 nanobubbles and 'V' (mL) is the final volume after ultrasonic coalescence

3.4 Results and discussion

3.4.1. Bubble characterization

Bubble characterization was made by measuring bubble size, image inspection and persistence time.

Bubble size distribution: was determined for five different combination of design parameters l and d at a 1.2 L/min flow rate. Analysis of the splitter design parameters, l and d effect on the trend of bubble size reduction was done. For this purpose, the bubble size generated by the system

before and after the installation of the bubble splitter was measured for the same flow rates. The influence of bubble flow path length on bubble size reduction was tested for two different bubble path lengths, l_1 and l_3. Similarly, the effect of splitter flow area on bubble size was studied by varying the flow diameters between d_1 and d_2. As presented in Fig. 3.3 and Fig. S2, installation of the bubble splitter affected bubble size. An increase in bubble flow path length in the splitter flow channel decreased the bubble size. This result is explained by the mechanism proposed in section 3.4, where the increase in flow length is related with the exposure time of acting forces on the bubbles. The D_{32} of inlet mother microbubbled water having 67 μm diameter in to the nanobubble splitter decreased to 58 μm in the first 2 m of the flow path, and further decreased to 897 nm after 15 m. Moreover, the decrease in the flow area showed the same effect of size reduction (compare Fig. 3.3 and S2). These results have similar result with that observed by (Kim and Han 2014). Considering that the flow rate and effective distance traveled by the bubble were the same, the decrease in bubble size due to the flow area reduction could be related to an increase in flow velocity in the flow channel. This increase in flow velocity contributes to stronger shear and turbulent forces acting on the bubbles in the channel.

Image inspection: Photographic images of the bulk liquid sample from the bubble column were compared at the time of saturation. Milky white

water was observed during microbubble production (Fig. 3.4a). In contrast, clear and transparent bubbled water was observed during the production of nanobubbles (Fig. 3.4b). This is because of the light-diffracting nature of microbubbles (Tschun-Il and Han 2007, Xu, Nakajima et al. 2008). To confirm the presence of ultrafine bubbles in the transparent water sample from the splitter, ultrasonic wave was applied on it to facilitate coalescence of ultrafine bubbles to form bigger bubbles. After the exposure to the ultrasonic wave, milky water was observed. This confirming the formation of microbubbles from the coalescence of already existing nanobubbles due to an increase of collusion forces (Fig. 3.4b).

Bubble persistence time: was measured and compared using an indirect method for both microbubbled and ultrafine bubbled waters. After O_2 saturation is achieved, bubble generation was terminated and the O_2 concentration in the bulk liquid is allowed to come to equilibrium with the atmosphere. The total time this O_2 desorption process took was measured Fig. S3.

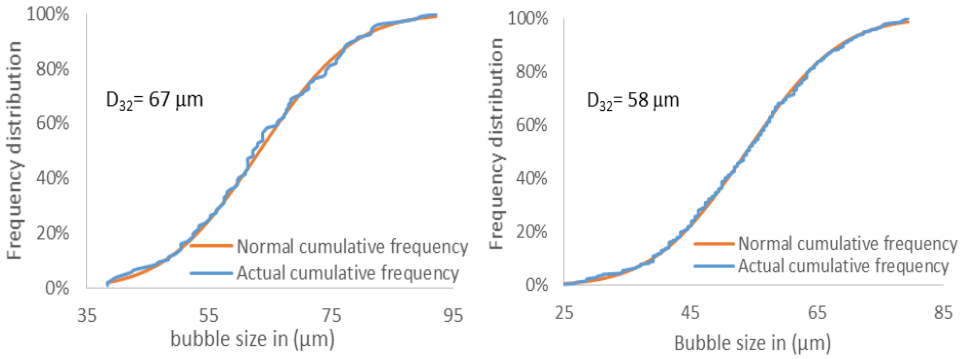

(a)

(b)

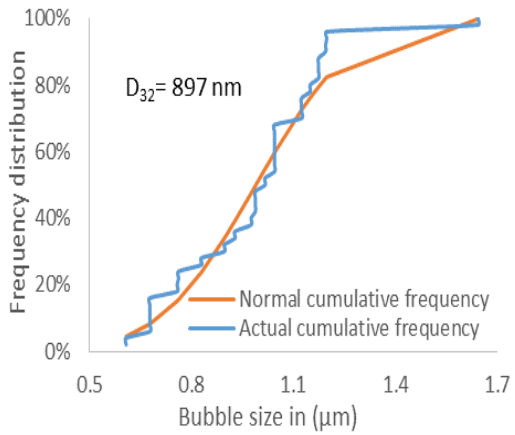

(c)

Figure 3.3 Bubble size distributions for bubbles generated by (a) microbubble generation system with nozzle diameter *Dn2*, (b) splitter with flow diameter d_2 in 2 m effective flow length, and (c) splitter with flow area d_2 in 15 m effective flow length

Desorption volumetric mass transfer rate coefficient $'kla_d'$ for O_2 was determined for comparison. Results showed that the milky water cloud stayed in the bubble column for 2–3 min after generation of microbubbles, which is similar to reports by other researchers (Xu, Nakajima et al. 2008). The desorption volumetric mass transfer coefficient, kla_d, value for microbubbled

water was two times higher than that of nanobubbled water. It indirectly explain that ultrafine bubbles stay for longer periods inside the bulk fluid and minimize the rate of mass transfer from the liquid phase to the gas phase compared to microbubbles (Fig. 3.5). Final equilibrium for desorption of O_2 gas was achieved after 50 h for microbubbled water, whereas it was achieved after 12 d in the case of nanobubbled water Fig. S3.

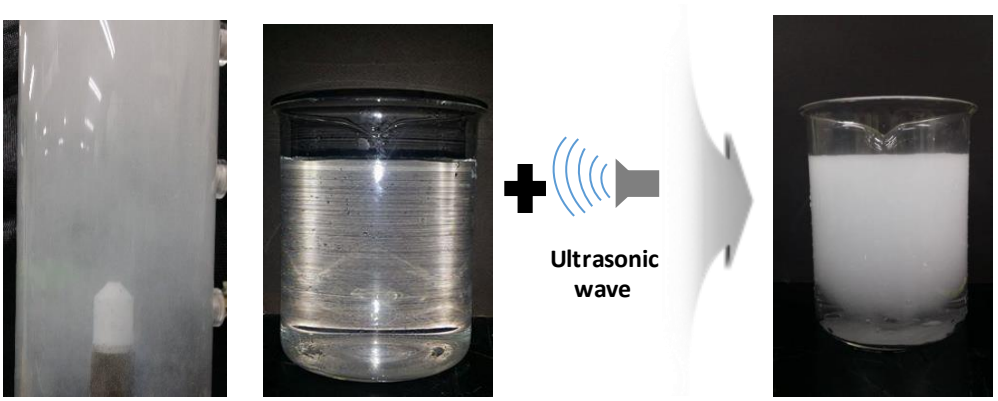

(a) (b)

Figure 3.4 Photographic images of (a) milky water during microbubble generation in the bubble column and (b) ultrafine bubbled water sample before and after ultrasonic wave application for coalescence

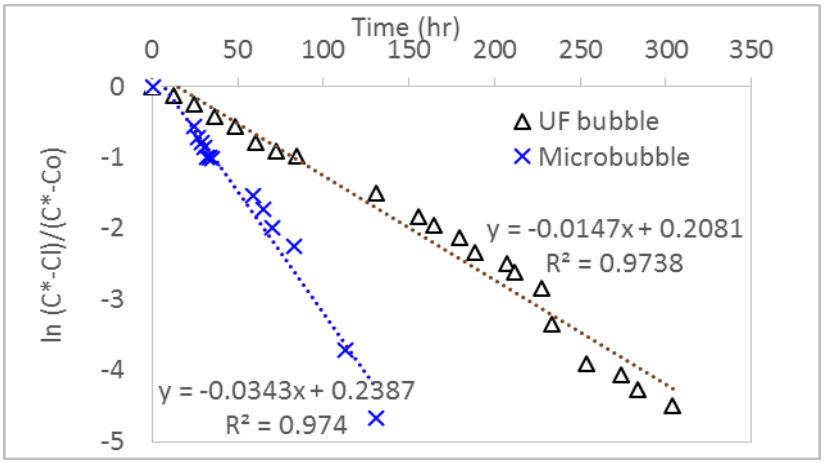

Figure 3.5 Comparison of desorption kla for indirect measurement in persistence times of micro- and nanobubbles in stagnant bulk liquid

3.4.1. Flow type in the bubble column

The flow type in the bubble column is checked by the tracer test method using NaCl as a tracer chemical. Both pulse input and step input tests are performed. For the semi-batch system applied in this research it is assumed that the ultrafine bubbles in the recycled bubbled water disappear the recycling pump before reaching the NB splitter due to coalescence because of high mixing. With this assumption a 50 ml NaCl is used for the pulse input experiment on the lowest flow rate applied in this research (0.6 L/min) to determine the dispersion number or the inverse of Peclet number ($P_e^- = \frac{D}{uL}$). The concentration versus residence time data is collected for the bubble column at the outlet of the recycling port. Using equation 3.1 and iteration technique the dispersion number is found to be 0.17. Compared to already determined charts on (Levenspiel 1972) the value is close

to 0.2 which is largely dispersed system. The normalized pulse tracer response graph is given by Fig S4 a. Similarly a step input test was performed for the lowest flow rate applied in this research (0.6 L/min), and the data is compared with ideal plug flow and ideal mixed flow bubble columns at the same inlet flow conditions. The result show that the system can be more represented by a mixed flow system before almost one ideal hydraulic retention time (HRT) which is equal to 16.7 min Fig S4 b. Considering these results, the DO versus time data for six randomly selected combinations of design and operation parameters, the comparison of *kla* value determined by the whole bubble generation time data and without the first HRT DO data is done. The maximum error found was 5% Fig S4 c. Therefore, in this research determination of *kla* using the overall data is considered acceptable with this tolerable error. Further research is important in this aspect to reassure this assumption.

3.4.2. Comparison of *kla* between different size bubble generation systems

Mass transfer intensification through the production of ultrafine bubbles via hydrodynamic size reduction of microbubbles was evaluated by calculating the *kla* for each bubbling experiment using equation 3.3. The k_la values of water bubbled with the conventional system (milli-sized bubbles), microbubbles, and ultrafine bubbles were compared and the results are presented in Fig.3.6. For the purpose of comparison, conventional bubbling was done by injecting O_2 gas directly into the center of the bubble column using a stone diffuser of 2.5 cm diameter. At a constant gas-liquid flow rate of

1.2 L/min and a given flow diameters Dn_2 and d_2, for microbubble production and nanobubble splitting, bubble splitting to nano size increased the *kla* significantly up to two fold (Fig. 3.6). Moreover, bubble splitting with the smallest flow path length l_1 in the splitter reduced the bubble size from 67µm to 58µm as shown in Fig. 3.3. This reduction in size improved *kla* by 50 % compared to the value of the mother micro bubble produced by Dn_2 nozzle.

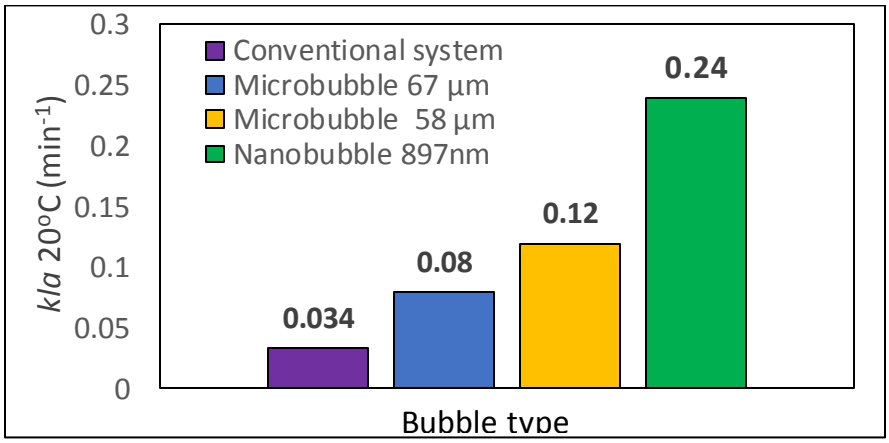

Figure 3.6 Change in *kla* with generated bubble type

3.4.3. Effect of operational and design parameters of bubble splitter on mass transfer

The shear and turbulent forces inside the hydrodynamic splitter are assumed to be responsible for bubble size reduction. In the assumed PF system, these hydrodynamic forces are mainly affected by pressure drop across the flow channel, flow rate, effective flow distance, flow area, flow channel friction and shape factors. For this research, the shape factor is assumed to have minimal effect. The effect of friction factor is kept constant by using

same channel material for all experiments. The effect of pressure can also be addressed by the combined effects of effective flow path length, flow area and flow rate. Therefore, for this research l and d as a design parameters and Q as operating parameter are selected as the main factors assumed to influence kla and ε. Therefore, the influence of these parameters was studied and related to their effect on the hydrodynamic bubble size reduction in the bubble splitter.

Effect of flow rates (Q). In different studies researchers attempted to increase *'kla'* by increasing the superficial gas flow rate of the incoming gas to the column. On the other hand, this increases operating cost during utilization of expensive gases or when off gas treatment leaving the system is regulated. Similar studies reveal that increasing the liquid velocity in the column decreased the *'kla'* (Weiguo, Jinfu et al. 2001, Lau, Peng et al. 2004). In this research, four water flow rates in the splitter, 0.6, 0.8, 1 and 1.2 L/min, were tested for a different combination of effective flow path lengths l_1, l_2, l_3 and effective flow diameters d_1, d_2, d_3 in the bubble splitter. The effect of 'Q' on 'kla' is presented as shown in Fig. 3.7 and S5. In contrast to other studies, results of this experiment showed that increasing water flow rate in the bubble splitter increased the $k_l a$ value in the bubble column for fixed design parameters of the splitter. This is highly related to a reduction in bubble size due to an increase in the shear and turbulent forces as a result of high flow velocity inside the flow channel. The result also depicts that the generation of

nanobubbles through hydrodynamic splitting of microbubbles could highly reduce the amount of consumed gas by increasing the rate of mass transfer. In many operations, this reduces operating and off-gas treatment costs.

Effect of design parameters. In section 3.1, observations on the selected design parameters 'l'and 'd' revealed that an increase in bubble flow path length and/or decrease in flow diameter inside the splitter reduces the bubble size of micro bubbles to nano size. This bubble size reduction is assumed to contribute for the mass transfer improvement in the bubble column. With this assumption, the effect of bubble splitter design parameters l and d, on the $k_l a$ and ε was investigated. For this experiment, the bubble splitting time inside the bubble splitter was controlled by adjusting l while keeping d and Q constant. Four flow rates 0.6, 0.8,1 and 1.2 L/min and three flow area diameters d_1, d_2 and d_3 are used in different combinations. The effect of bubble size reduction on $k_l a$ due to increment of l from l_1 to l_2 and l_3 is presented in Fig. 3.8 or S6. In another test the effect of these design parameters on 'ε' was done for a flow rate of 1.2 L/min and the result is presented in Fig. 3.9.

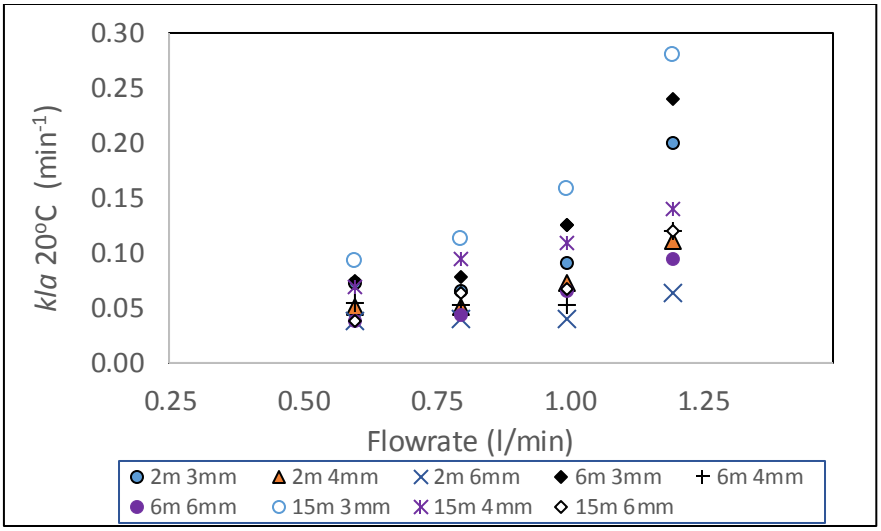

Figure 3.7 Effect of gas-water mixture flow rate of the splitter on kla in the bubble column

For all the experiments done, the k_la showed a direct relationship with an increase in l for the range of flow paths tested. This result can be supported theoretically by the fact that bubble size reduction via increasing l in the splitter caused an increase in *kla*. However, the ε in the bubble column increased up to l_2= 6m in the splitter and then remained constant or decreased slightly as "l" further increased (Fig. 3.9). This result also confirms that, the type of bubbles generated by the splitter tend to totally have nano size with an increase of "l". For the short residence time in the splitter (l < 6m), the majority of bubbles produced are microbubbles. These bubbles have a tendency of floating out or escaping from the bubble column during operation time. Increasing the flow path length "l", increased the amount of nanobubbles which have the tendency of staying more in the bubble column. This

increasing tendency of bubbles staying more time in the bubble column slowly increased the gas volume in the bulk liquid. This slow increase of the gas volume continues until l reaches the level at which all the microbubbles changed to nano size. Because of no escaping tendency of nanobubbles all the incoming gas stays in the bulk liquid in the form of nanobubbles beyond this value of "l". The slight decrease in ε while $k_l a$ continued to increase beyond l_2= 6m (Fig. 3.8 and 3.9) is may be because of the fast volume reduction or diminishing nature of ultrafine bubbles smaller than 10 µm, as explained theoretically via the Laplace-Young equation (Li, Takahashi et al. 2009).

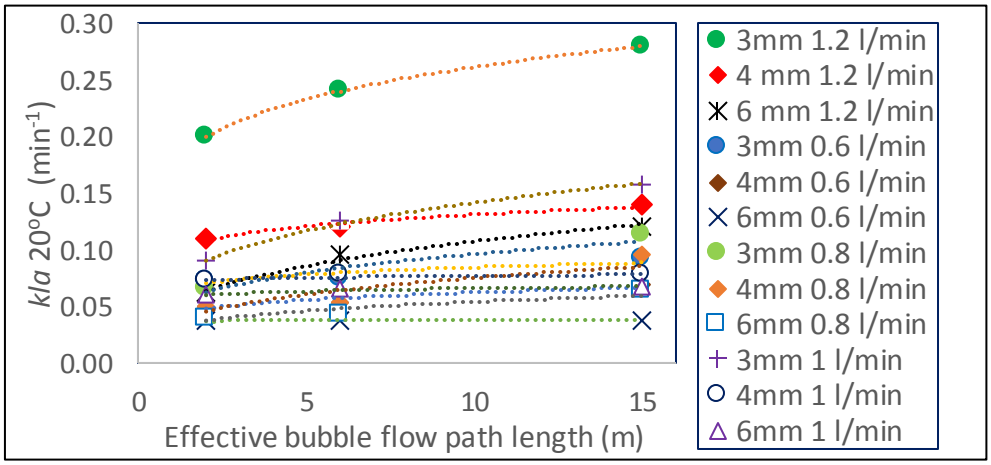

Figure 3.8 Influence of effective bubble flow path of the splitter on kla inside the bubble column

Similarly, since decreasing flow area decreased bubble size for a constant flow rate and effective flow path length, another experiment was performed to study the effect of d inside the splitter on $k_l a$. Three flow diameters d_1, d_2 and

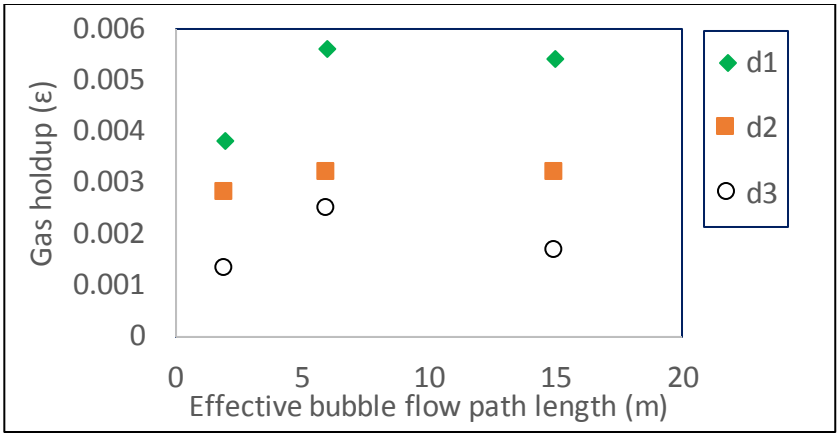

Figure 3.9 Effect of effective bubble flow distance on the splitter on ε in the bubble column

d_3, were used while keeping other design and operating parameters constant. For the range of gas-liquid mixture flow rate of 0.6, 0.8, 1 and 1.2 L/min and a flow path set of l_1, l_2 and l_3, it was found that the splitter flow diameter has an inverse relationship with $k_l a$, as shown in Fig. 3.10 and S7. This could also be because of an increase in velocity resulting from the decrease in flow area which leads to an increase in shear forces causing the reduction in bubble size. Furthermore, the effect of flow area on ε was tested for constant flow rate of 1.2 L/min on the three flow path lengths l_1, $l_2$and l_3 (Fig. 3.11). The result depicted that the reduction in bubble size due to reduction in flow diameter caused an increase in gas holdup for the same flow path distance traveled by the bubble inside the splitter.

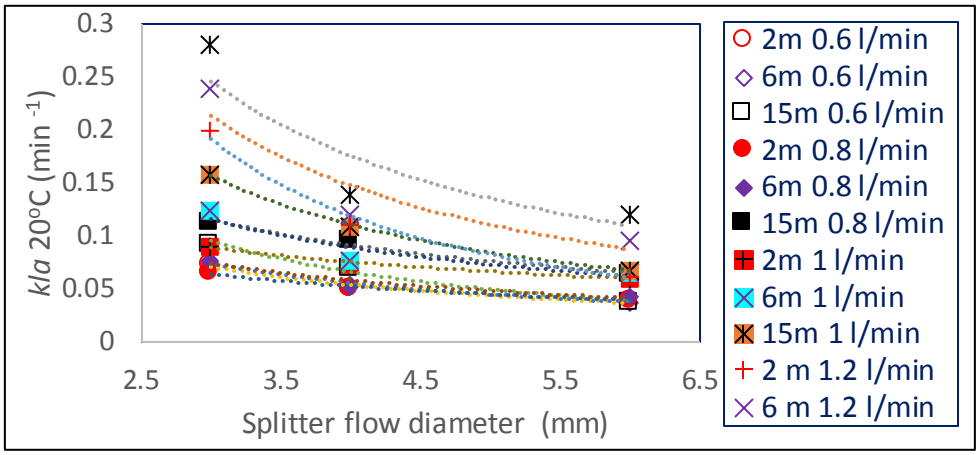

Figure 3.10 Influence of change in splitter flow diameter on kla in the bubble column

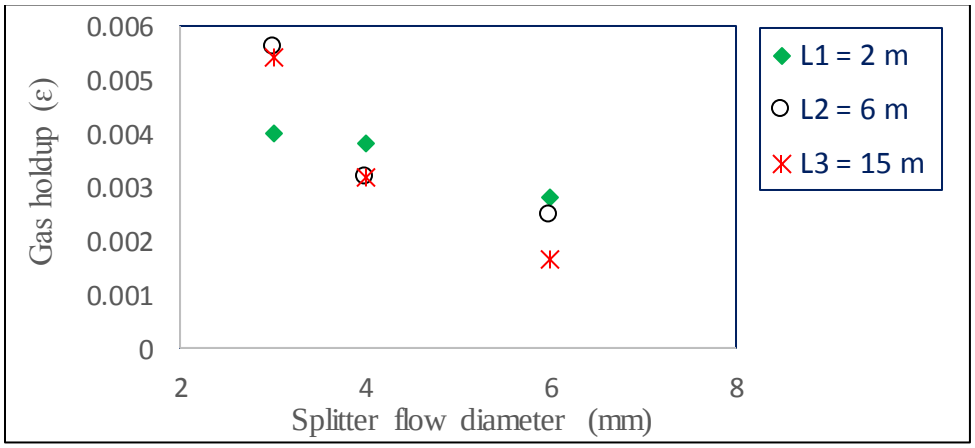

Figure 3.11 Effect of change in splitter flow diameter on ε in the bubble column

3.4.4. Mechanism of bubble size reduction

The mechanism of microbubbles generation in this experiment is via the cavitation effect in both the rotary pump and nozzles. To produce ultrafine bubbles, these microbubbles were further reduced by applying a nanobubble

splitter. Hypothetically, two major mechanisms are assumed to occur in the nanobubble splitter: splitting or shredding of the mili and microbubbles and further compression of the already-shredded bubbles. The shredding dominantly expected to occurs in the first few meters of the PF channel inside the splitter. At this stage milli and micro-sized bubbles produced by the pump and injected into the bubble splitter will fall under the influence of two opposing forces. These two opposing forces are friction forces from the channel wall and pumping forces generated by the pump. These forces hypothetically split the incoming milli and microbubbles to a smaller size until the level at which the size of the majority of the bubbles cannot be reduced further by splitting, which is the end of stage one. Beyond this stage, the second process will start by further increasing the residence time of the bubble in the splitter by extending "l". This further allow the size reduction of already-produced sub-micron and ultrafine bubbles, possibly because of internal pressure development as described by (Li, Takahashi et al. 2009). By this time, the remaining big bubbles or those formed by coalescence will also continue to be reduced in size owing to the presence of hydrodynamic forces. This theoretical hypothesis is deduced from the experimental results performed on bubble size, $k_l a$, and ε in preceding sections.

3.4.5. Model Correlation

In section 3.3 above, the major variables affecting kla are assumed as l, d and Q. To prove this assumption and address to what extent the three variables can express kla, statistical model is developed. The independent experimental results on the influence of these three variables l, d and Q on kla_{20^oC} had a significant correlation Fig. 3.7, 3.8 and 3.10. Therefore, kla is expressed as a function of l, d and Q assuming the influence of other flow affecting variables stated in section 3.3 to be minimal, equation 3.6. The relation between the dependent variable kla with all the independent variables is observed to follow a power law trend Fig S5, S6 and S7. Based on these trend a power law was assumed to relate kla_{20^oC} with l, d and Q as it is expressed in equation 3.7:

$$kla_{20^oC} = f\,(\,l, d, Q) \qquad 3.6$$

$$kla_{20^oC} = p\;\; l^a\, d^b\, Q^c \qquad 3.7$$

Applying multilinear regression analysis (See S7) and analysis of variance (ANOVA) technique, the variables p, a, b and c are determined and the relationship formula is given by equation 3.8:

$$kla_{20^oC} = 2.04\;\; l^{0.14}\, d^{-0.9}\, Q^{1.2} \quad , \quad R^2 = \; 0.8566 \qquad 3.8$$

The extent at which the chosen independent variables could express the change in kla_{20^oC} has been assessed by determining the regression

coefficient. The calculated (R^2 =0.8553) explains that the three independent variables can approximately estimate the value of the kla_{20^oC} up to 86% by equation 3.8. Moreover, the parity plot for the model correlation and experimentally determined value of kla_{20^oC} was plotted for the 36 test data sets (Fig. 3.12). The 36 test data sets had different combination of independent variable values. The average error of the prediction was approximately 15 %. 'F' statistics was used as global test to evaluate the significance of the three variables on the total model. Similarly 't' statistics was used to check statistical significance of each independent variable in the presence of other influencing variables. The result supports that all the three variables are significant in the model.

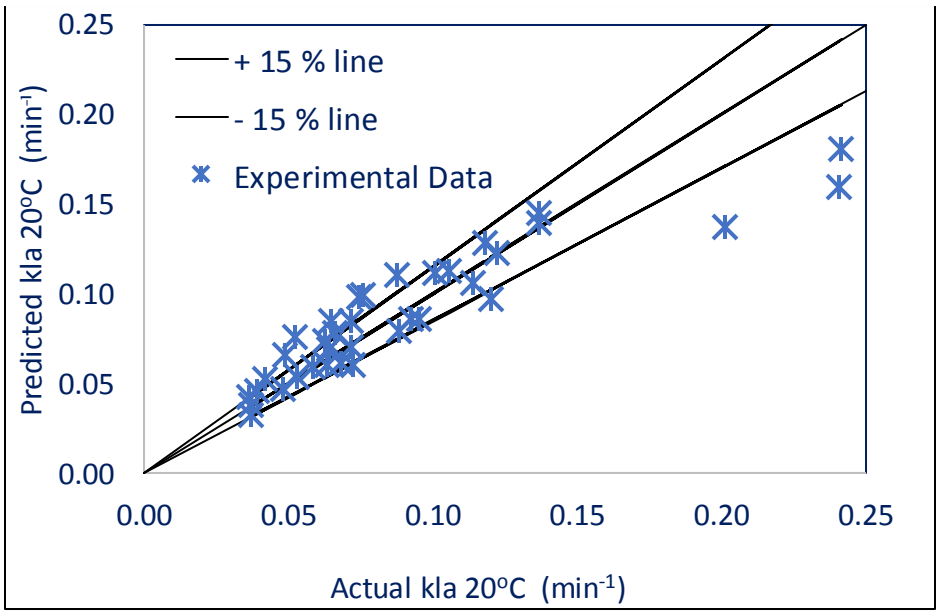

Figure 3.12 Actual versus predicted volumetric mass transfer coefficient *kla*

3.5 Conclusion

Mass transfer intensification via bubble size reduction was tested in this study. A bubble splitter was used to reduce the bubble size at constant oxygen gas flow rates inside the splitter and improve the kla of the bubble column. A dynamic oxygen desorption method was used to determine the k_la of the liquid phase in the bubble column while bubble size was checked using image analysis and indirect visual inspections. It was found that the change in bubble size reduction has dependence on design and operational parameters of the splitter. The increase in bubble flow path length and/or decrease in splitter flow path diameter decreased bubble size and improved kla and ε in the bubble column. In another test, increase in gas-liquid mixture flow rate in the splitter decreased bubble size by increasing shear forces on the bubbles leading to an increase in kla inside the bubble column. These results show that kla is directly proportional to l and Q whereas it is inversely related to d inside the bubble splitter. Multilinear regression model developed in this study shows that the three chosen factors contribute the highest share in bubble size reduction and kla improvement and can be used to predict kla with a limited error. The three outliers are registered for the smallest flow diameter and higher flowrate used for this research. There is a wider jump in kla values as shown in Fig 3.8. This might be caused by an additional effect of turbulence created by increase of velocity at the outlet of the splitter in the column. The

error due to outliers could emerge from these values. Therefore, further researchers could consider more factors for these set of design and operation parameters for better results. Moreover, by this study the major factors that affect bubble size reduction to nano size using the PF splitter are identified. The mechanism of bubble splitting and how to improve mass transfer via bubble size reduction are also explained with experimental evidence.

3.6 References

Al-Ahmady, K. K. (2006). "Analysis of Oxygen Transfer Performance on Sub-surface Aeration Systems." International Journal of Environmental Research and Public Health 3(3): 301-308.

Bartrand, T. A., B. Farouk and C. N. Haas (2009). "Countercurrent gas/liquid flow and mixing: Implications for water disinfection." International Journal of Multiphase Flow 35(2): 171-184.

Bouaifi, M., G. Hebrard, D. Bastoul and M. Roustan (2001). "A comparative study of gas hold-up, bubble size, interfacial area and mass transfer coefficients in stirred gas–liquid reactors and bubble columns." Chemical Engineering and Processing: Process Intensification 40(2): 97-111.

Dhaouadi, H., S. Poncin, J. M. Hornut and N. Midoux (2008). "Gas–liquid mass transfer in bubble column reactor: Analytical solution and experimental confirmation." Chemical Engineering and Processing: Process Intensification 47(4): 548-556.

Garcia-Ochoa, F. and E. Gomez (2009). "Bioreactor scale-up and oxygen transfer rate in microbial processes: An overview." Biotechnology Advances 27(2): 153-176.

Han, L. and M. H. Al-Dahhan (2007). "Gas–liquid mass transfer in a high pressure bubble column reactor with different sparger designs." Chemical Engineering Science 62(1–2): 131-139.

Kim, H. and M. Han (2014). A study on the development of sub-micron bubble generator and characterization of sub-micron bubble. PhD degree, Seoul National University

Lau, R., W. Peng, L. G. Velazquez-Vargas, G. Q. Yang and L. S. Fan (2004). "Gas−Liquid Mass Transfer in High-Pressure Bubble Columns." Industrial & Engineering Chemistry Research 43(5): 1302-1311.

Levenspiel, O. (1972). Chemical reaction engineering, Wiley.

Li, P., M. Takahashi and K. Chiba (2009). "Enhanced free-radical generation by shrinking microbubbles using a copper catalyst." Chemosphere 77(8): 1157-1160.

Linek, V., M. Kordač and T. Moucha (2005). "Mechanism of mass transfer from bubbles in dispersions: Part II: Mass transfer coefficients in stirred gas–liquid reactor and bubble column." Chemical Engineering and Processing: Process Intensification 44(1): 121-130.

Parmar, R. and S. K. Majumder (2013). "Microbubble generation and microbubble-aided transport process intensification—A state-of-the-art report." Chemical Engineering and Processing: Process Intensification 64: 79-97.

Shu, L., W. Qunhui, M. Hongzhi, H. Peikun, L. Jun and K. Takashige (2010). "Effect of micro-bubbles on coagulation flotation process of dyeing wastewater." Separation and Purification Technology 71(3): 337-346.

Stenstrom, M. K. and R. G. Gilbert (1981). "Effects of alpha, beta and theta factor upon the design, specification and operation of aeration systems." Water Research 15(6): 643-654.

Terasaka, K., A. Hirabayashi, T. Nishino, S. Fujioka and D. Kobayashi (2011). "Development of microbubble aerator for waste water treatment using aerobic activated sludge." Chemical Engineering Science 66(14): 3172-3179.

Tschun-Il, K. and M. Han (2007). Analysis of bubble potential energy and its application to disinfection and oil washing. Doctorate degree, Seoul National University.

Weiguo, Y., W. Jinfu and J. Yong (2001). "Gas-liquid mass transfer in a slurry bubble column reactor under high temperature and high pressure." Chinese Journal of Chemical Engineering 9(3): 253-257.

Wu, C., K. Nesset, J. Masliyah and Z. Xu (2012). "Generation and characterization of submicron size bubbles." Advances in Colloid and Interface Science 179–182: 123-132.

Xu, Q., M. Nakajima, S. Ichikawa, N. Nakamura and T. Shiina (2008). "A comparative study of microbubble generation by mechanical agitation and sonication." Innovative Food Science & Emerging Technologies 9(4): 489-494.

Chapter 4

Effect of Ultrafine/ Nanobubble utilization on Ozone based Advanced Oxidation Process in Wastewater Treatment

4.1.Introduction

Ozone (O_3) is a powerful oxidant which reacts with a wide range of organic and inorganic compounds in water system (Ouederni, Mora et al. 1987, Katsoyiannis, Canonica et al. 2011, Khuntia, Majumder et al. 2015). It has been used widely in water and wastewater treatment because of its high reactivity, ease of production using ultraviolet rays or electric charges, self-decomposition to oxygen and most of all its ability to be used in combination with other treatment methods and chemicals for enhanced efficiency (Sano, Yamamoto et al. 2007, Khuntia, Majumder et al. 2015). Investment and operational costs mainly related to energy and off gas treatment were challenges of O_3 based treatment systems. But, it attracted attention because of its enhanced energy efficiency of O_3 generation in the last few decades (Sievers 2011),stringent regulations in water treatment, frequent water shortages and growing public perceptions towards safe water systems attracted the need of ozonation (Loeb, Thompson et al. 2012).

In wastewater treatment, advanced oxidation process (AOPs) are known to have the capacity of converting most organic compounds in to

carbon dioxide, water and mineral acids or salts. This mineralization process is achieved by an elevated amount of radicals generated in the system. AOP can be classified in to three main classes based on the way of radical generation. Generation of radicals by (1) direct (physical) based processes, (2) addition of oxidants, and (3) use of solid catalysts (Sievers 2011). Among AOPs O_3 based system is categorized under the oxidant addition systems and have been showing better efficiency in water treatment. In O_3 based AOP processes the predominant radical species are the hydroxyl radical (˙OH) (Lucas, Peres et al. 2009, Lucas, Peres et al. 2010, Sievers 2011). In this kind of systems the oxidation of any compound could occur via either of the following two mechanisms. The oxidation of compounds via O_3 molecule (direct reaction) or the oxidation through the reaction of the compound with the hydroxyl radicals formed by O_3 (indirect reaction) (Sievers 2011, Khuntia, Majumder et al. 2015). In the direct reaction O_3 acts directly and selectively with specific inorganic or organic pollutants. The indirect oxidation of water pollutants via ˙OH generation is highly reactive and non-selective to almost all kinds of organic pollutants. Since the standard oxidation potential of O_3 (2.07V) is lower than the hydroxyl radical (2.80V), the oxidation reaction with the pollutants is better accelerated by the indirect reactions (Lucas, Peres et al. 2010). This is true especially for those slow reactions with O_3. But because of its non-selective nature the ˙OH oxidation capacity of the system for a specific

pollutant could substantially decrease. This is due to the fast scavenging of ˙OH by different components of the water to be treated. In O_3 based AOP, because of their importance, enhancing both types of reactions mechanisms is necessary to increase the efficiency of the overall oxidation process.

Substantial studies have been done to optimize ozonation and AOPs by influencing water properties, operating conditions and optimizing design parameters.

Water properties: Different studies explained that ozonation and ozone based AOP is affected by water properties like; pH, alkalinity, concentration and type of organic matter as well as temperature (Glaze, Weinberg et al. 1993, Siddiqui and Amy 1993, Kim, von Gunten et al. 2003, Tang, Adu-Sarkodie et al. 2005). The pH of water is very important because the decomposition of O_3 is accelerated by an increase in pH or concentration of OH^- (Tomiyasu, Fukutomi et al. 1985, Sehested, Corfitzen et al. 1991, von Gunten 2003). In conventional bubbling systems generation of ˙OH is not detected in acidic pH (Takahashi, Chiba et al. 2007). Similarly, (Lucas, Peres et al. 2009) studied the degradation of organic substances in winery wastewater, and observed that reduction of chemical oxygen demand under the action of O_3 for acidic pH is negligible and more accelerated in neutral and alkaline pH by the fast ˙OH formation. Similar phenomenon has been observed by (Poznyak, Tapia et al. 2006, Lucas, Peres et al. 2010, Yang, Wang

et al. 2012). To understand the effect of pH on O_3 decomposition reaction, governing reaction mechanisms of O_3 in different pH proposed in previous researches is adopted and presented in table 4.1. In alkaline solution the OH^- ions serve as the initiators of fast chain reaction whereas in the acidic media this is not the case. Temperature is the other influencing operating condition in AOP. Increase in process temperature increases the O_3 depletion rate while it has no effect on ˙OH exposure (Elovitz, von Gunten et al. 2000). In the other hand, an increase in temperature during AOP have a positive influence on bromate formation as a AOP byproduct (Siddiqui and Amy 1993). Therefore, rise in process temperature have a dual effect. It decreases solubility of O_3 at the same time it increases the reaction rate of AOP reactions. Higher alkalinity reduce the efficiency of AOP because of the ˙OH scavenging nature of bicarbonates and carbonate ions. But for the case of organic matters, since different varieties exist in the water to be treated and each organic matter have its own feature towards the O_3 or ˙OH reactions, the effect vary widely.

Table 4.1 Decomposition of O_3 in alkaline and acidic media (Tomiyasu, Fukutomi et al. 1985, Khuntia, Majumder et al. 2015)

Alkaline	Acidic
$O_3 + OH^- \rightarrow HO_2^- + O_2$, $k_2 = 40$	$O_3 \leftrightarrow O + O_2$
$O_3 + HO_2^- \rightarrow {}^{\cdot}O_3^- + HO_2^{\cdot}$, $k_2 = 2.2 * 10^6$	$O + H_2O \rightarrow 2{}^{\cdot}OH$
$HO_2^{\cdot} + OH^- \leftrightarrow {}^{\cdot}O_2^- + H_2O$ $pK = 4.8$	${}^{\cdot}OH + O_3 \rightarrow HO_2^{\cdot} + O_2$ $k_2 = 1.1 * 10^8$
${}^{\cdot}O_2^- + O_3 \rightarrow {}^{\cdot}O_3^- + O_2$, $k_2 = 1.6 * 10^9$	$HO_2^{\cdot} + O_3 \rightarrow {}^{\cdot}OH + 2O_2$ $k_2 < 10^4$
${}^{\cdot}O_3^- + H_2O \rightarrow {}^{\cdot}OH + O_2 + OH^-$, $k_1 = 20 - 30\ s^{-1}$	$HO_2^{\cdot} \leftrightarrow .O_2^- + H^+$ $pK = 4.8$
${}^{\cdot}O_3^- + {}^{\cdot}OH \rightarrow {}^{\cdot}O_2^- + HO_2^{\cdot}$, $k_2 = 6 * 10^9$	${}^{\cdot}O_3^- + H^+ \rightarrow {}^{\cdot}OH + O_2$ $k_2 = 9 * 10^{10}$
${}^{\cdot}O_3^- + {}^{\cdot}OH \rightarrow O_3 + OH^-$, $k_2 = 2.5 * 10^9$	${}^{\cdot}OH + HO_2^{\cdot} \rightarrow H_2O + O_2$ $k_2 = 7 * 10^9$
${}^{\cdot}OH + O_3 \rightarrow HO_2^{\cdot} + O_2$, $k_2 = 3 * 10^9$	

$*$ k values are in $M^{-1}s^{-1}$ unless otherwise specified

Design of contactors: different process and reactor design parameters including the hydrodynamics affect the O_3 based AOP efficiency. Process design of O_3 based AOP combined with different initiators is one method of optimizing the process efficiency. Many AOPs are achieved by hybridization of two or more of the ${}^{\cdot}OH$ generation techniques mentioned earlier. Combining these generation techniques was applied to increase the efficiency of the system by shifting the reaction mechanisms from direct to indirect for different types of pollutants. (Katsoyiannis, Canonica et al. 2011) investigated the efficiency of a conventional ozonation in comparison to O_3/H_2O_2 (hydrogen peroxide) and ultraviolet rays (UV)/H_2O_2 for the treatment of specific organic micropollutants namely atrazine, sulfamethaxazole and N-

nitrosodimethylamine. The use of O_3/H_2O_2 for treatment showed an increased rate of micropollutant transformation with a significant reduction of bromate formation compared to conventional ozone based AOP. On the other hand the UV/H_2O_2 system consumes substantially higher energy despite its efficiency in oxidizing the micropollutants. Similarly, (Acero, Stemmler et al. 2000) also showed that the degradation of atrazine depends on the mechanism of oxidation. They studied the contribution of the two mechanisms to the overall degradation process. The other factor affecting the overall chemical and inactivation reactions is the hydrodynamics in the O_3 contactor. Its optimization mainly depend on modification of design features of gas-liquid contacting schemes. The ultimate purpose of optimizing these features in the O_3 contactors is to improve the utilization efficiency and mass transfer (Siddiqui and Amy 1994, Tang, Adu-Sarkodie et al. 2005). The O_3 utilization and mass transfer efficiency can be improved by increasing the concentration of O_3 in the bulk liquid with the reduction in O_3 concentration in the off gas. Any improvement attempt of both is intuitively expected to influence the AOP and disinfection efficiency by shifting reaction mechanisms and suppressing effect of operating parameters. Different researches have been done to improve the O_3 mass transfer and utilization efficiency. Agitation speed, gas flow, O_3 generator gas pressure and power are identified as predominant factors affecting the O_3 absorption rate in water (Ouederni, Mora et al. 1987).

In another study, (Zhou, Smith et al. 2000) investigated the O_3 mass transfer in water and wastewater and found out that the gas sparger type and the water type as the most important factors while the O_3 dose and gas flow rate are the list to affect the bubble size. But because of the high gas holdup, the specific surface area was highly dependent on the increase in gas flow rate which consequently increased the mass transfer coefficient (Zhou, Smith et al. 2000).There are a limited number of studies done on the application of fine bubble for ozonation. These few researches briefly discuss the effect of bubble size on ozonation and especially on the mechanism of AOP. (Zhang, Xi et al. 2013) reported the bubble diameter reduction in the bubble column as a result of an increase in inlet O_3 concentration due to the faster solubility of O_3. (Chu, Xing et al. 2008) also studied the mass transfer, COD and color removal of textile wastewater in comparison to the conventional bubbles. The COD removal efficiency and de-coloration time was improved for microbubbles. Additionally, since the high pressure inside microbubbles induced the decomposition of O_3 and contributed to hydroxyl radical formation, the COD degradation is also enhanced by indirect oxidation. Similarly, (Chu, Yan et al. 2008) performed a microbubble ozonation test on sludge solubilization and showed an improved COD mineralization and solubility of sludge for the similar reasons. But, considering the contradictive nature of ultrafine bubbles stability and expected high mass transfer, none has been done on the effect of

ultrafine bubbles on O_3 based AOP. Therefore, in this chapter, previously unaddressed influences of bubble size on O_3 based AOP is tested. Influence of bubble size reduction on operating parameters affecting AOP, temperature and pH, and their impact on the mechanism and possibility of oxidation efficiency improvement was investigated by comparing the difference between microbubble and nanobubble generation systems.

4.2. Experimental Setup

The gas-liquid mass transfer experiments for the AOP were conducted in a semi-batch system similar to the one in chapter 3. The Plexiglas column has internal diameter of 0.152 m, height of 0.7 m, and working volume of 10 L with a gas tight lid to force the off gas to pass through the O_3 washing bottle before the off-gas is released to the fume hood. The experimental setup is shown in Fig.4.1. The bubble generation system is fitted with, an air-water mixing variable speed pump with an outlet saturator pipe of 8 mm diameter. A hydrodynamic microbubble splitter with an interchangeable flow path length "*l*" and flow area was installed between the air-water mixing pump and the bubble column as shown in Fig. 4.1. The flow channel in the splitter is designed to simulate a plug flow (PF) scheme. As discussed in chapter 3, it is made to have a rough wall to further reduce the size of the milli- and microbubbles created by the mixing pump and saturation pipe. Because of the

corrosive nature of O_3, oxygen was used as a surrogate gas to measure the bubble size. For a splitter flow area with nominal diameters of d = 3 mm and two bubble flow path lengths l_1 = 2 m and l_2= 15 mm the generated bubble size was 58 µm and 897nm respectively at a flow rate of 1.2 L/min (refer chapter 3). Gas-liquid mixture flow rate of Q= 0.8 L/min inside the bubble splitter was used for the AOP experiments performed. Oxygen (O_2, 99%) is supplied to a laboratory scale O_3 generator at a flow rate of 200 ml/min to generate O_3-O_2 mixture gas. The O_3 gas mixture concentration leaving the ozone generator and entering to the mixing pump is measured to be 49 mg/L.

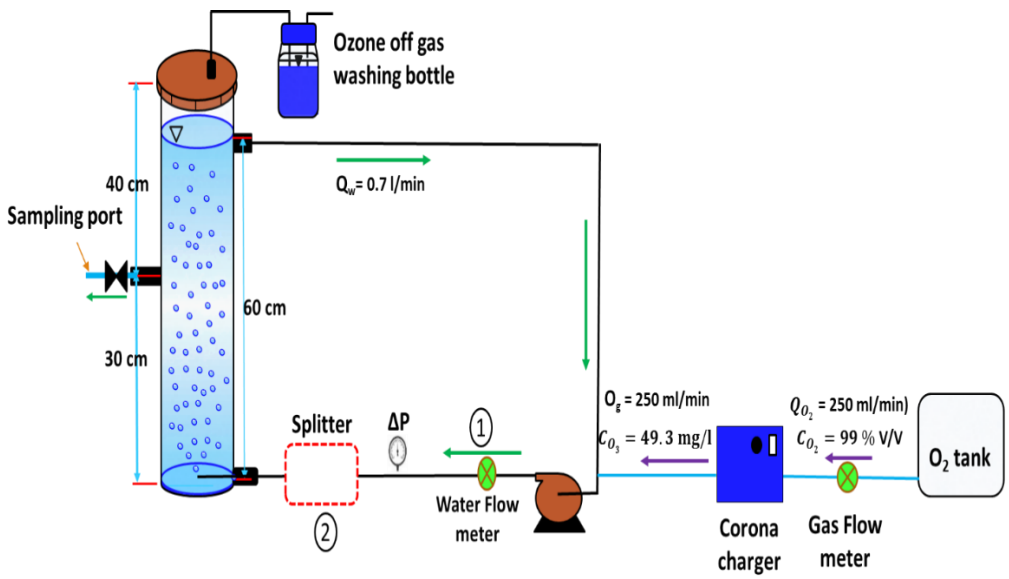

Figure. 4.1 Schematic diagram for nanobubble generation system

4.3.Material and Methods

4.3.1. Materials

Chemicals

Potassium indigotrisulfonate ($C_{16}H_7N_2O_{11}S_3K_3$) and p-Chlorobenzoic acid (*p*CBA, 99%) high purity was purchased from Sigma Aldrich whereas HPLC grade methanol (CH_3OH) from Fisher chemical, Sodium dihydrogen phosphate dehydrate ($NaH_2PO_4.H_2O$) from Junsei Chemicals and Hydrochloric acid (HCl, >35%), Phosphoric acid (H_3PO_4) and Sodium hydroxide (NaOH) pellet are purchased from Daejung chemicals. All the chemicals were used as received from their manufacturers.

4.3.2. Methods

Experimental techniques

In all experiments, deionized (DI) water from [made: Millipore (USA), model: Elix@ Advantage System] was used as a bulk liquid base. The initial pH of the bulk water was adjusted by 0.1M HCl and 0.1MNaOH solutions. The pH was measured by using a pH meter [made: DKK-TOA (Japan), model: HM-31P].

In the aqueous solution, dissolved O_3 concentration can be measured by electrochemical method directly or optically using colorimetric techniques. For this research optical technique was applied according to the standard

indigo colorimetric method (APHA et al. 200). The gaseous O_3 concentration is measured by the modified indigo method developed for gaseous ozone analysis by (Chiou, Mariñas et al. 1995). Potassium indigotrisulfonate is used as an indicator and its color change was measured using UV spectrophotometer [made: Humas (Korea), model: HS 3300] at 600nm. For this purpose, a 20 mL ozonated DI water was drown out from the middle of bubble tank through the sampling port at a given time interval using a gas tight syringe. The syringe was pre-filled with a predetermined amount of Potassium indigotrisulfonate based on the initial pH of the experiment to automatically react with the O_3 in the solution. Then the resulting solution color is measured using spectrophotometry and related to the O_3 concentration.

The concentration of ˙OH was measured by using *p*CBA as a radical probe (Elovitz and von Gunten 1999). The concentration of *p*CBA was determined by HPLC [made: YL instrument (Korea) model: YL9100] using a 55% methanol and 45% 10 mM phosphoric acid as a mobile phase. A 50µL sample was injected in to the C18 column [made: Waters (Ireland), model:SunFire C18, 150 mm length, 4.6 mm internal diameter, 5µm particle size] and *p*CBA was detected at 234 nm wave length. *p*CBA is selected as a ˙OH-probe chemical since it has a very low reactivity with O_3 ($k_{O_3/pCBA} <$ $0.15 M^{-1}S^{-1}$ (David Yao and Haag 1991)) but readily reacts with ˙OH ($k_{.OH/pCBA}$ = 5 x 10^9 $M^{-1}S^{-1}$) as reported by (Elovitz and von Gunten 1999)

quoting (Neta and Dorfman 1968). For this indirect determination of ˙OH concentration, a sample of 20 ml ozonated DI water was drown out of the bubble column through the sampling port using a gas tight syringe. It is then allowed to react with up to 250 µM *p*CBA, pre-filled in the gas tight syringe, depending on the starting pH. The reacted solution is taken to HPLC for the unreacted *p*CBA concentration detection and the ˙OH exposure is determined. The O_3 containing gas from the bubble column is washed by passing the off gas through an indigo solution in a gas washing bottle as shown in Fig. 4.1.

Determination of volumetric O_3 mass transfer coefficient

Dynamic measurement technique is used for determination of the volumetric mass transfer. In this process O_3 bubbles are generated until saturation is reached Fig 4.2, a. When O_3 saturation was reached, bubble generation was interrupted to start recording the O_3 consumption by scavenging processes Fig 4.2, b. A model for the relationship between normalized concentration and testing time is developed from the O_3 gas mass balance in the bulk liquid using equation 2.5. The O_3 gas consumption rate (GCR) is given by equation 4.1 as explained in section 4.4. Then the pseudo first order O_3 consumption constant k_d is found by determining the slope of the curve fit for the data of O_3 concentration versus time graph Fig 4.2,b. Finally the value of k_d determined by this method will be substituted in equation 4.2 and after integrating equation 4.2, $k_l a$ value will be determined

by curve fitting of the normalized O_3 concentration Vs time data graph with the model in equation 4.3.

$$\frac{C_l}{C^*} = \frac{k_L a}{k_L a + k_d} * \left(1 - e^{-(k_L a + k_d)t}\right) \qquad \frac{C_l}{C^*} = e^{-k_d t}$$

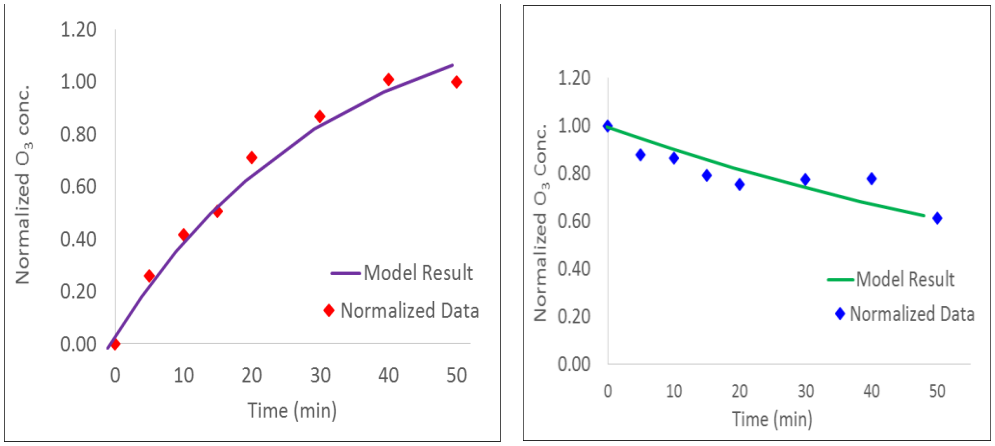

(a) (b)

Figure 4.2 Illustration for the dynamic technique of volumetric mass transfer coefficient determination

4.4. Model development for volumetric mass transfer coefficient determination

The model for volumetric mass transfer coefficient of the O_3 gas in the bubble column is derived from the mass balance equation in the bulk liquid given by equation 2.5.

$$\frac{dC}{dt} = GTR - GCR \qquad 2.5$$

where, GTR is the gas transfer rate to the bulk liquid given by equation 2.4 and GCR is the gas consumption rate in the bulk liquid by any reaction in this case O_3 scavenging.

$$GTR = J * a = k_L a * (C^* - C_L) \qquad 2.4$$

where, GTR is the gas transfer rate in (mg/l min) C^* is the saturation O_3 concentration (mg/l), C_L is O_3 concentration at any time t (mg/l) and $k_L a$ O_3 volumetric mass transfer coefficient in (min^{-1}).

Assuming that the O_3 concentration is much higher than the scavengers (mainlyOH^-) reacting with O_3 in the bulk DI water of the bubble column, the O_3 gas consumption rate (GCR) by the reaction is approximated to follow pseudo first order with respect to the O_3 concentration as:

$$GCR = \frac{dC_{O_3}}{dt} = -k_d * C_L \qquad 4.1$$

where, k_d is pseudo first order O_3 reaction constant (min^{-1}) and C is the concentration of O_3 (mg/l) in the bulk liquid

Then the net rate of mass transfer is given by

$$\frac{dC}{dt} = k_L a * (C^* - C_L) - k_d * C_L \qquad 4.2$$

Solving for equation 4.2 (refer S3)

$$\frac{C_L}{C^*} = \frac{k_L a}{k_L a + k_d}\left(1 - e^{(-k_L a + k_d)t}\right) \qquad 4.3$$

Equation 4.3 is the final model developed for the determination of the volumetric mass transfer coefficient

4.5.Results and discussion

4.5.1 Impact of nanobubbles in affecting the trend of pH on O_3 residual

The effect of pH on O_3 residual concentration is long known and explained by different researchers (Lucas, Peres et al. 2010, Khuntia, Majumder et al. 2015). The fast reduction of O_3 residual with an increase in pH was better explained by its reaction with OH^- ions as a scavenger to start the fast radical reaction presented in table 4.1(Khuntia, Majumder et al. 2015). This pH effect reduce the efficiency of O_3 selective reactions (direct reactions) because of an increase in competitive reactions with scavengers which reduce O_3 concentration in the bulk liquid. The experiment done for this research using either MBs or NBs as an O_3 delivery method show the same effect as previous studies in this aspect. For both bubble type applications, an increase in residual O_3 concentration is observed with a reduction in pH of the DI water Fig 4.3. But the effect of bubble size reduction for a specific pH is compared for the three pH zones used in this research to observe how it influence the effect of pH on O_3 residual concentration Fig 3.

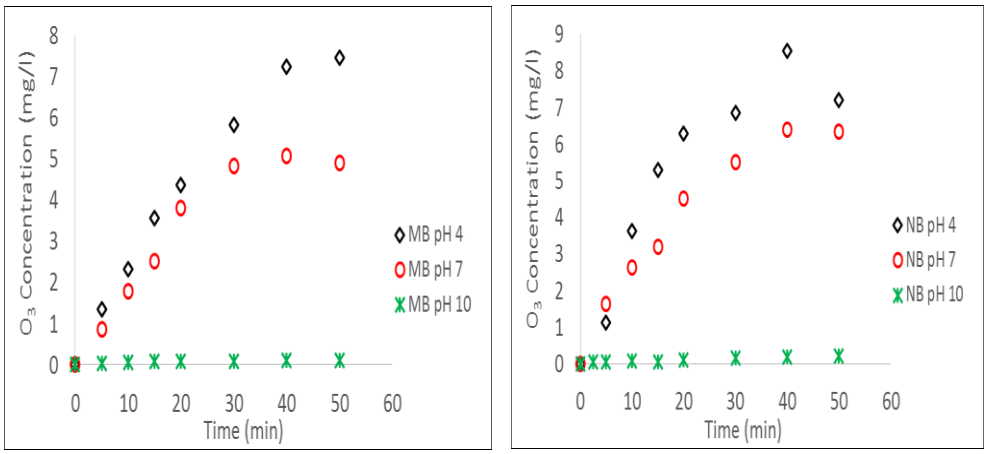

(a) (b)

Figure 4.3 Effect of pH on O_3 residual concentration for two different bubble types (a) result for MBs (b) result for NBs

During the bubble production there was an uncontrolled temperature increment due to friction in the splitter for both MB and NB systems. This temperature increment is higher for NB production and its effect will be discussed in the next session. Despite the negative impact on O_3 solubility of this temperature increment in NB production systems, the residual O_3 concentration for all the pH zones measured show that application of NBs increased the concentration of O_3 residual in the bulk liquid. This result can explain the potential of NBs towards improving mass transfer. For the same volume of O_3 gas supplied, an increase in residence time and surface area to volume ratio of NBs in the bulk liquid compared to MBs is the reason for the increase in O_3 residual concentration in NB application. Therefore, from these observed increment of residual O_3 concentration due to NB application, it can

be assumed that there is a possibility of improving disinfection efficiency by reducing bubble size and also reduce the amount of O_3 off gas by retaining more in the bulk liquid.

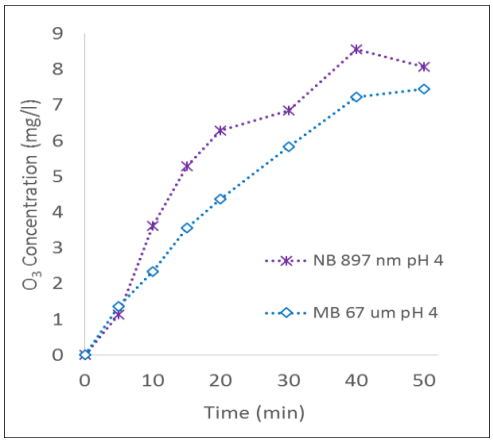

(a)

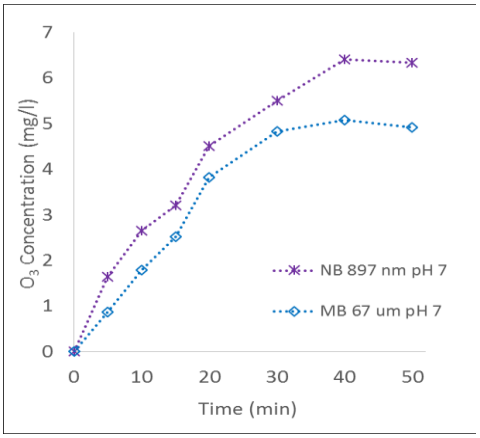

(b)

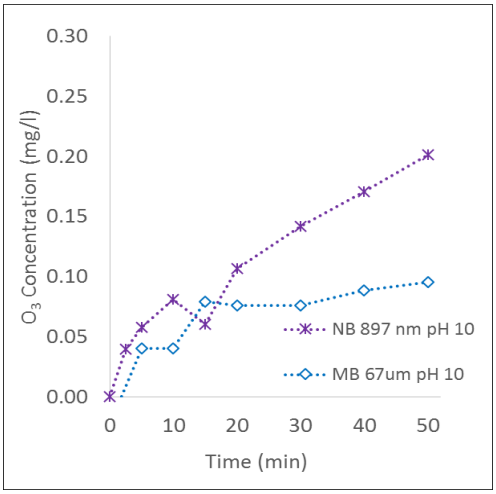

(c)

Figure 4.4 Effect of bubble size on residual O_3 concentration in different pH (a) at pH= 4 (b) at pH=7 and (c) at pH= 10

4.5.2 Impact of nanobubble application on the influence of temperature

It is known that an increase in process temperature reduces the solubility of gaseous O_3 in the bulk liquid. Similar result was observed by the experiments done for this research under the same bubble types Fig 4.5 and S8. For all experiments done, the gas concentration decreases when the process temperature increased from 10 ^oC to 20 ^oC under the same bubble type and process pH. But because of the process water circulation through the bubble splitter, the water temperature increased gradually through whole bubble generation operation time until the process is stopped. A higher temperature increment was observed for NB generation systems compared to the MB system. This temperature increment for MB and NB systems from the initial temperature of 20^oC is shown in Fig 4.6 a. Similarly, the residual O_3 concentration of the two bubble type processes at different pH values under the influence of this change in temperature is presented in Fig. 4.6 (b-d). In spite of the relatively high temperature increase in nanobubbled system compared to the MB one and the high possibility of O_3 by scavenging reactions due to enhanced reaction surface area to volume ration of NBs compared to MBs, the dissolved O_3 concentration showed slightly higher concentration at all pH which shows that bubble size reduction is suppressing the effect of temperature on solubility. Furthermore, a relatively higher temperature

increment in NB is also expected to favor the forward reaction with the scavengers compared to the MB system, which is expected to contribute to the reduction in O_3 concentration. But the result found showed that the amount of O_3 gas transferred by NBs is higher compared to MBs, despite the expected higher consumption of O_3 gas by scavenging reactions for nanobubbled system. From these results it can be concluded that application of NB can suppress the negative influence of temperature on the residual concentration of O_3 gas in the bulk liquid to a given extent and favor a wider operating temperature range for O_3 based treatment plants. This is most probably because of the mass transfer improvement possibility of NBs due to high persistence time and high surface area to volume ratio compared to MBs.

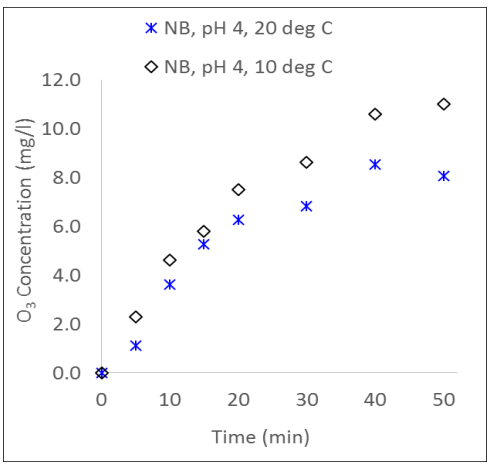

(a)

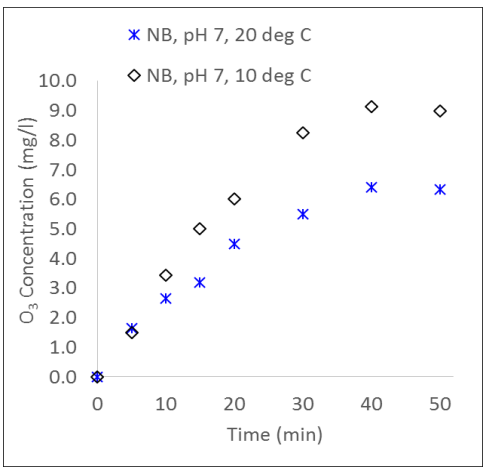

(b)

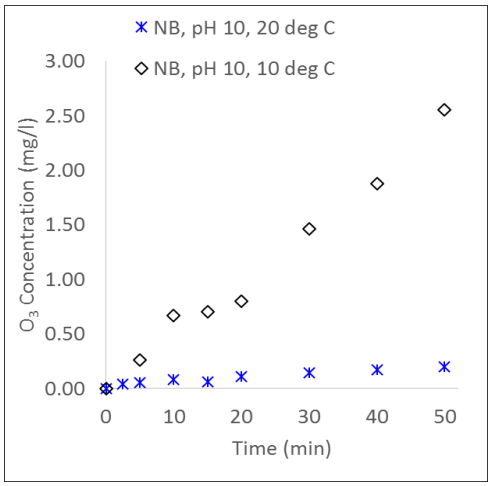

(c)

Figure 4.5 Effect of process initial temperature on O_3 residual concentration for NB under different pH (a) at pH=4, (b) at pH=7 and (c) at pH=10

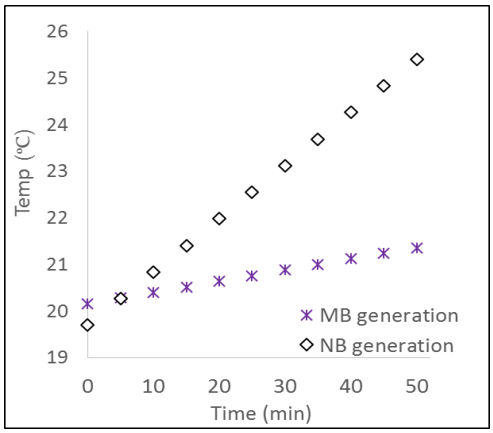

(a)

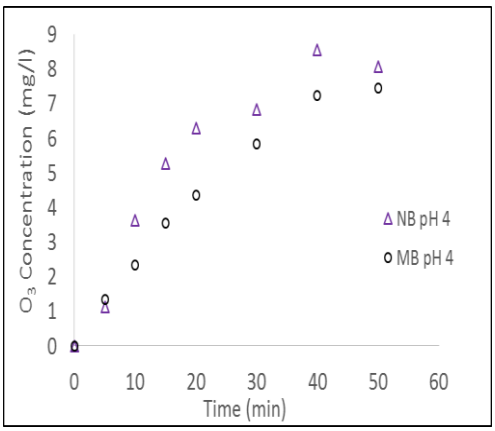

(b)

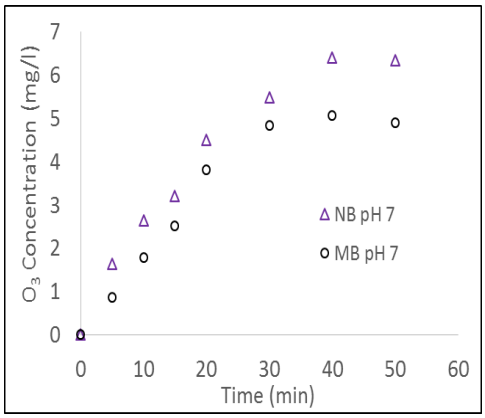

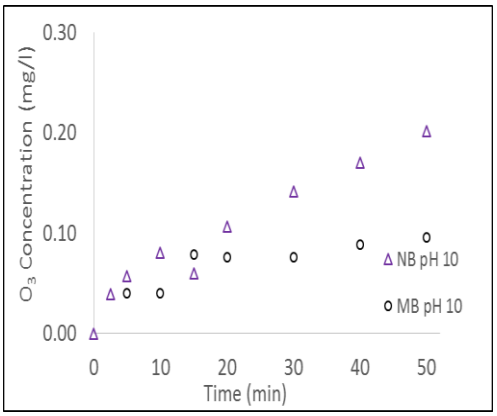

(c) (d)

Figure 4.6 (a) Change in bubble column process temperature for different bubble generation systems (at initial temperature of 20°C) (b-d) effect of bubble size on influence of temperature over O_3 residual concentration at different pH.

4.5.3 Impact of bubble size on the net mass transfer of O_3

The net O_3 mass transfer equation developed earlier (equation 4.3) is used to determine the volumetric mass transfer coefficient ($k_l a$) of both systems at different pH using the dynamic technique. As already discussed in the preceding chapter, $k_l a$ is used as a measuring parameter for mass transfer. The effect of the variation on the surface area to volume ratio "a" from the initial time up to the complete mixing period which is approximately one HRT of the system is considered not to affect the $k_l a$ value significantly for nanobubbled system. The comparison for the result is displayed in Fig 4.7, a . The $k_l a$ showed an increment with an increase in pH for both bubble types. This could be because of the improvement in an enhancement factor (E) due

to the reaction with scavengers. For pH of 4 and 7 the nanobubbled system showed better $k_l a$ may be because the O_3 mass transfer process is the rate limiting process and the reaction with scavengers most probably occur slowly in the bulk liquid. The gap between the $k_l a$ values for micro bubbled and nano bubbled DI water closes down as the pH increases. This could be because of an increase in OH^- concentration which help the initiation of the fast radical reactions. This fast radical reactions occur instantaneously and could cause the shift of reaction zone closer to the gas liquid interphase. As a result the liquid film thickness "δl" (refer chapter 2 Fig 3.) decreases and the film mass transfer resistance "$\frac{1}{k_l}$" gets low to the extent at which the liquid film resistance to mass transfer can no more be the rate determining parameter. Therefore, in higher pH operations where fast radical reactions occur, liquid film mass transfer is no more the rate controlling parameter to the overall process. In the other hand, the value for the O_3 consumption rate constant, k_d, shows an increment with pH as expected due to an increase in OH^-. At pH of 4 and 7, the value of k_d shows an increased value for the NB systems in comparison to the one with MBs under the same pH Fig 4.8. This again confirm that at acidic and neutral pH where the radical reaction initiator OH^- ions are small in concentration, the NB size and its expected longer residence time contributes to the increase in dissolved O_3 concentration which shifts the reaction equilibrium towards O_3 scavenging by OH^- ions. At the basic pH the effect of

bubble size between micro and NB didn't show a difference. This could be because the fast reactions is occurring very close to the gas-liquid interface.

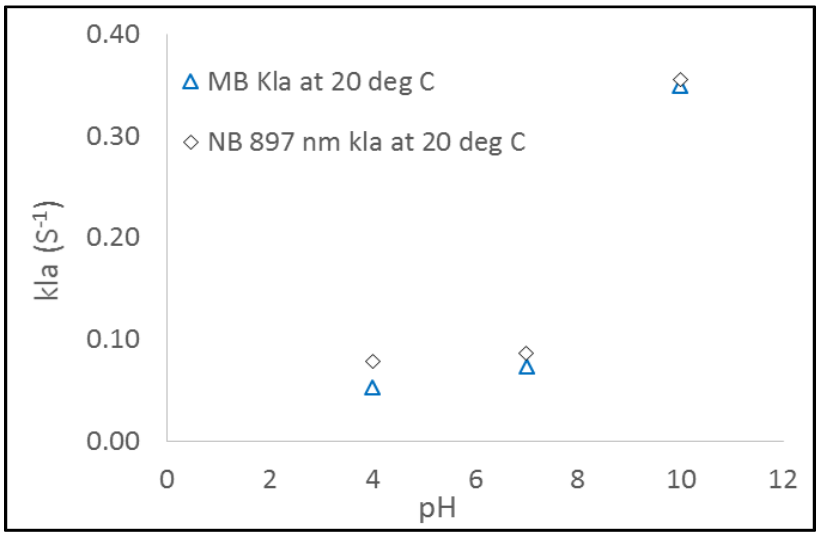

Figure 4.7 Influence of pH and bubble size on k_la of O_3

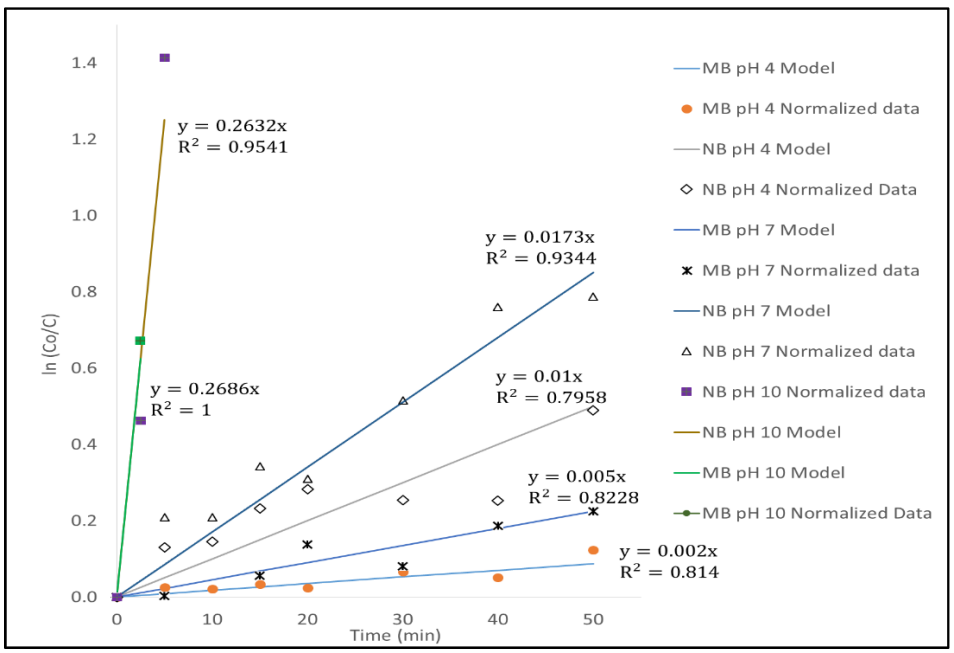

Figure 4.8 Influence of pH and bubble size on k_d of O_3

4.5.4 Impact of bubble size on the formation of ˙OH

The possibility of improving the AOP efficiency for a given O_3 based water treatment unit mainly depend on the increment of the ˙OH exposure. But it is very difficult to directly measure the concentration of ˙OH. Therefore, *p*CBA is used as a probe compound and the degradation reaction is modelled as a second order reaction with ($k_{\cdot OH,pCBA} = 5 \times 10^9\ \mathrm{M^{-1}s^{-1}}$, (Elovitz, von Gunten et al. 2000) and the reaction rate equation is expressed as in equation 4.4. Integrating this equation to determine the ˙OH exposure ([˙OH]*t) which is given by equation 4.5 then figure 4.9 is plotted.

$$-\frac{\mathrm{d}[p\mathrm{CBA}]}{\mathrm{dt}} = k_{\cdot OH,pCBA}[\cdot\mathrm{OH}][p\mathrm{CBA}] \qquad 4.4$$

Integrating equation 4.4 gives:

$$-\ln\left[\frac{\mathrm{pCBA}}{\mathrm{pCBA_0}}\right] = k_{\cdot OH,pCBA}[\cdot\mathrm{OH}]\mathrm{t} \qquad 4.5$$

The result shows that an increase in pH increases the ˙OH exposure for both micro bubbled and nano bubbled systems as it is expected. But the ˙OH exposure is very high for nano bubbled system compared to the micro bubbled systems at the same pH. This result supports the outcomes in section 4.1.1 which suggests that NBs facilitate the forward reactions for the radical chain reactions. It is reported that ˙OH are produced at higher pH conditions for conventional systems using macrobubbles (Tomiyasu, Fukutomi et al. 1985).

In other research (Takahashi, Horibe et al. 2015) reported that O_3 microbubbles tend to collect OH^- at the surface even at lower pH which almost simulates the situation in high pH case. This help the initiation of $^{\bullet}OH$ chain reactions even in the acidic pH for the case of microbubble application. As shown in Fig. 4.9, the result of this research also confirms the generation possibility of $^{\bullet}OH$ in acidic conditions using O_3 microbubbles. The new finding of this research show that further reduction in bubble size to nanobubble tend to improve the concentration of $^{\bullet}OH$ by a minimum of 3.5 fold compared to the microbubbled systems even in the acidic pH. After a longer time of operation the effect of the forward reactions tend to produce other radicals and start to decrease the $^{\bullet}OH$ concentration due to the scavenging of the $^{\bullet}OH$ in forward reactions. In NB system at pH 10, the amount of $^{\bullet}OH$ reached its maximum in between 300-600 s and decreased to zero. This is may be because of the fast initiation of the forward radical chain reactions or fast scavenging of $^{\bullet}OH$ by OH^- ion in forward reactions. In this case the high concentration in OH^- ion and NB application resulted in the fast forward reaction resulting in fast reduction of $^{\bullet}OH$. This phenomena can be supported by the possibility of the reaction zone shift close to gas-liquid interface. Based on this outcome, since an increase in $^{\bullet}OH$ is directly related with an increase in AOP efficiency, it can be concluded that bubble size

reduction to NB can have higher possibility of improving O_3 based AOP systems efficiency.

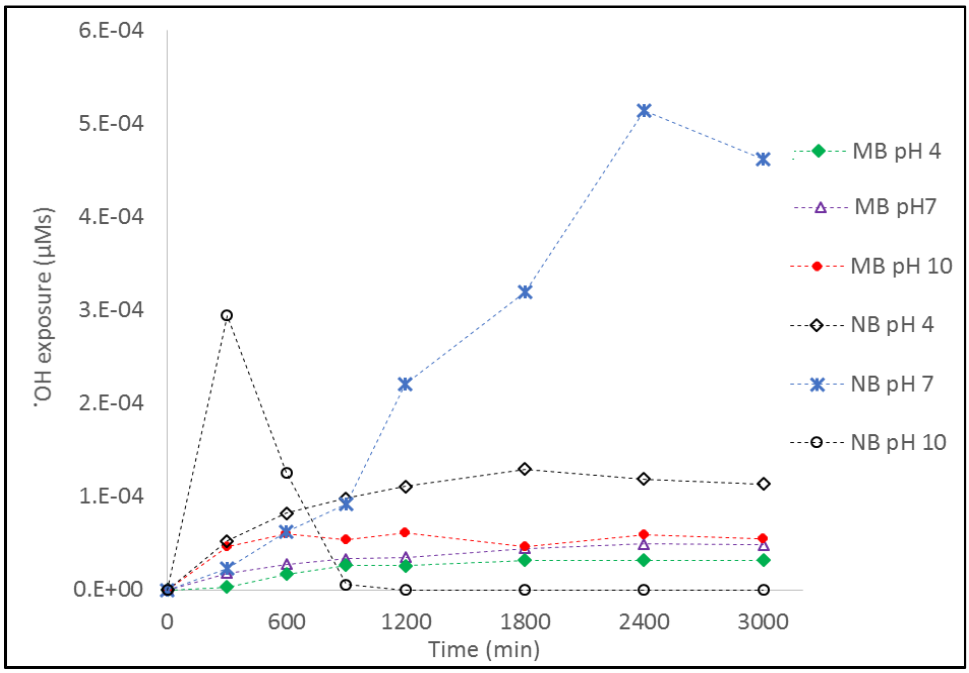

Figure 4.9 ·OH exposure versus time of ozonation process

4.6. Conclusion

In this chapter the influence of bubble size reduction from MB to NB in the application for O_3 based AOP is investigated. The results showed the promising possibility of NB application in O_3 based AOP. It is also observed that, NBs suppressed the negative influence of pH and operating temperature on the efficiency of ozonation. Therefore, application of NBs tend to improve the solubility of O_3 and rate of mass transfer under the influence of relatively wider range of temperature and pH. Moreover, application of NB highly

encourage the ˙OH radical initiation reactions which improve the possibility of O_3 based AOP systems efficiency compared to O_3 micro bubbled AOP systems.

4.7.References

Acero, J. L., K. Stemmler and U. von Gunten (2000). "Degradation Kinetics of Atrazine and Its Degradation Products with Ozone and OH Radicals: A Predictive Tool for Drinking Water Treatment." Environmental Science & Technology 34(4): 591-597.

APHA, AWWA and WEF (2005) Standard methods for the examination of water and wastewater, American Public Health Association, American Water Works Association, Water Environment Federation, Washington, DC.

Chiou, C.-F., B. J. Mariñas and J. Q. Adams (1995). "Modified Indigo Method For Gaseous And Aqueous Ozone Analyses." Ozone: Science & Engineering 17(3): 329-344.

Chu, L.-B., X.-H. Xing, A.-F. Yu, X.-L. Sun and B. Jurcik (2008). "Enhanced treatment of practical textile wastewater by microbubble ozonation." Process Safety and Environmental Protection 86(5): 389-393.

Chu, L.-B., S.-T. Yan, X.-H. Xing, A.-F. Yu, X.-L. Sun and B. Jurcik (2008). "Enhanced sludge solubilization by microbubble ozonation." Chemosphere 72(2): 205-212.

David Yao, C. C. and W. R. Haag (1991). "Rate constants for direct reactions of ozone with several drinking water contaminants." Water Research 25(7): 761-773.

Elovitz, M. S. and U. von Gunten (1999). "Hydroxyl Radical/Ozone Ratios During Ozonation Processes. I. The Rct Concept." Ozone: Science & Engineering 21(3): 239-260.

Elovitz, M. S., U. von Gunten and H.-P. Kaiser (2000). "Hydroxyl Radical/Ozone Ratios During Ozonation Processes. II. The Effect of Temperature, pH, Alkalinity, and DOM Properties." Ozone: Science & Engineering 22(2): 123-150.

Glaze, W., H. Weinberg And J. Cavanagh (1993). "Evaluating the formation of brominated DBPs during ozonation." Journal-American Water Works Association 85(1): 96-103.

Katsoyiannis, I. A., S. Canonica and U. von Gunten (2011). "Efficiency and energy requirements for the transformation of organic micropollutants by ozone, O3/H2O2 and UV/H2O2." Water Research 45(13): 3811-3822.

Khuntia, S., S. K. Majumder and P. Ghosh (2015). "Quantitative prediction of generation of hydroxyl radicals from ozone microbubbles." Chemical Engineering Research and Design 98: 231-239.

Kim, J.-H., U. von Gunten and B. J. Mariñas (2004). "Simultaneous Prediction of Cryptosporidium parvum Oocyst Inactivation and Bromate Formation during Ozonation of Synthetic Waters." Environmental Science & Technology 38(7): 2232-2241.

Loeb, B. L., C. M. Thompson, J. Drago, H. Takahara and S. Baig (2012). "Worldwide Ozone Capacity for Treatment of Drinking Water and Wastewater: A Review." Ozone: Science & Engineering 34(1): 64-77.

Lucas, M. S., J. A. Peres, B. Y. Lan and G. Li Puma (2009). "Ozonation kinetics of winery wastewater in a pilot-scale bubble column reactor." Water Research 43(6): 1523-1532.

Lucas, M. S., J. A. Peres and G. Li Puma (2010). "Treatment of winery wastewater by ozone-based advanced oxidation processes (O3, O3/UV and O3/UV/H2O2) in a pilot-scale bubble column reactor and process economics." Separation and Purification Technology 72(3): 235-241.

Neta, P. and L. M. Dorfman (1968). Pulse Radiolysis Studies. XIII. Rate Constants for the Reaction of Hydroxyl Radicals with Aromatic Compounds in Aqueous Solutions. Radiation Chemistry, American Chemical Society. 81: 222-230.

Ouederni, A., J. C. Mora and R. S. Bes (1987). "Ozone Absorption in Water: Mass Transfer and Solubility." Ozone: Science & Engineering 9(1): 1-12.

Poznyak, T., R. Tapia, J. Vivero and I. Chairez (2006). "Effect of pH to the Decomposition of Aqueous Phenols Mixture by Ozone." Journal of the Mexican Chemical Society 50(1).

Sano, N., T. Yamamoto, D. Yamamoto, S.-I. Kim, A. Eiad-Ua, H. Shinomiya and M. Nakaiwa (2007). "Degradation of aqueous phenol by simultaneous use of ozone with silica-gel and zeolite." Chemical Engineering and Processing: Process Intensification 46(6): 513-519.

Sehested, K., H. Corfitzen, J. Holcman, C. H. Fischer and E. J. Hart (1991). "The primary reaction in the decomposition of ozone in acidic aqueous solutions." Environmental Science & Technology 25(9): 1589-1596.

Siddiqui, M. and G. Amy (1994). "Empirically and Theoretically–Based Models for Predicting Brominated Ozonated By–Products." Ozone: Science & Engineering 16(2): 157-178.

Siddiqui, M. S. and G. L. Amy (1993). "Factors affecting DBP formation during ozone-bromide reactions." Journal of the American Water Works Association: 63-72.

Sievers, M. (2011). 4.13 - Advanced Oxidation Processes A2 - Wilderer, Peter. Treatise on Water Science. Oxford, Elsevier: 377-408.

Takahashi, M., K. Chiba and P. Li (2007). "Formation of Hydroxyl Radicals by Collapsing Ozone Microbubbles under Strongly Acidic

Conditions." The Journal of Physical Chemistry B 111(39): 11443-11446.

Takahashi, M., H. Horibe, K. Matsuura and K. Tatera (2015). "Effect of Microbubbles on Ozonized Water for Photoresist Removal " Journal of Photopolymer Science and Technology 28(2).

Tang, G., K. Adu-Sarkodie, D. Kim, J.-H. Kim, S. Teefy, H. M. Shukairy and B. J. Mariñas (2005). "Modeling Cryptosporidium parvum Oocyst Inactivation and Bromate Formation in a Full-Scale Ozone Contactor." Environmental Science & Technology 23(39): 9343-9350.

Tang, G., K. Adu-Sarkodie, D. Kim, J.-H. Kim, S. Teefy, H. M. Shukairy and B. J. Mariñas (2005). "Modeling Cryptosporidium parvum Oocyst Inactivation and Bromate Formation in a Full-Scale Ozone Contactor." Environmental Science & Technology 39(23): 9343-9350.

Tomiyasu, H., H. Fukutomi and G. Gordon (1985). "Kinetics and mechanism of ozone decomposition in basic aqueous solution." Inorganic Chemistry 24(19): 2962-2966.

von Gunten, U. (2003). "Ozonation of drinking water: Part I. Oxidation kinetics and product formation." Water Research 37(7): 1443-1467.

Yang, D.-m., B. Wang, H.-y. Ren and J.-m. Yuan (2012). "Effects and mechanism of ozonation for degradation of sodium acetate in aqueous solution." Water Science and Engineering 5(2): 155-163.

Zhang, F., J. Xi, J.-J. Huang and H.-Y. Hu (2013). "Effect of inlet ozone concentration on the performance of a micro-bubble ozonation system for inactivation of Bacillus subtilis spores." Separation and Purification Technology 114: 126-133.

ZHOU, H., SMITH, #160 and D. W. (2000). Ozone mass transfer in water and wastewater treatment : Experimental observations using a 2D laser particle dynamics analyzer. Kidlington, Royaume-Uni, Elsevier.

Chapter 5

Effect of Ultrafine/Nanobubble Application on Aerobic Biological Wastewater Treatment

5.1. Introduction

Aerobic digestion is a biological treatment process facilitated by microorganisms under the help of continuous aeration. It is used to reduce total organic matter by the action of microorganisms to the extent of its stabilization. At the stage of stabilization, the waste is assumed to be at its lowest amount of waste mater to support the cell activities of microorganisms. Aerobic digestion processes are widely applied in several industrial or environmental processes (Zupančič and Roš 2008, Garcia-Ochoa and Gomez 2009). It is usually used in wastewater treatment activated sludge processes (Zupančič and Roš 2008), membrane bio reactors (Gander, Jefferson et al. 2000), algal-bacterial symbiosis systems (Tang, Zuo et al. 2016), intensification of yeast production (Hanotu, Kong et al. 2016), minimization of excess sludge before disposal (Abbassi, Dullstein et al. 2000) and many more. Usually the limiting substrate in all this process is Oxygen (Garcia-Ochoa and Gomez 2009).

In wastewater treatment systems the application of aerobic digestion is limited to the treatments of low strength wastewater having chemical oxygen demand (COD) less than 1000 mg/l. Treating wastes with COD more than this value may not be cost effective compared to the anaerobic systems. This is

because of the possibility of less energy requirement of anaerobic systems with a potential of energy and nutrient recovery (Chan, Chong et al. 2009). Moreover, according to the review by (Liu and Tay 2001), the current challenge in activated sludge processes is the high amount of activated sludge needing further treatment that could cost 25-65 % of the total plant operation. In summary, the high cost of aerobic digestion processes mainly emerge from their relative big size and operation costs, especially aeration, mixing and sludge treatment costs. In the contrary its advantage in achieving a complete mineralization or better efficiency of COD removal urged the need of continuous research on different techniques on how to improve its efficiency.

Many researchers studied on utilizing the advantages of aerobic digestion to improve efficiency of water treatment processes. (Chan, Chong et al. 2009) discussed the advantages of utilizing aerobic-anaerobic combined system in the treatment of industrial and municipal waste water. By the comparison the researchers did on different systems they found out that the integrated systems have the advantage of minimal space requirement, low capital cost, and excellent COD removal efficiency. Considering the main limiting factor which is oxygen concentration, (Abbassi, Dullstein et al. 2000) applied pure oxygen and experimented in a laboratory scale on how the effect of increasing the inlet oxygen concentration facilitate the degradation of biological matter for the purpose of sludge minimization. Their result show

that an increase in oxygen concentration improved the sludge minimization efficiency. On another study, (Ago, Nagasawa et al. 2005) tried to improve the aeration system for aerobic fermentation using microbubbles. They reported that cultivation of selective yeasts can be achieved at low flow rates of microbubble aeration. On another study (Kim and Han 2010) shows the tendency of disinfection of different bacteria by the potential energy of bursting microbubbles. Other studies confirm that in the operation of membrane bioreactor (MBR), the cost of aeration and sludge treatment are the basic operational costs to control. In their research, (Yoon, Kim et al. 2004) stated that aeration cost for the wastewater treatment is inversely proportional to sludge treatment cost. Based on the optimization they did, it was found out that the sludge treatment cost is much higher than the aeration cost over a reasonable operational conditions. Therefore, they concluded that sludge minimization must be considered as a key for the economical operation of MBR. Moreover, low solubility of oxygen in broths result in high residence time of organic waste degradation due to low oxygen mass transfer rate in the wastewater, need of intensive mixing due to bigger bubble applications and fast membrane fouling in MBR systems because of excess sludge formation were found to be the gaps in wastewater aerobics digestion systems.

In this chapter, the effect of nanobubble aeration on microorganism growth, sludge minimization and membrane fouling reduction are taken as a

major indicators for the possibility of improving the oxygen mass transfer efficiency on biological wastewater treatment using ultrafine bubbles. A comparison is done with a conventional bubbling system as a representative for current existing aerobic digestion systems.

5.2.Floc matrix model

In general, microorganisms in wastewater treatment plants exist in a group of colony as a suspension of floc. The process of substrate degradation by a floc of microorganisms in a suspended aerobic mixed culture requires availing both the substrate and oxygen into the inner side of the floc to reach enough amount of microorganism colony. Different authors proposed different microorganism floc (matrix) models. (Benintendi 2016) proposed a floc having a single core based on the diffusion of the substrate. In this model the mass transfer of the substrate occurs from the bulk liquid to the inner core of the floc diffusing through the liquid film layer followed by the diffusion in the floc. In the proposed floc model, biodegradation of the substrate or biological reaction of the substrate happens in parallel to diffusion. In this model the transport of oxygen was not taken in to consideration as shown in Fig. 5.1a. In another research, different biomass floc matrix model is used by (Abbassi, Dullstein et al. 2000) (as proposed by (G. 1996)) to represent a situation for high concentration of oxygen in the bulk liquid. It has three zones inside the floc based on the oxygen and substrate concentration as shown in

fig. 5.1b. As explained by (Abbassi, Dullstein et al. 2000) in zone **A** both the substrate and oxygen exist in enough amount. As a result microbial degradation and complete consumption of the diffused substrate will occur in this zone. In zone **B** since the oxygen gas concentration is higher than the amount needed for the biological degradation of the diffused substrate in zone A, the rest continue to diffuse to the internal core of the floc where the oxygen concentration is low. In zone **B** since the floc contains nitrogen compounds and dead cells, these start to be degraded by facilitative microorganisms with the help of enough oxygen presence. The more this area expands because of an increase in oxygen concentration in the bulk liquid, more degradation will occur resulting in reduction of the floc size. This would result in reduction of excess sludge. In zone **C** the microorganisms are dormant and do not participate in degradation process. But because of the presence of facultative bacteria lysis is present and new substrates could be produced. For the case of this research, taking the small DO concentration level in the conventional aerobic digestion systems, the suspension of bacteria floc is represented as a two zone solid system. The model by (Benintendi 2016) is modified to consider both the diffusion of oxygen and substrate concentrations as shown in Fig. 5.1 c. In this case both oxygen and the substrate will diffuse through the liquid film surrounding the floc to reach the microorganisms in zone **A**. In zone **A**, oxygen and substrate will diffuse and at the same time biodegradation

reaction occur until all the diffused oxygen is utilized by the microorganisms for the biodegradation reaction of the substrates. In this case the limiting reactant for the reaction is oxygen. Then in zone **C,** the remaining substrate (if any) and the dead cell due to lysis will increase the concentration of the substrate. This could increase the size of the internal core and excess sludge could be produced.

The hypothesis of this chapter is basically to transform the nature of the floc matrix from the proposed conventional case which is given by Fig 5.1 b to high oxygen concentration case adopted by (Abbassi, Dullstein et al. 2000), Fig 5.1 c, by applying ultrafine bubbles. The ultrafine bubbles as shown in chapter three have a tendency of long residence time in the bulk liquid and have a better rate of mass transfer. These features of NBs increases the DO concentration of the bulk liquid which definitely could increase the distance oxygen can diffuse inside the core of the floc resulting in increase of the oxygen concentration in zone **B** of Fig 5.1 c. As a result we expect an increase in substrate degradation, dead cells and digestion wastes in zone **B** as well as reduction in excess sludge volume.

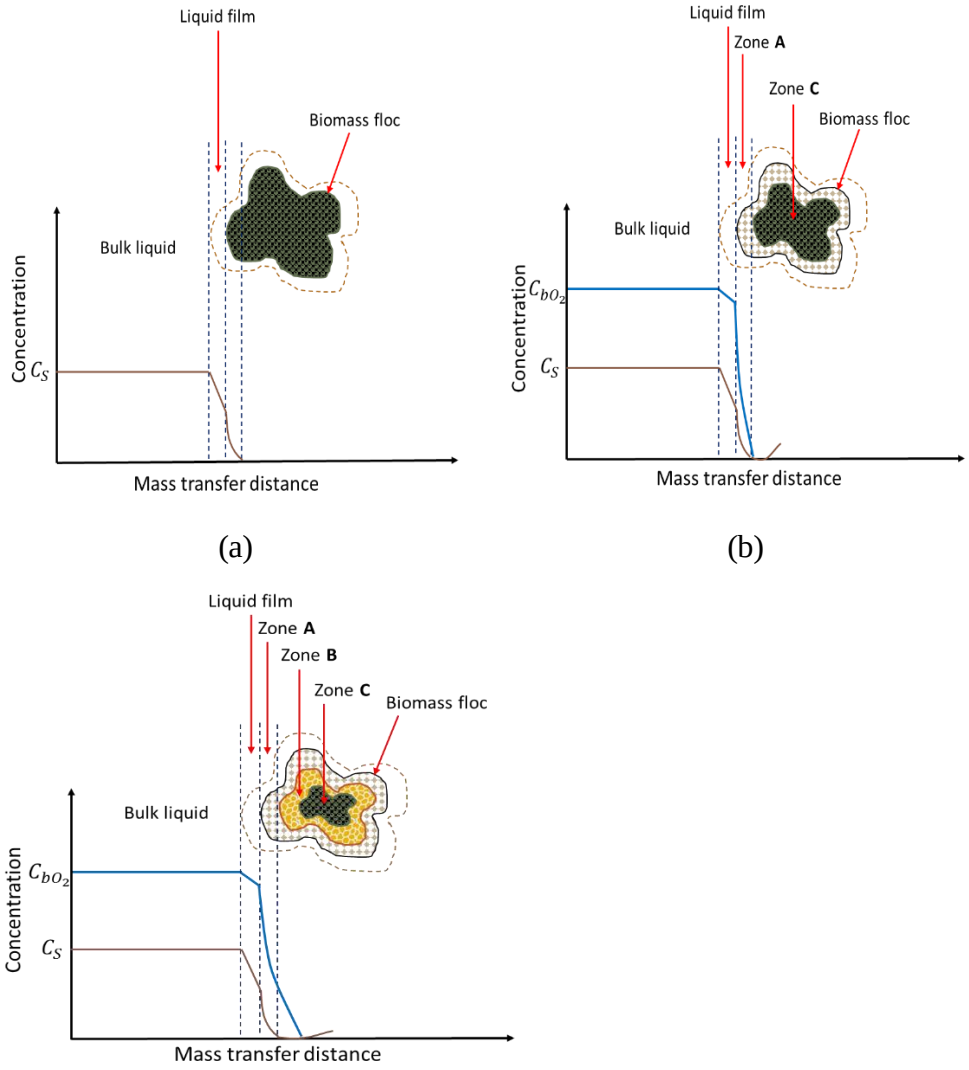

Figure 5.1 Conceptual microorganism floc model for mass transfer a) Only substrate diffusion (Benintendi 2016), b) Both substrate and oxygen diffusion when oxygen is the limiting factor in the biodegradation reaction in the floc and c) substrate and oxygen diffusion at high oxygen concentration (Abbassi, Dullstein et al. 2000) where, $C_{b\,O_2}$ and $C_{b\,S}$ are bulk concentrations of oxygen and substrate.

5.3.Experimental setup

Two separate semi-batch systems having Plexiglas bubble column with a diameter of 10 cm and height of 65 cm are used as an aerobic reactors for the peptone synthetic sewage (see S4) digestion. Each reactor have a working volume of 4 liter. The first reactor has a stone diffuser connected to a continuous supply of air from small air blower. The second reactor is connected to a splitter NB generator which recycle the water from the reactor at a rate of 5.5 ml/s for NB generation. To simulate the shear effect of the splitter on the floc due to recycling, a splitter was allowed to run without bubble generation during conventional bubble generation test. Air flow rate of 150 ml/min was supplied continuously for both systems separately as shown in Fig. 5.2. A side stream Polyvinylidene difluoride (PVDF) made membrane prepared by Hyosung Corporation, Korea, was attached to the reactors for membrane filtration after the bubbling is stopped on the sixth day. The membrane module has a diameter of 1cm and length of 30 cm with seven PVDF membrane fibers. A sample outlet at the middle of the tanks depth was fixed for sampling purpose in each experiment.

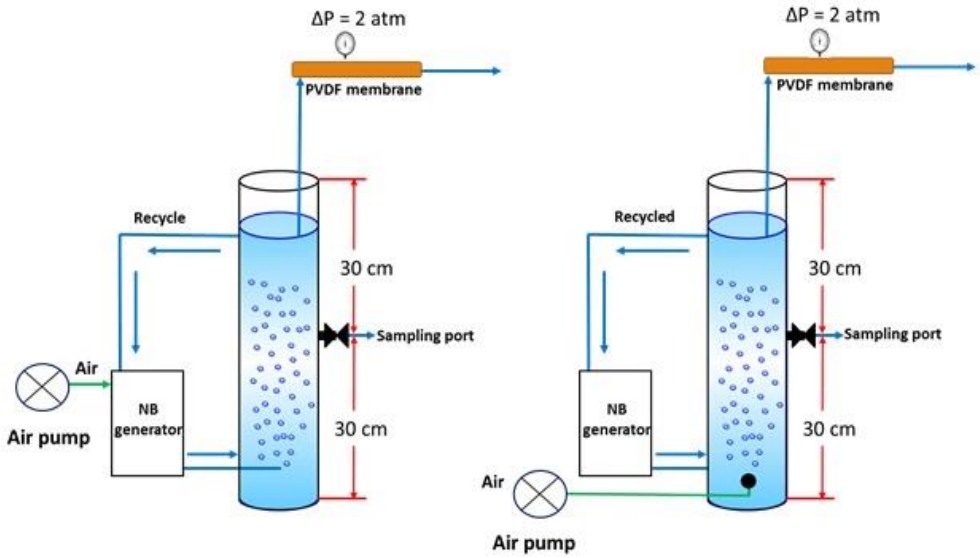

(a) (b)

Figure 5.2 Aerobic waste digestion reactor laboratory setup (a) for nanobubble (b) for conventional bubble application

5.4.Material and Methods

5.4.1. Materials

Chemicals

Peptone from Sigma-aldrich, Beef extract (Bacto™ Beef extract desiccated) from Difco, potassium phosphate monobasic (KH_2PO_4) and magnesium sulfate heptahydrate ($MgSO_4.7H_2O$) from Daejung, Sodium chloride (NaCl), calcium chloride dihydrate ($CaCl_2.2H_2O$) from Samchun Chemicals and Urea from Bioshop and Antifoam emulsion (TS-105A) from Taeyoung Biochem was purchased and used as received from the manufacturer.

5.4.2. Methods

Experimental Procedures

In all experiments, deionized (DI) water from [made: Millipore (USA), model: Elix@ Advantage System] was used for the synthetic water preparation. The Organization for Economic Cooperation and development (OECD) recipe (See S4) for synthetic sewage feed was used to simulate the wastewater. Bio-seed was collected from the MBR unit of the hybrid wastewater treatment plant at building 39 of Seoul national university. A 40 ml fresh bio-seed from a well-mixed batch was inoculated to both columns at the start of the operation. Both operations are run at the same environmental conditions. Both bubble columns were stationed in an incubator [made: Vision Scientific Co. LTD (Korea), model: VS-8480SL] at 20^{o}C. The digesters were allowed to operate for five days. In both cases samples were collected from the tap mounted at the mid-way of the column height. The mixed liquor suspended solid (MLSS) is measured to determine the amount of biological matter in the suspension at a given time. To confirm the trend, optical method was also used by using UV spectrophotometer [made: Humas (Korea), model: HS 3300] at 600nm. Dissolved oxygen was measured by an optical DO meter [made: YSI (U.S.A), model: ProODO] with a response time of approximately 25 s. At the sixth day the bubbling was interrupted and membrane filtration was done at a constant pressure drop of 2 atm to measure the change of

filtration capacity of the membrane due to clogging. The COD was measured by closed reflux colorimetric method using a COD kit [Humas. Co. LTD] and UV spectrophotometer. Field-emission scanning electron microscope [made: ZEISS (Germany), model: Sigma] was used to take images of membrane surface before and after filtration. The extent of surface clogging of these membranes were checked from this pictures for both experiments and comparison is made.

Measurement of volumetric oxygen transfer coefficient

Dynamic measurement technique is followed for determination of the volumetric mass transfer. In this process air bubbles are generated in both systems until saturation is reached Fig 5.3, a. When oxygen saturation in the synthetic wastewater was reached, bubble generation was interrupted to start recording the oxygen consumption rate by the microorganisms Fig 4.2, b. A model for the relationship between oxygen concentration and testing time is developed from the oxygen mass balance in the reactor using equation 2.5. In equation 2.5 the GCR will be substituted by the oxygen utilization rate (OUR) by microorganisms. The oxygen utilization rate (OUR) is given by equation 5.1. Then the OUR constant k_u is found by determining the slope of the curve fit for the data of oxygen concentration Vs time graph as in Fig 4.2,b. Finally the value of k_u determined by this method will be substituted in equation 5.3

below and $k_l a$ value will be determined by curve fitting of the oxygen concentration Vs time data graph with the model in equation 5.3.

$$C = C^* - \frac{k_u C_x}{k_l a} - e^{-k_l a}(C^* - \frac{k_u C_x}{k_l a} - C_o) \qquad (C - C_o) = -k_u C_x t$$

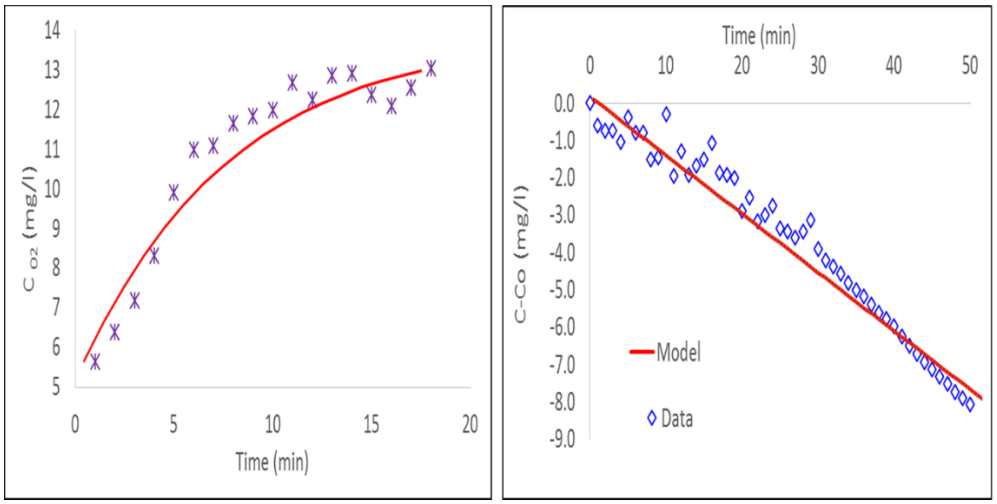

(a) (b)

Figure 5.3 Illustration for the dynamic technique of *kla* determination

5.5. Model development for volumetric mass transfer coefficient determination in aerobic digestion systems

To develop the volumetric mass transfer coefficient of oxygen in the digester the mass balance equation given by equation 2.5 is used.

$$\frac{dC}{dt} = GTR - GCR \qquad 2.5$$

where, GTR is the oxygen gas transfer rate given by equation 2.4 and GCR is substituted by OUR of microorganisms.

Then,

$$\mathrm{GTR} = \frac{\mathrm{dC}}{\mathrm{dt}} = \mathrm{J} * \mathrm{a} = k_L a * (\mathrm{C}^* - \mathrm{C_L}) \qquad 2.4$$

when the bubbling is terminated the oxygen gas in the reactor decreases at a rate equal to the oxygen utilization rate for respiration by the microorganism (Garcia-Ochoa and Gomez 2009). Therefore, at this stage the rate of oxygen mass transfer is given by:

$$\mathrm{GCR} = \frac{\mathrm{dC_{O_2}}}{\mathrm{dt}} = k_u * \mathrm{C_m} \qquad 5.1$$

where k_u is oxygen utilization rate constant (mass of O_2/mass of microorganism) and $\mathrm{C_m}$ is the average microorganism concentration in the reactor at the measurement time (mass of microorganism/volume)

Then the net rate of mass transfer is given by

$$\frac{\mathrm{dC}}{\mathrm{dt}} = k_L a * (\mathrm{C}^* - \mathrm{C_L}) - k_u * \mathrm{C_m} \qquad 5.2$$

Solving for equation 5.2 (Similar steps in S3 are applied for the solution)

$$\mathrm{C} = \mathrm{C}^* - \frac{k_u \mathrm{C_x}}{k_l a} - \mathrm{e}^{-\mathrm{k_l a}}(\mathrm{C}^* - \frac{k_u \mathrm{C_x}}{k_l a} - \mathrm{C_o}) \qquad 5.3$$

Equation 5.3 is the final model developed for the determination of the volumetric mass transfer coefficient.

5.6. Biological kinetic parameters estimation

The most important biological kinetics parameters are the cell yield coefficient, Y (mg VSS/mg COD), and the endogenous decay rate, K_d (1/day). The net yield represents the net biomass produced per substrate removed and the endogenous decay rate represents the rate of biomass loss due to the endogenous respiration. The net yield and the endogenous decay rates can be determined experimentally. Equation 5.4 is applied to determine Y as a slop of the curve fitted from the graph of the rate of change of concentration of MLSS ($\frac{dX}{dt}$) (mg/l. day) versus that of the rate of change of substrate ($\frac{dS}{dt}$) (mg/l. day). Similarly the endogenous decay rate can be demined during the decay time of the biomass from the graph given by the solution of equation 5.5.

$$\frac{dX}{dt} = Y\frac{dS}{dt} - K_d X \qquad 5.4$$

$$\frac{dX}{dt} = -K_d X \qquad 5.5$$

where, "x" is the concentration of mixed liquor volatile suspended solid (MLSS) (mg/L),"t" is time (hrs), "s" is substrate concentration (mg/L) Y is yield coefficient (mg SS/mgCOD) and "K_d" fraction of MLSS or cells oxidized by endogenous respiration per unit time (1/hr).

5.7. Results and discussion

5.7.1 Influence of applying NB for mass transfer in aerobic digester

The volumetric mass transfer coefficient for both bubbling systems was determined by the dynamic method explained earlier. The result show that the value for the volumetric mass transfer coefficient of the system using NB aeration is almost double to that of the conventional bubbling. The oxygen utilization rate for the NB aerated system is also double to that of the system utilizing conventional bubbles as shown in the table 5.1.

Table 5.1 Analysis results of oxygen mass transfer parameters for each system.

Aeration system	OUR (mg O_2/min)	$k_l a$ (min^{-1})
Conventional Bubbling	0.0748	0.07
Nano bubbling	0.159	0.13

The value of $k_l a$ determined from the experiment show that application of smaller bubbles have higher possibility of improving the rate of gas diffusion to the inner side of floc. Similarly, the OUR value suggest that NBs could enhance the growth rate of microorganisms. This growth rate enhancement could lead to high consumption of substrates leading to better efficiency of organic matter degradation. It also can result in fast endogenous decay rate for microorganisms in a semi batch system where substrate

concentration decreases with time. Finally, this endogenous decay rate could result in better excess sludge reduction. To confirm these assumptions made based on the mass transfer analysis data, further experiments on measurement of organic matter degradation, microorganism growth rate and biological kinetic parameter estimation was done.

5.7.2 Organic matter reduction

In the experiments performed the only carbon sources are the organic chemicals used for the preparation of the synthetic sewage. Since there is no inorganic carbon source, COD can be used to determine the organic matter reduction through time. The COD reduction versus hydraulic retention time data given in Fig. 5.4 depicts that almost 72 % of the substrate is digested in the first 48 hours for the NB aeration system whereas, it took 120 hours to achieve almost the same concentration in the system driven by conventional bubbles. One of the assumptions from the mass transfer data, which predicts better biodegradation rate of organic matter for nanobubbled system is proofed to be true. Despite a high efficiency of biological degradation rate, the result also predicts a high possibility of reducing the hydraulic retention time (HRT) of the bio reactors.

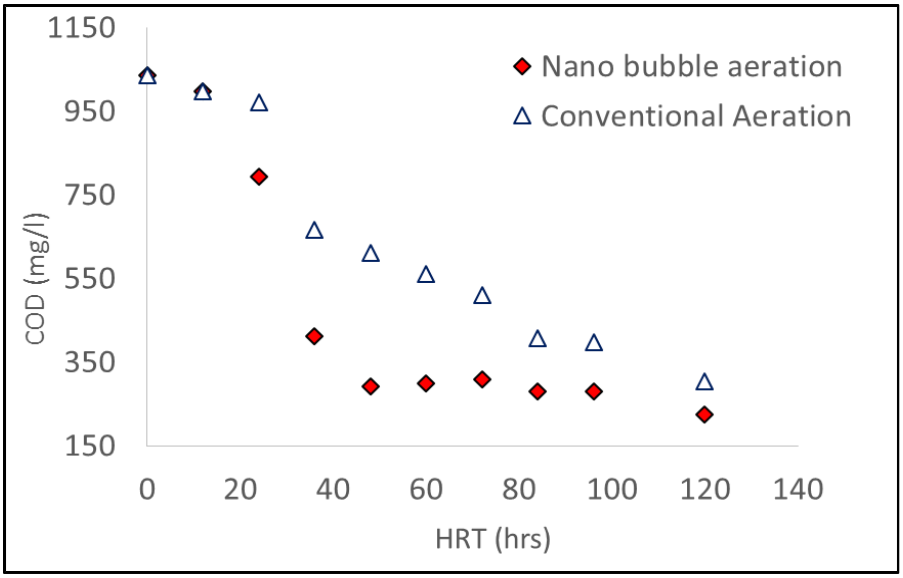

Figure 5.4 Organic matter reduction versus hydraulic retention time data

5.7.3 Biological matter growth rate

The biomass growth curve is developed by measuring the MLSS of the systems at a given time interval. The data is plotted and presented in Fig 5.5 for the fast growth period of both systems. The growth curve show that the NB supplied system reach its higher MLVS value in a short time, which is almost the same time at which the 72 % of the organic matter is degraded, compared to the system with the conventional bubbling. After this time the NB curve shows a fast decline may be because of the fast endogenous decay rate.

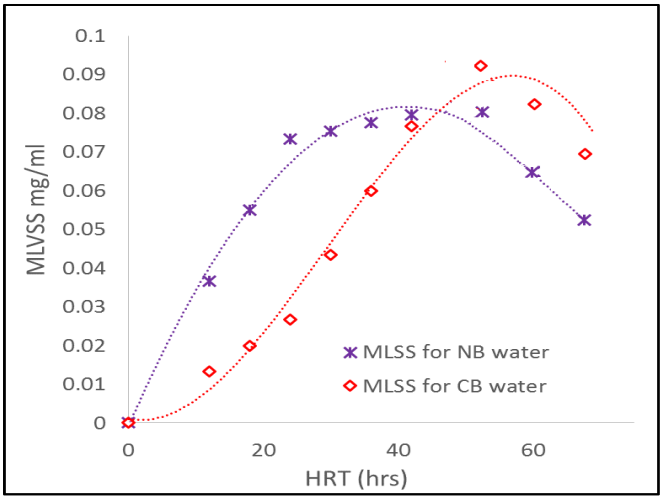

Figure 5.5 Biological matter growth curve

5.7.4 Biological kinetic parameters estimation

The cell yield coefficient, Y, and the endogenous decay rate K_d are determined for both bubbling systems. The NB supported system has shown a better value of Y= 0.12 while the conventional bubbled one showed around half of the value for the nanobubbled system which is Y= 0.06 Fig. 5.6 a. This shows that NB supports the growth yield of microorganisms. Similarly, the decay rate coefficient K_d was also determined and NB was found to facilitate the decay process as predicted earlier from the oxygen mass transfer data Fig 5.6 b. The value of the decay rate for the biomass in the nanobubbled system is almost three times faster than the conventional bubble supported system. This also supports the fact that NBs improve reduction of excess sludge production in aerobic digesters.

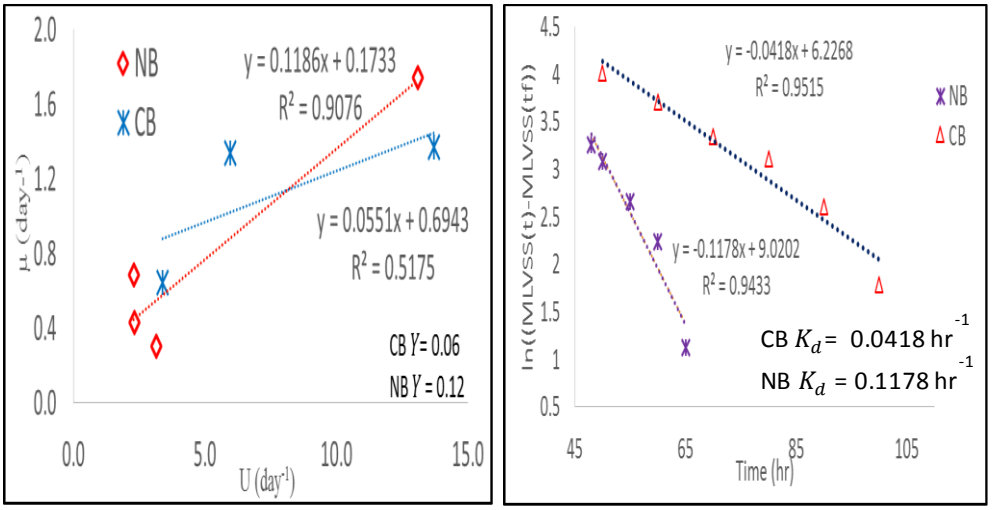

(a) (b)

Figure 5.6 Biological kinetic parameters, (a) Specific substrate utilization rate versus specific biomass growth rate for determination of yield coefficient (b) logarithmic change of biomass weight versus time graph for the determination of K_d

5.7.5 Effect of NB application on membrane filtration operation

It is known that aerobic MBR systems utilize aerobic digestion in conjunction with membrane filtration. Two types of membrane systems configurations, submerged and side stream are usually used in MBR systems. Comparatively, the side stream configuration is cost ineffective with respect to energy requirement and ease of fouling reduction (Gander, Jefferson et al. 2000). To support the outcomes of the previous session's experimental results and confirm the possibility of sludge reduction possibility by NB, simple membrane filtration test and membrane surface image analysis is done.

The membrane filtration was done for both systems at constant pressure of 2 atm. The volume of water filtered was measured with time and plotted as in Fig. 5.7 a. The flow rate at a given interval was calculated discretely and plotted with the average time of the interval taken as in Fig 5.7 b. The membrane filtration flow rate decreases with time for both systems, but it dropped fast for the CB system. The rate of filtration was slightly better for the NB system throughout the whole operation time while the cumulative filtered volume of the NB treated system increased better than that of CB treated one Fig 5.7. This may be is because of NBs action in reducing the sludge concentration which tend to clog the membrane pores very fast. To confirm this, the membrane image was taken before and after filtration for both types of treatment units and the result is displayed as in Fig 5.8. The pictures show that there was a remaining porous area on the NB treated water filter membrane after equal volume of filtration compared to the membrane used to filter the water from the conventional bubbled system. This clearly supports the assumption that NBs could reduce the excess sludge formation.

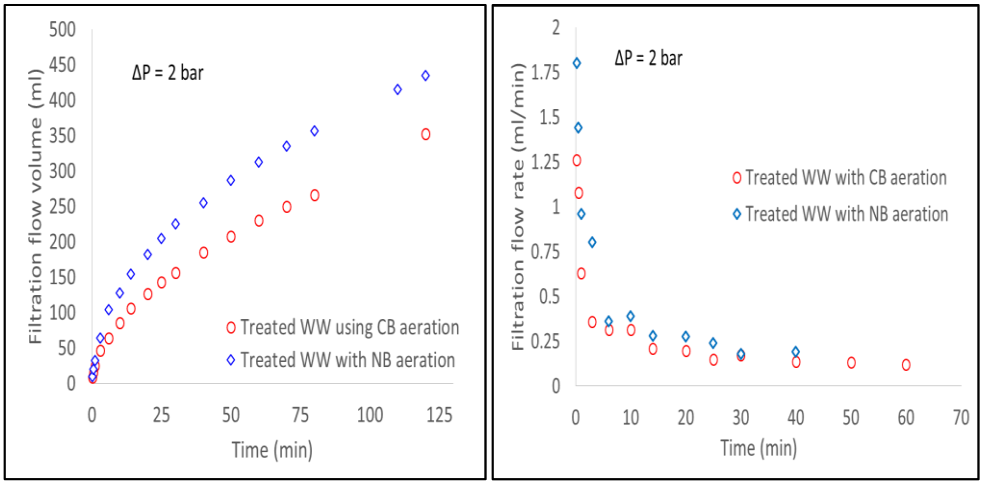

(a) (b)

Figure 5.7 (a) Cumulative filtrate volume from the two systems through filtration time (b) calculated discrete flow rate of filtration from the two systems.

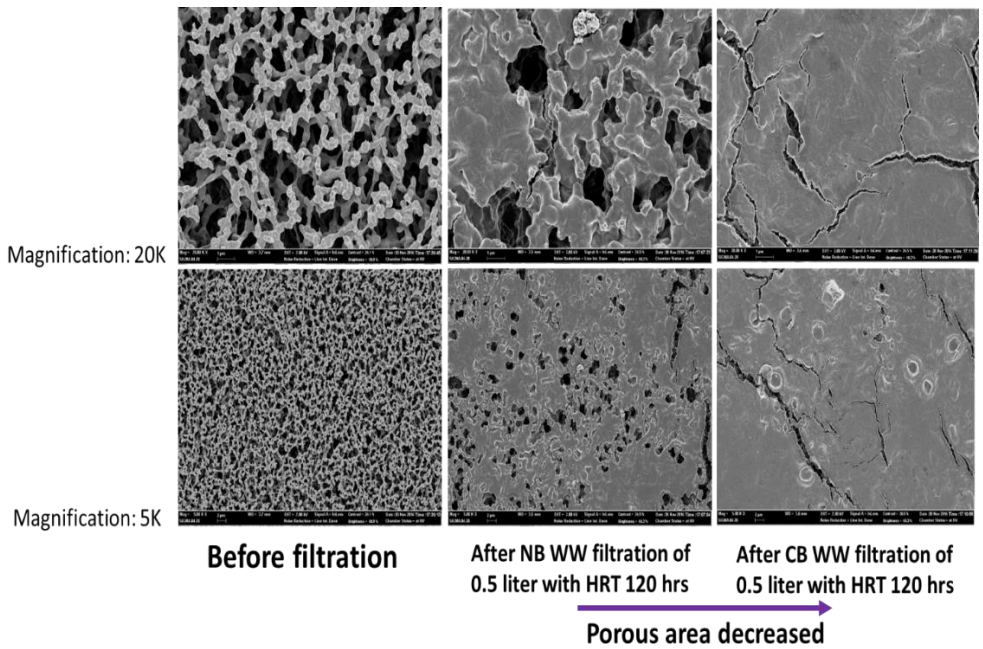

Figure 5.8 SEM image for the surface of membranes before and after filtration in the two systems

Finally, the results found suggest that NBs have a tendency of improving oxygen level in the biomass floc. As a result the mass transfer in the floc increases resulting in an increase of the oxygen sufficient portion of the floc volume. This create suitable environment for more aerobic microorganisms to function on the biodegradation of the substrate as well as dead cells in the floc. By this, more organic waste will be digested with better efficiency. Since most organic matter digestion is achieved, reduction of excess sludge production can also be achieved by applying air NBs without using pure oxygen or with no need of improving oxygen concentration of inlet gas as suggested by other researchers. The difference of oxygen mass transfer between conventional bubble and nanobubbles is summarized by modifying the floc models explained in section 5.2 incorporating the contribution of NBs as follows Fig 5.9.

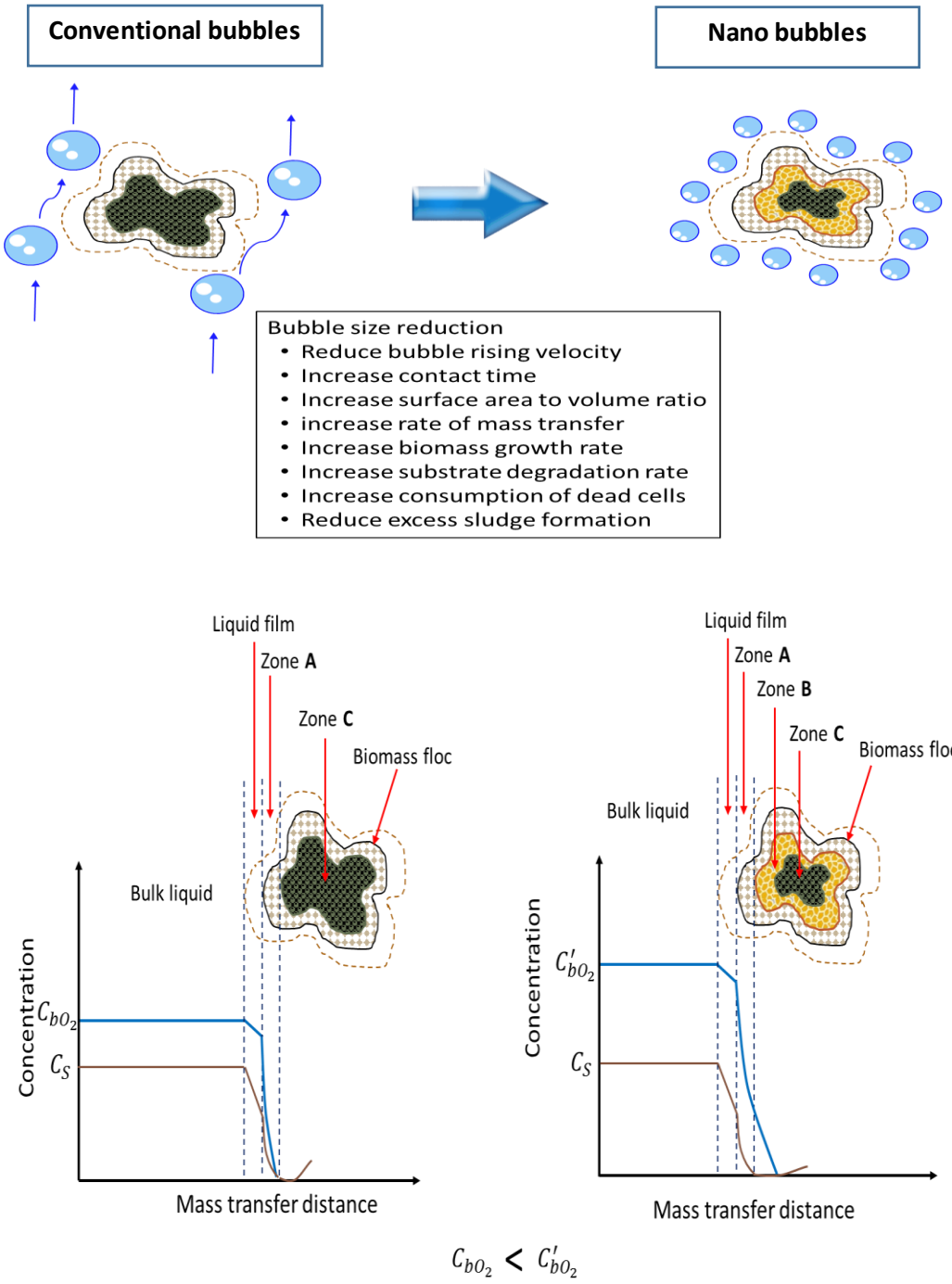

Figure 5.9 Floc model summary of the effect of size reduction to nano scale on aerobic digestion

5.8.Conclusion

In this chapter NB application was tested as an aeration mechanism in a laboratory scale, semi-batch, biological wastewater treatment unit and it is compared with similar scale unit using conventional bubbling technique. The result showed better OUR and $k_l a$ values for the NB supported system, indicating higher oxygen mass transfer rate to the bulk liquid. This is achieved by utilizing the nature of NBs capacity of availing enough residence time and high mass transfer surface area to volume ratio. This increase in dissolved oxygen level, increased the oxygen diffusion rate to the floc and improved biodegradation rate of organic matter on top of reducing the excess sludge formation. Preliminary results also depict the possible reduction of a sludge load and fouling rate for aerobic MBR systems.

5.9.Reference

Abbassi, B., S. Dullstein and N. Räbiger (2000). "Minimization of excess sludge production by increase of oxygen concentration in activated sludge flocs; experimental and theoretical approach." Water Research 34(1): 139-146.

Ago, K.-i., K. Nagasawa, J. Takita, R. Itano, N. Morii, K. Matsuda and K. Takahashi (2005). "Development of an Aerobic Cultivation System by

Using a Microbubble Aeration Technology." Journal of chemical engineering of japan 38(9): 757-762.

Benintendi, R. (2016). "Modelling and experimental investigation of activated sludge VOCs adsorption and degradation." Process Safety and Environmental Protection 101: 108-116.

Chan, Y. J., M. F. Chong, C. L. Law and D. G. Hassell (2009). "A review on anaerobic–aerobic treatment of industrial and municipal wastewater." Chemical Engineering Journal 155(1–2): 1-18.

G., Ö. (1996). Stickstoffelimination durch immobilisierte Biomasse und entkoppelte Substratversorgung bei hochbelasteten Abwässern (Elimination of nitrogen by immobilized biomass and decoupled substrate supply on highly charged waste waters). Ph.D., University of Bremen.

Gander, M., B. Jefferson and S. Judd (2000). "Aerobic MBRs for domestic wastewater treatment: a review with cost considerations." Separation and Purification Technology 18(2): 119-130.

Garcia-Ochoa, F. and E. Gomez (2009). "Bioreactor scale-up and oxygen transfer rate in microbial processes: An overview." Biotechnology Advances 27(2): 153-176.

Hanotu, J., D. Kong and W. B. Zimmerman (2016). "Intensification of yeast production with microbubbles." Food and Bioproducts Processing 100, Part A: 424-431.

Kim, T.-i. and M. Han (2010). Analysis of bubble potential energy and its application to disinfection and oil washing. Doctorate, Seoul National University.

Liu, Y. and J.-H. Tay (2001). "Strategy for minimization of excess sludge production from the activated sludge process." Biotechnology Advances 19(2): 97-107.

Tang, C.-C., W. Zuo, Y. Tian, N. Sun, Z.-W. Wang and J. Zhang (2016). "Effect of aeration rate on performance and stability of algal-bacterial symbiosis system to treat domestic wastewater in sequencing batch reactors." Bioresource Technology 222: 156-164.

Yoon, S.-H., H.-S. Kim and I.-T. Yeom (2004). "The optimum operational condition of membrane bioreactor (MBR): cost estimation of aeration and sludge treatment." Water Research 38(1): 37-46.

Zupančič, G. D. and M. Roš (2008). "Aerobic and two-stage anaerobic–aerobic sludge digestion with pure oxygen and air aeration." Bioresource Technology 99(1): 100-109.

Chapter 6

Conclusion and Recommendation

6.1. Conclusion

This research mainly focus on the investigation of gas-liquid mass transfer improvement for water and wastewater treatment technologies by applying ultrafine/NBs as a gas supplying method. To achieve this, potential water and wastewater treatment processes applying bubble technology were selected. The processes chosen are pure aeration, O_3 based AOP and MBR.

The literature review process for this research revealed a big gap of clearly categorizing bubbles with in a given range of intervals. Despite the presence of ample researches on bubble characterization, an overlap in the researcher's definitions of size ranges was identified. To overcome these ambiguity of categorization, size ranges were proposed for each bubble type based on their common features and according to the properties they share on different researches.

For the generation of fine and ultrafine bubbles, hydrodynamic splitting technique was applied. In this technique the bubble splitter hydrodynamic shear and turbulent forces play an important role for the generation of smaller bubbles from already produced big bubbles in the rotary pump. Even though, the bubble splitter system was used before for another

research, the effect of its design and operating parameters were not exhaustively related to mass transfer parameters. In this study, the effect of design and operating parameters of the splitter on the bubble size reduction trend, that was studied before, was confirmed for the purpose of relating bubble size indirectly with mass transfer through design parameters. Splitter flow path length, flow diameter and gas-liquid recycle flow rate are assumed to be the major parameters affecting bubble size and in turn mass transfer. Keeping other parameters constant, it was confirmed that, an increase in splitter flow path length or decrease in flow path diameter decreases the bubble size to the extent of nano level. Taking the effect of these parameters on bubble size reduction and with a theoretical knowledge of intensifying mass transfer using finer bubbles, the effect of these splitter design and operation parameters on mass transfer was checked. An increase in splitter flow path length, a decrease in flow area diameter and an increase in gas-liquid recycle flow rate improved the mass transfer as expected, because of their effect on bubble size reduction. The reduction of bubbles by the change of design and operating parameters contributes to mass transfer intensification. Based on the experimental results for pure gas liquid mass transfer, a linear regression model relating the volumetric mass transfer coefficient and the three design and operating parameters was developed. From the significance test of the model the three parameters are found to be significant for their effect on the

volumetric mass transfer coefficient. Moreover, the effect of bubble size reduction on non-reactive water systems was examined. The results found proved that ultrafine bubbles provide better rate of mass transfer over their liquid film despite their persistent and stable shells.

In another set of experiment involving O_3 based AOP, influence of bubble size reduction from MB to NB on the process was investigated. A model was developed to estimate the volumetric mass transfer coefficient. The results showed that NB application in O_3 based AOP could revolutionize the inefficiencies of currently existing plants. Experiments depicted that, NBs can suppress the negative influence of pH and operating temperature on AOP. In the experiment it is observed that, better O_3 solubility and rate of mass transfer under the influence of relatively wider range of temperature and pH can be achieved by application of NBs. Moreover, bubble size reduction have encouraged the $^{\cdot}OH$ radical initiation reactions which improve the possibility of O_3 based AOP systems.

Similarly, the effect of NBs on mass transfer in aerobic MBR system were studied and showed good result. In this area NBs increased the oxygen concentration in the bulk liquid and improved rate of mass transfer. The resulting increase in mass transfer rate improved microorganism growth rate, organic matter degradation and reduction in excess sludge production.

6.2. Recommendation

Many researches have been done on bubble field, but the studies in fine an ultrafine bubbles are limited. Most studies in fine and ultrafine bubble areas focus on fundamental properties or characterization of bubbles. As far as the researcher's knowledge is concerned this research might be considered as one of the few studies relating ultrafine bubbles to applications in water and wastewater treatment field. Considering this fact, there are some limitations that could be considered for further studies. The application of the dynamic method in the conventional systems for the determination of volumetric mass transfer coefficient assumes constant surface area to volume ratio "a" from the start of the operation assuming that the distribution of the bubbles in the bubble column reach constant in a very short time. But for the case of nanobubbles this is assumed to take some time therefore more work has to be needed to modify this technique for the application of NB systems. Therefore as a limitation of this study this must be considered in detail for further studies. The regression model developed to relate the design and operating parameters with the volumetric mass transfer coefficient could be improved more by adding the effects of more specific parameters like gas flowrate, flow channel wall friction, flow path shape (straight channel, coiled channel, alternate channel), pressure drop across the channel, contacting scheme (concurrent counter current flows) and water head in the bubble column. According to the

statistical tests done, even though the three variables presented here majorly effect the mass transfer coefficient, applying more variables could improve the model. Moreover, it was very difficult to determine the gas-holdup of nanobubbles for lower flow rate experiments using the given technique in this dissertation. Furthermore, the effect of temperature during nanobubble generation in the splitting system on the mass transfer need to be addressed in detail. Using the hydrodynamic splitting technique applied, there is a possibility of producing smaller bubbles that cannot be detected by the microscopic image analysis. Therefore, applying more advanced instruments could improve the model and it could be possible to directly relate the mass transfer with bubble size, volume and number. Similarly, application of more tests on different surrogate chemicals could show the contribution of NBs for the AOP mechanisms in further studied for specific wastes. Since, all the experiments in this research are semi batch systems, further works on continuous methods are also recommended.

Finally, considering the limited number of prior works on applied researches of NB in water and wastewater treatment, it is very important to work on this direction to address the gap. By the course of this research it was observed that, the application of NBs could be a solution for the challenges in eutrophication, treatment of water contaminants from pharmaceutical and personal care product (PPCPs), specific industry wastes from wineries, leather

and textile industries and so forth. Similarly, the challenges of chemical resistant microorganisms like *cryptosporidium parvum* and the issue of bromine formation while applying higher concentration of O_3 for disinfection could also be solved by applying the property of NBs. Therefore, it is recommended to test NBs for all these application areas. Moreover, from different experiments in this research, the advantages of NBs observed on water and wastewater technologies, depict that researchers can also relate their researches of NB application with plant HRT, reactor size and economic analysis as well.

Appendix

Supporting Document

S1: Supporting document figures

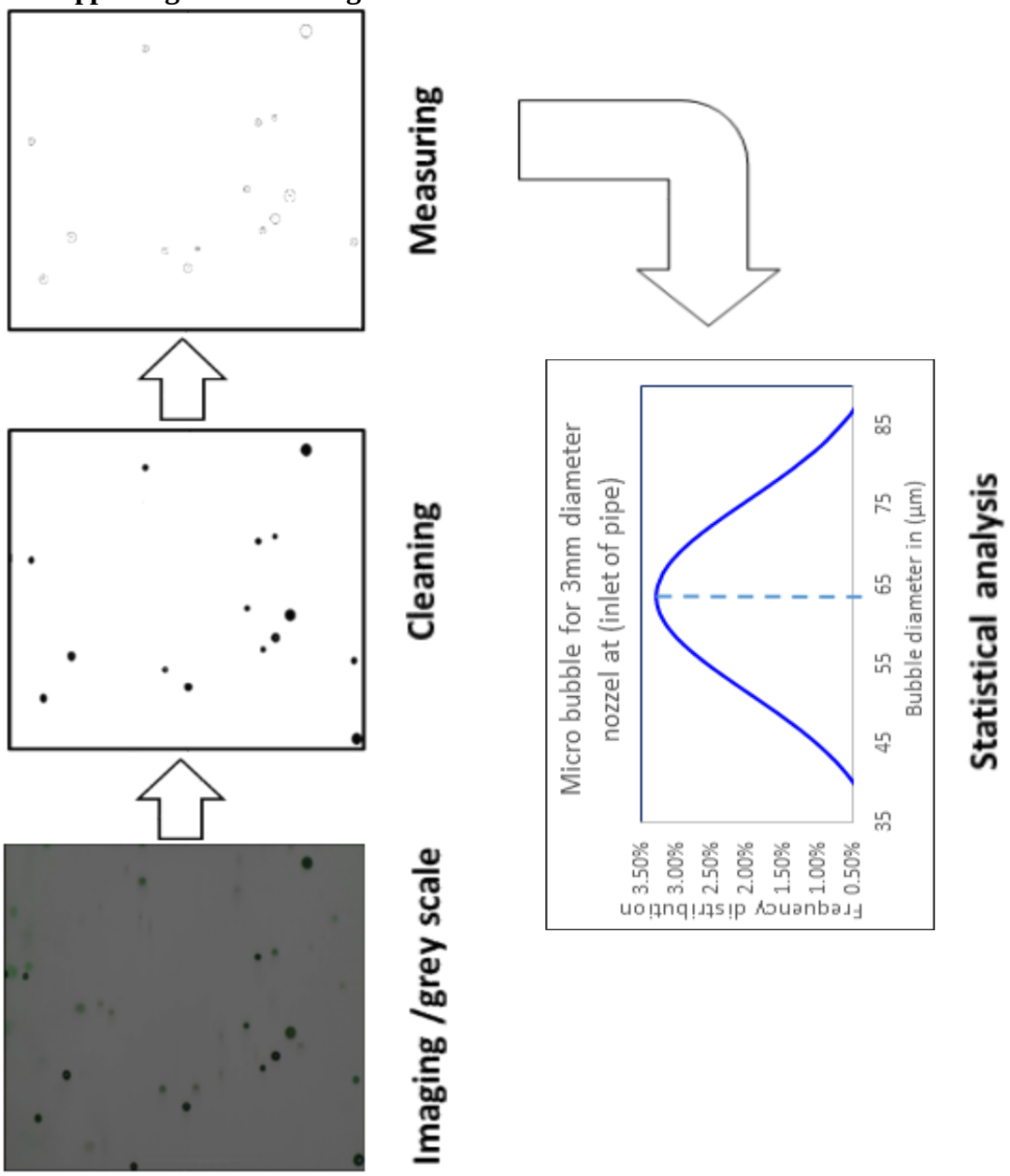

Figure S1 Sample microbubble image and stapes in the three stages of image analysis technique

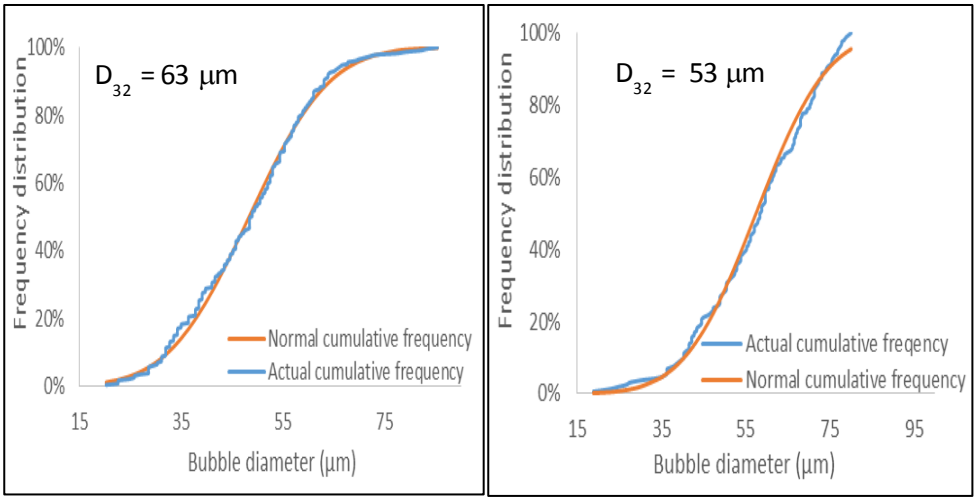

(a) (b)

Figure S2 Bubble size distributions for bubbles generated by (a) microbubble generation system with nozzle diameter d_{n1}, and (b) splitter with flow diameter d_1 in 2 m effective flow length

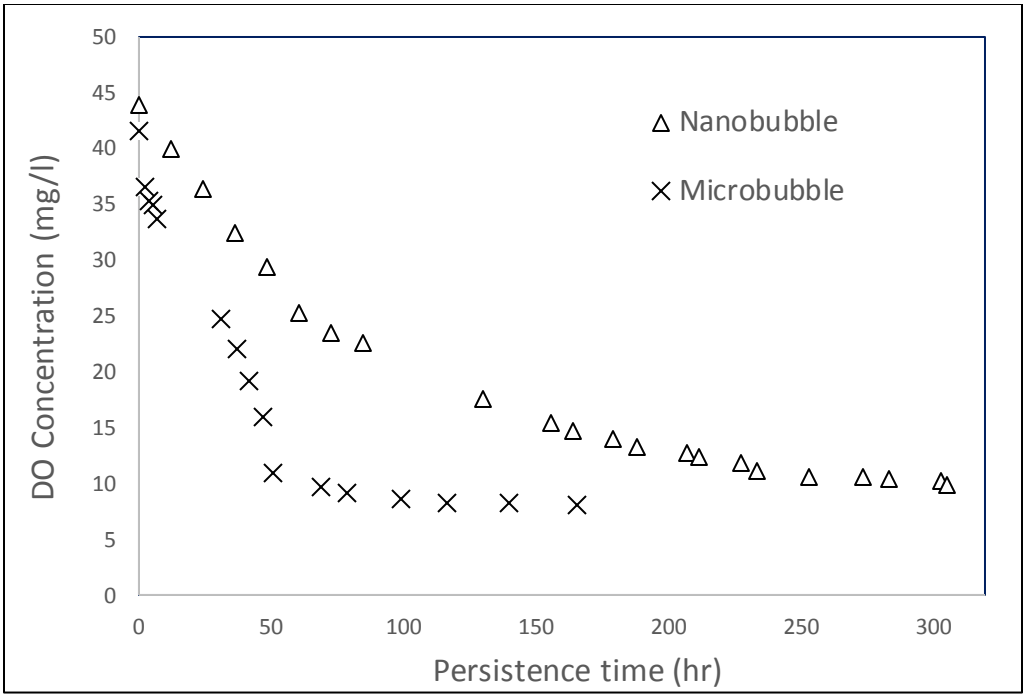

Figure S3 DO concentration reduction/desorption Vs bubble persistence time of micro- and nanobubbles in stagnant bulk liquid

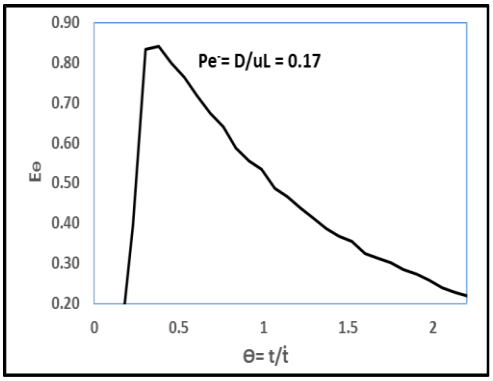

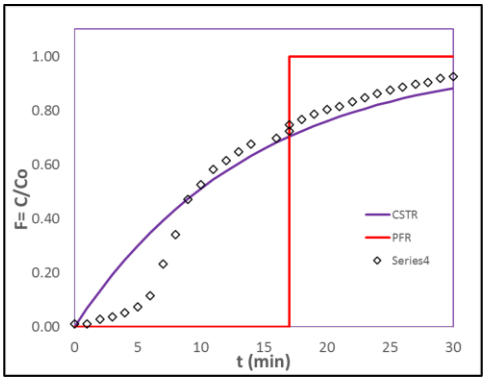

(a) (b)

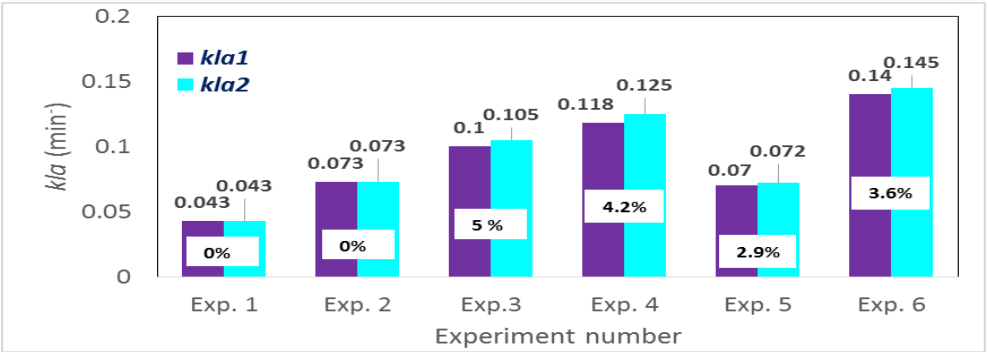

Experimental parameters	Experiment Number	kla1	kla2	Error (%)
Q=0.8 l/min, l=6m, D=6mm	Exp. 1	0.043	0.043	-
Q=0.6 l/min l=15m, D=4mm	Exp. 2	0.073	0.073	-
Q=0.8 l/min, l=15m, D=4mm	Exp.3	0.1	0.105	5
Q=1 l/min, l=2m, D=3mm	Exp. 4	0.118	0.125	4.2
Q=1 l/min, l=6m, D=6mm	Exp. 5	0.07	0.072	2.9
Q=1.2 l/min, l=15m, D=4mm	Exp. 6	0.14	0.145	3.57

** $k_l a1$ is determined by considering all the data and
$k_l a2$ is the value determined from the data after one HRT

(c)

Figure S4 Tracer test response results (a) Normalized concentration pulse input response for 50 ml NaCl solution at Q= 0.6 L/min inlet flow rate at d= 3 mm inlet (b) Comparison of step input response for 2.5 mg/L NaCl solution at Q= 0.6 L/min inlet flow rate at d= 3 mm inlet with ideal reactors at the same inlet conditions (c) comparison of kla values determined from the application of full data and starting after the first HRT data

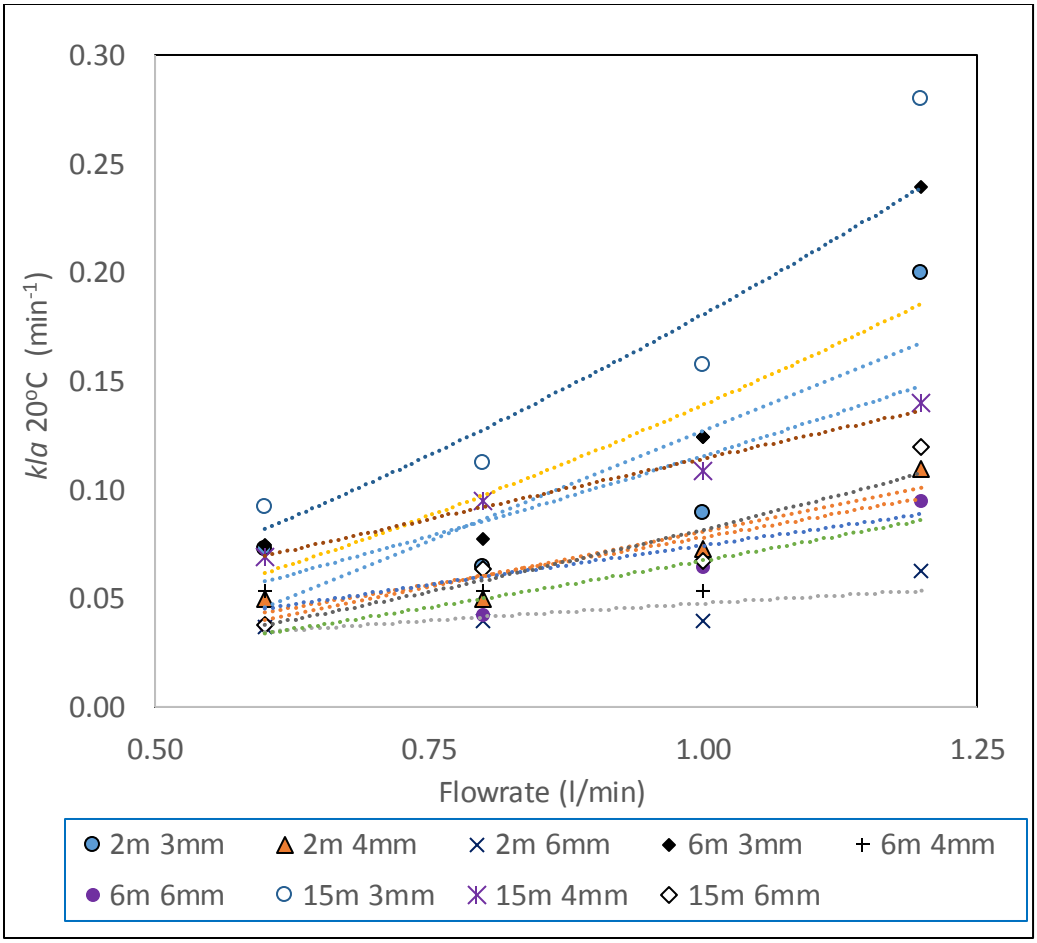

Splitter design parameter combination (l x d)	Trend equation	Regression coefficient (R^2)
2m x 3mm	$kla_{20^oC} = 0.12\ Q^{1.35}$	0.6336
2m x 4mm	$kla_{20^oC} = 0.08\ Q^{1.14}$	0.8163
2m x 6mm	$kla_{20^oC} = 0.05\ Q^{0.63}$	0.6341
6m x 3mm	$kla_{20^oC} = 0.14\ Q^{1.59}$	0.7995
6m x 4mm	$kla_{20^oC} = 0.08\ Q^{0.97}$	0.5045
6m x 6mm	$kla_{20^oC} = 0.07\ Q^{1.34}$	0.9057
15m x 3mm	$kla_{20^oC} = 0.18\ Q^{1.54}$	0.8973
15m x 4mm	$kla_{20^oC} = 0.12\ Q^{0.97}$	0.9847
15m x 6mm	$kla_{20^oC} = 0.08\ Q^{1.51}$	0.9142

Figure S5 Trend of the effect of change in gas-liquid flowrate in the splitter on kla inside the bubble column

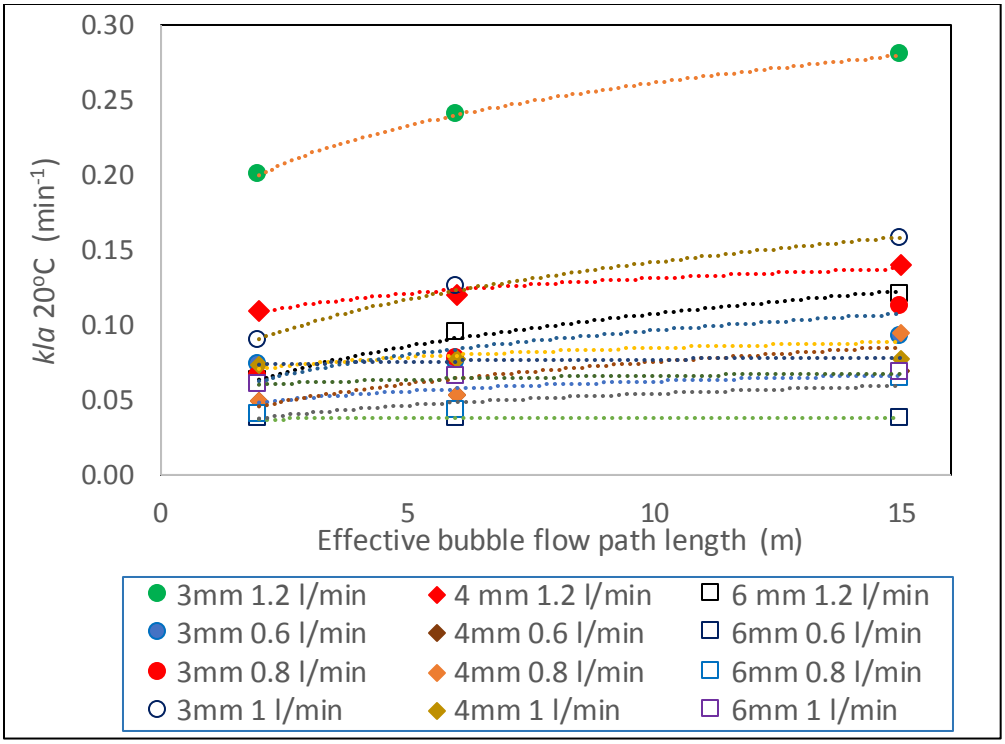

Splitter flow diameter, $d\ (mm)$	Flow rate in the splitter, Q (l/min)	Trend equation	Regression coefficient (R^2)
3mm	1.2	$kla_{20^oC} = 0.18\ l^{0.17}$	1.0000
4mm	1.2	$kla_{20^oC} = 0.10\ l^{0.12}$	0.9559
6mm	1.2	$kla_{20^oC} = 0.05\ l^{0.33}$	0.9879
3mm	1.0	$kla_{20^oC} = 0.08\ l^{0.28}$	0.9977
4mm	1.0	$kla_{20^oC} = 0.07\ l^{0.03}$	0.7938
6mm	1.0	$kla_{20^oC} = 0.06\ l^{0.06}$	0.9770
3mm	0.8	$kla_{20^oC} = 0.05\ l^{0.27}$	0.9357
4mm	0.8	$kla_{20^oC} = 0.04\ l^{0.31}$	0.7801
6mm	0.8	$kla_{20^oC} = 0.03\ l^{0.23}$	0.8053
3mm	0.6	$kla_{20^oC} = 0.07\ l^{0.11}$	0.7959
4mm	0.6	$kla_{20^oC} = 0.04\ l^{0.16}$	0.8624
6mm	0.6	$kla_{20^oC} = 0.04\ l^{0.01}$	0.7938

Figure S6 Trend of change in effective bubble flow path of the splitter on *kla* inside the bubble column

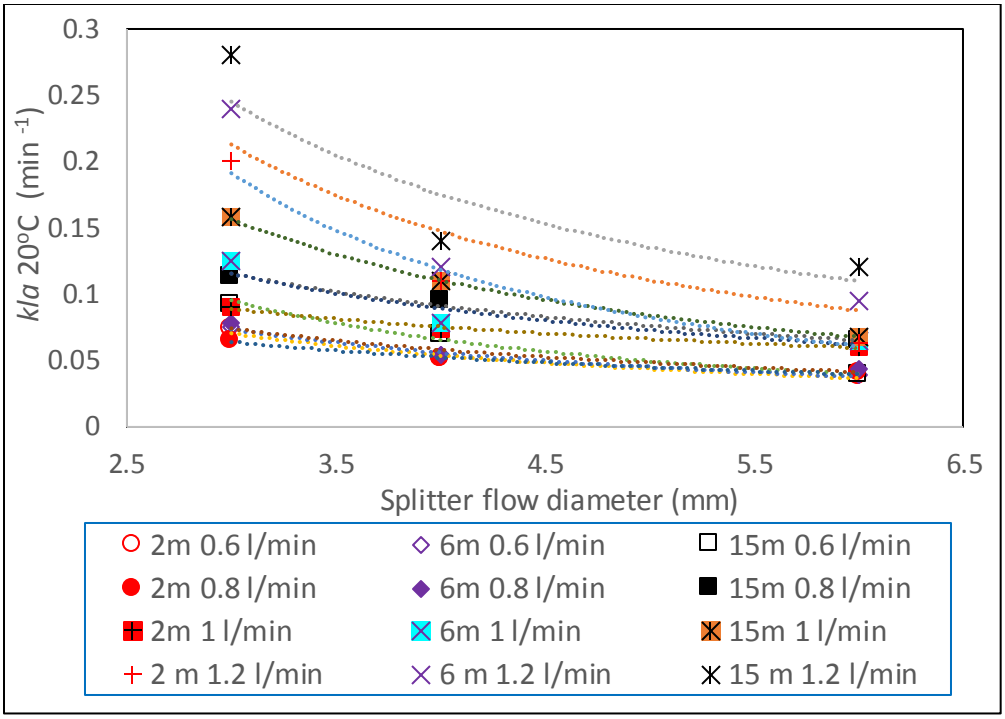

Splitter flow path length, $l\,(m)$	Flow rate in the splitter, Q (l/min)	Trend equation	Regression coefficient (R^2)
2mm	1.2	$kla_{20^oC} = 1.18\,d^{-1.66}$	0.9871
6 mm	1.2	$kla_{20^oC} = 0.88\,d^{-1.29}$	0.8647
15 mm	1.2	$kla_{20^oC} = 0.89\,d^{-1.17}$	0.8110
2mm	1.0	$kla_{20^oC} = 0.17\,d^{-0.58}$	0.9865
6 mm	1.0	$kla_{20^oC} = 0.31\,d^{-0.91}$	0.8769
15 mm	1.0	$kla_{20^oC} = 0.60\,d^{-1.22}$	0.9995
2mm	0.8	$kla_{20^oC} = 0.14\,d^{-0.69}$	0.9793
6 mm	0.8	$kla_{20^oC} = 0.19\,d^{-0.85}$	0.9423
15 mm	0.8	$kla_{20^oC} = 0.29\,d^{-0.82}$	0.9833
2mm	0.6	$kla_{20^oC} = 0.20\,d^{-0.96}$	0.9714
6 mm	0.6	$kla_{20^oC} = 0.21\,d^{-0.97}$	0.9912
15 mm	0.6	$kla_{20^oC} = 0.39\,d^{-1.29}$	0.9879

Figure S7 Trend on effect of splitter flow diameter change on *kla* inside the bubble column

S2: Multilinear Regression Model Procedure

Variables assumed to affect kla inside the bubble splitter:

- Flow path length (l)
- Flow area diameter (d)
- Flowrate (Q)
- Flow channel wall friction (f)
- Flow path shape (straight channel, coiled channel, alternate channel)
- Pressure drop across the channel (P)
- Water head in the bubble column (h)
- Temperature (T)

Assumption

- The flow in the splitter follows a Plug flow scheme with a flow area diameter of d.
- The dominant factors assumed to affect kla are taken to be
    - Flow path length (l in m)
    - Flow area diameter (d in m)
    - Flowrate (Q in m^2/min)
    - Temperature (T) : For this all the experimentally determined values of kla are corrected to a standard temperature by the following equation:

      $kla_{20} = \frac{kla_{(T)}}{1.024^{(T-20)}}$, in ($min^{-1}$)

      Where: 'kla_{20}' is the value of 'kla' at 20°C, '$kla_{(T)}$' is 'kla' value at test water temperature and 'T' is the test water temperature in °C.

- In comparison to the four parameters stated above other parameters are assumed to have minimal effect on bubble size reduction to influence the kla in the bubble column.
- Considering the experimental result trend of kla with each assumed dominant variable, a nonlinear function of power law is assumed to represent the model.

Multi-linear regression steps

Step 1: Representing the temperature corrected kla as a function form

$$kla_{20^0C} = f\ (\ l, d, Q) \qquad 3.6$$

Step 2: Expressing the model in power form and introducing proportionality constant (p) and power constants of each independent variable a, b and c.

$$kla_{20^0C} = p\ \ l^a\ d^b\ Q^c \qquad 3.7$$

Step 3: Taking the log of both sides equation 3.7 is reduced to a linear form (Linearization),

$$kla_{20^0C} = \log p + a \log l + b \log d + c \log Q$$

Let $y = \log\ (kla_{20^0C}), P = \log p, x_1 = \log l, x_2 = \log d$ and $x_3 = \log Q$

$$kla_{20^0C} = P + a \log l + b \log d + c \log Q \qquad 3.7.1$$

$$y = P + a\ x_1 + b\ x_2 + c\ x_3 \qquad 3.7.2$$

Step 5: Matrix of observations (Expressing experimental data results in matrix form)

But the 36 sets of observations can be represented collectively by matrix similar to the form in equation 3.7.3;

$$y = \beta x \qquad 3.7.3$$

Where: y is matrix of kla experimental results, β is matrix of coefficients and x is matrix of logarithmic value of independent variables l, d and Q. It is given by matrices in S3.

Step 4: Using least square method the parameters (P, a, b and c) are estimated by solving:

$$\beta = (x'x)'x'y \qquad 3.7.4$$

Using MATLAB the result of β is given to be

$$\beta = \begin{bmatrix} 0.3085 \\ 0.1374 \\ -0.8992 \\ 1.1929 \end{bmatrix} \qquad 3.7.5$$

From this P= 0.3085, a = 0.1374, b = -0.8992, c = 1.1929.

By substituting these values in equation 3

$$kla_{20^oC} = 0.3085 + 0.1374 \log l - 0.8992 \log d + 1.1929 \log Q \qquad 3.7.6$$

Step 5: Checking the statistical significance of the fitted curve by ANOVA technique

Summary of ANOVA

	df	*SS*	*MS*	*F*
Regression	3	1.408	0.4693	64.8
Residual	33	0.239	0.00724	
Total	34	1.638		

Step 6: Using the global test (F- statistics), for α = 0.05, observed "F" value is much higher than the tabulated value confirming that all the β values are not equal to zero.

Observed value = 64.8 >> Tabulated value $F_{0.025,3,33} = 2.9$

Step 7: The t- test is used to check the contribution of each variable given the presence of the rest of the variables.

1- Significance of x_1 contribution given that x_2 and x_3 are already in the regression model

2- Significance of x_2 contribution given that x_1 and x_3 are already in the regression model

3- Significance of x_3 contribution given that x_1 and x_2 are already in the regression model

The t- statistics

Tested variable in the presence of the rest of the variables	Calculated/ Observed /t/ value	Tabulated 't' value at α = 0.05 $t_{0.025,\ 33}$
x_1	3.486	≈2.042
x_2	7.812	≈2.042
x_3	9.44	≈2.042

In all the cases the calculated value is higher than the tabulated value confirming the significant contribution of all the three variables.

Therefore, equation 8 can be utilized as a representative multilinear regression model.

Finally, simplifying and writing equation 8 in power form

$$kla_{20^oC} = 2.04\ l^{0.14}\ d^{-0.9}\ Q^{1.2},\ R^2 = 0.8566 \qquad 3.8$$

Error percent

$$e(\%) = \left(\sum \frac{(kla_{20^oC})_E - (kla_{20^oC})_m}{(kla_{20^oC})_E}\right) * 100 = 15\ \%$$

S3: Matrix of experiment sets

$$y = \begin{bmatrix} -1.1400 \\ -1.3160 \\ -1.1435 \\ -1.1900 \\ -1.3140 \\ -1.4090 \\ -1.0560 \\ -1.1450 \\ -1.2330 \\ -0.6960 \\ -0.9430 \\ -1.2050 \\ -1.1450 \\ -1.2740 \\ -1.4320 \\ -1.1290 \\ -1.2820 \\ -1.3770 \\ -0.9290 \\ -1.1210 \\ -1.1930 \\ -0.6180 \\ -0.9140 \\ -1.0210 \\ -1.0560 \\ -1.1670 \\ -1.4360 \\ -0.9960 \\ -1.0350 \\ -1.1990 \\ -0.8650 \\ -0.9760 \\ -1.1810 \\ -0.6160 \\ -0.8640 \\ -0.9210 \end{bmatrix}_{36x1} \quad x = \begin{bmatrix} 1.00 & 0.30 & -2.52 & -3.20 \\ 1.00 & 0.30 & -2.40 & -3.20 \\ 1.00 & 0.30 & -2.22 & -3.20 \\ 1.00 & 0.30 & -2.52 & -3.10 \\ 1.00 & 0.30 & -2.40 & -3.10 \\ 1.00 & 0.30 & -2.22 & -3.10 \\ 1.00 & 0.30 & -2.52 & -3.00 \\ 1.00 & 0.30 & -2.40 & -3.00 \\ 1.00 & 0.30 & -2.22 & -3.00 \\ 1.00 & 0.30 & -2.52 & -2.92 \\ 1.00 & 0.30 & -2.40 & -2.92 \\ 1.00 & 0.30 & -2.22 & -2.92 \\ 1.00 & 0.78 & -2.52 & -3.20 \\ 1.00 & 0.78 & -2.40 & -3.20 \\ 1.00 & 0.78 & -2.22 & -3.20 \\ 1.00 & 0.78 & -2.52 & -3.10 \\ 1.00 & 0.78 & -2.40 & -3.10 \\ 1.00 & 0.78 & -2.22 & -3.10 \\ 1.00 & 0.78 & -2.52 & -3.00 \\ 1.00 & 0.78 & -2.40 & -3.00 \\ 1.00 & 0.78 & -2.22 & -3.00 \\ 1.00 & 0.78 & -2.52 & -2.92 \\ 1.00 & 0.78 & -2.40 & -2.92 \\ 1.00 & 0.78 & -2.22 & -2.92 \\ 1.00 & 1.18 & -2.52 & -3.20 \\ 1.00 & 1.18 & -2.40 & -3.20 \\ 1.00 & 1.18 & -2.22 & -3.20 \\ 1.00 & 1.18 & -2.52 & -3.10 \\ 1.00 & 1.18 & -2.40 & -3.10 \\ 1.00 & 1.18 & -2.22 & -3.10 \\ 1.00 & 1.18 & -2.52 & -3.00 \\ 1.00 & 1.18 & -2.40 & -3.00 \\ 1.00 & 1.18 & -2.22 & -3.00 \\ 1.00 & 1.18 & -2.52 & -2.92 \\ 1.00 & 1.18 & -2.40 & -2.92 \\ 1.00 & 1.18 & -2.22 & -2.92 \end{bmatrix}_{36x4} \quad \beta = \begin{bmatrix} \mathrm{P} \\ a \\ b \\ c \end{bmatrix}_{4x1}$$

S3: Model development for O_3 volumetric mass transfer coefficient determination

The model for volumetric mass transfer of the O_3 gas in the bulk liquid is derived from the mass balance equation in the bulk liquid given by equation 2.5.

$$\frac{dC}{dt} = GTR - GCR \qquad 2.5$$

Where, GTR is the gas transfer rate given by equation 2.4 and GCR is the gas consumption rate in the bulk liquid by any reaction type.

$$GTR = \frac{dC}{dt} = J * a = k_L a * (C^* - C_L) \qquad 2.4$$

Assuming that the O_3 concentration is much higher than the radicals (mainly $^{\bullet}OH$) reacting with it in the bulk DI water of the bubble column, the O_3 gas consumption rate (GCR) by the reaction is approximated to follow pseudo first order as:

$$GCR = \frac{dC_{O_3}}{dt} = k_d * C_L \qquad 4.1$$

Where k_d is pseudo first order reaction constant or the O_3 consumption rate constant and C is the concentration of O_3 in the bulk liquid

Then the net rate of mass transfer is given by

$$\frac{dC}{dt} = k_L a * (C^* - C_L) - k_d * C_L \qquad 4.2$$

$\frac{dC}{dt} = k_L aC^* - (k_L a + k_d) * C_L$ multiply both sides by $(\frac{1}{k_l a + k_d})$

$(\frac{1}{k_l a + k_d}) * \frac{dC}{dt} = (\frac{k_L aC^*}{k_l a + k_d}) - C_L$ then re-arranging variables together

$\frac{dC}{(\frac{k_L aC^*}{k_l a + k_d} - C_L)} = (k_l a + k_d)dt$ let $= \frac{k_L aC^*}{k_l a + k_d}$, then substituting this in the equation

$\int_0^{C_L} \frac{dC}{u - C} = \int_0^t (k_l a + k_d)dt$ Integrate both sides within the boundaries given

$-\ln(\frac{u - C_L}{u}) = (k_l a + k_d)t$ since all the components of *u* are constants

$e^{-(k_l a + k_d)t} = \frac{u - c_L}{u} = \frac{\left(\frac{k_L aC^*}{k_l a + k_d} - C_L\right) - C_L}{(\frac{k_L aC^*}{k_l a + k_d} - C_L)}$, re-arranging this equation

$\frac{C_L}{C^*} = \frac{k_L a}{k_l a + k_d}\left(1 - e^{-(k_l a + k_d)t}\right)$ is the final model equation for curve fitting with the data

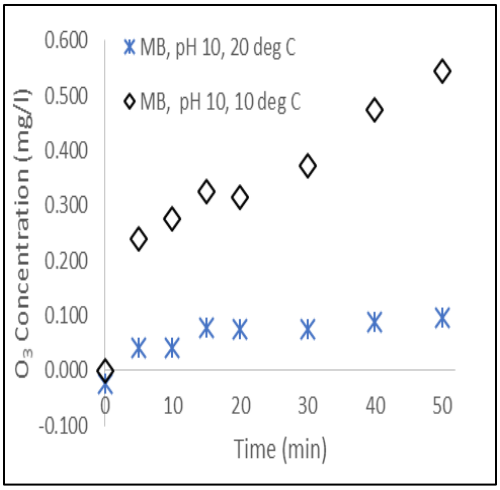

(a)

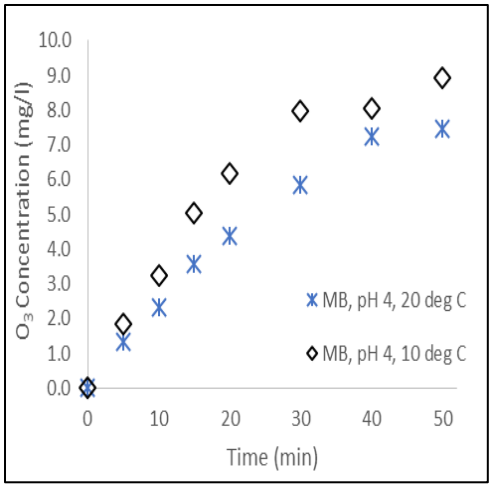

(b)

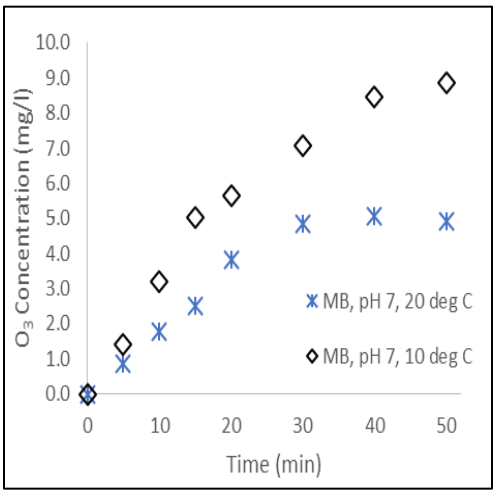

(c)

Figure S7 Effect of process initial temperature on O_3 residual concentration for NB under different pH (a) at pH=4, (b) at pH=7 and (c) at pH=10

S4: Modified synthetic sewage recipe from the Organization for Economic Cooperation and development (OECD)

Chemical component	Concentration (in mg/l)
Peptone	280
Meat extract	770
Potassium phosphate monobasic (KH_2PO_4)	196
Sodium chloride (NaCl)	49
Calcium chloride dihydrate ($CaCl_2.2H_2O$)	28
Magnesium sulfate heptahydrate ($MgSO_4.7H_2O$)	14
Urea	210
Bio-seed	10 (ml/l)

**The COD of this solution is measured and it is found to be 1036 mg/L

초록

초미세/나노버블을이용한물및상수및폐수처리에서의 기체액체 물질 전달 및 (생)화학적 반응 강화

타텍 테메스겐 테르파사
건설환경공학부
서울대학교

일정 조건 하에서 네 가지 주요 물질의 상태 간 물질 전달 효율은 공정에 가장 큰 영향을 미친다. 서로 다른 상 간의 상호 작용은 자연적 또는 인공적인 공정에서 대부분 관찰된다. 상과 관련된 공정들 중에 기체-액체간의 상호 작용은 환경 산업, 상수 및 하수 처리장, 기체 흡착 공정, 수생 시스템 복원 기술, 수경 재배, 표면 세척, 기타 화학 및 석유 산업 등에서 볼 수 있다. 대부분의 공정에서 기체-액체간 물질 전달 효율은 주요한 처리 제한 인자가 된다.

본 연구에서는 초미세/나노 기포를 이용하여 물질 전달 효율을 향상시킬 수 있는 가능성을 조사하였으며, 이를 ·상 하수 처리 기술에 적용하는데 중점을 두었다. 이를 위하여 폭기, 오존 고도산화, 호기성 MBR 수처리 공정 등에서 이용 가능한 기체-액체간 물질 전달 방법을 연구하였다. 아래의 세 가지 공정에서 초미세/나노 기포의 영향을 연구하였다.

1- 순수한 기체-액체의 물질 전달 시스템
2- 액체 막에서의 빠른 반응을 가진 시스템
3- 고형물질이 많이 포함된 액체에서의 느린 반응을 가진 시스템.

각 시스템의 효율 향상에 나노 기포가 미치는 영향을 규명하기 위해 최종 결과물을 비교 검토 하였다.

논문의 첫 번째 장에서는 물질 전달에 중점을 두고 나노기포를 적용하는 수처리 기술 분야의 일반론을 정리하였다. 기포를 적용한 수처리 기술과 관련된 성과들을 간략하게 요약하여 제시하였다. 각 기술들의 명확한 목표와 구체적인 대상을 상세히 기술하였다.

논문의 두 번째 장에서는 기포 기술과 물질 전달에 관한 이론들을 요약하였다. 본 장에서는 기포의 측정법들을 바탕으로 기포 크기 범위에 대한 명확한 정의를 제안하였다. 아직까지 기포 크기에 대한 명칭이 정의되지 않아 기포의 크기에 대해 다양한 표현을 사용하고 있기 때문에 다른 기포 크기에 대한 용어 정리가 필요하다고 판단하였다. 이를 위해 기포 크기에 대해 연구한 문헌을 정리하여 공통적인 사항을 정리하였다. 본 장에서 제시된 기포 크기에 대한 정의를 모든 연구자들이 사용하지 않더라도 최소한 본 연구에서 기포의 크기를 이해하는데 도움이 될 것이다. 또한 물질 전달과 관련된 기포의 특성들과 본 논문의 각각의 장들에서 언급될 특성들에 대해 간단히 논의하였다. 본 연구에서 사용되는 이중경막이론을 위한 기초적인 물질 전달 이론과 가정들 또한 정의되었다.

논문의 세번째 장에서는 순수한 기체-액체의 물질 전달에서 나노기포의 효과에 대해 다루었다. 나노기포는 큰 기포를 유체역학적으로 쪼개어 작은 기포를 생성하는 방식으로 발생시켰다. 기포 발생 장치의 설계 및 운전 인자가 기포 크기의 감소에 미치는 영향을 연구하였다. 물질 전달 지표에 대한 설계 및 운전 인자의 영향을 규명함으로써, 물질 전달에 대한 기포 크기 효과를 간접적으로 다루었다. 또한, 주요 설계 및 운전 인자의 영향을 보다 정밀하게 표현하기 위해 기포발생장치의 설계 매개 변수를 용적 물질 전달 계수와 연결시키기 위한 회귀 모델을 개발하였다. 회귀 모델을 통해 기포발생장치의 유로 길이, 유로 면적, 순환 속도가 기포를 쪼개는 주요한 인자로

판단되었으며, 유로의 길이가 길고, 면적이 작으며 기체와 액체의 혼합 속도가 빠를수록 기포의 크기는 작아져 나노 크기까지 도달하였다. 이를 통해 나노 기포 시스템은 용적 물질 전달 계수를 기존 기포 시스템에 비해 최대 600 %까지 향상시켰고, 미세기포 시스템에 비해 100-200%까지 향상시켰다.

네 번째 장에서는 물질전달 효율 향상을 통한 오존고도산화공정의 공정 효율 개선에 대해 다루었다. 세미 배치 테스트에서 나노 기포는 온도와 pH 가 공정에 미치는 부정적인 영향을 억제하는 경향을 보였다. 나노 기포를 사용 할 경우 공정의 온도가 상승하여 오존의 용해도가 감소하면서 발생하는 부정적인 영향을 감소시켰다. 이와 유사하게 오존 나노 기포는 일반적인 미세 기포보다 산성일 때 높은 농도의 하이드록실 라디칼을 발생시키는 경향을 보였다. 이것은 다른 하이드록실 라디칼 개시제를 첨가하지 않는 이상 큰 기포를 이용한 연구에서는 불가능했다. 이 결과는 나노기포를 통하여 낮은 pH 조건에서의 고급 산화 공정 효율을 개선할 수 있음을 알려준다. 또한, 체적 물질 전달 계수를 예측하기 위해 이중 경막설 이론에 기초하여 수학적 모델을 개발하였다. 물질 전달 계수는 미세 기포에 비해 나노 기포가 상대적으로 더 높은 값을 보였다. 오존 소비 속도도 나노 기포를 적용했을 때 더 높았으며, 낮은 pH 조건에서도 마찬가지였다. 하이드록실 라디칼의 농도를 확인한 결과 나노 기포를 적용했을 때 모든 pH 범위에서 더 높은 하이드록실 라디칼 농도를 나타내었다. 이 실험들은 나노 기포가 고도산화처리 공정의 효율을 향상시킬 수 있다는 것을 보여준다.

마지막으로 생물학적 반응 과정이 포함된 호기성 폐수 처리 공정에서 나노 기포의 효용성을 실험하였다. 이론적인 플록 모델을 기체-액체-고체 간의 물질 전달에 적용하고 모델을 개선하였다. 물질

전달율, 생물학적 폐기물 분해 속도, 바이오매스 생성 속도, 맴브레인 여과 공정 실험을 통하여 모델을 검증하였다. 나노 기포를 사용한 호기성 소화조에서 용적 물질 전달 계수는 0.13 으로 계산되었는데, 일반적인 기포에서 0.07 임을 고려할 때 이는 약 2 배에 달하는 수치이다. 산소 섭취 속도 역시 기존 기포 시스템의 2 배에 달했다. 이러한 물질 전달 효율의 향상은 생물학적 반응에 산소 공급을 증가시켜 기존의 호기성 소화조에서의 산소 부족 현상을 감소시켰다. 나노기포를 적용하여 바이오 매스 생장 속도 증가, 생물학적 폐기물 분해 속도 증가를 확인하였고, 잉여 슬러지 생산량과 막 오염도를 감소시킬 수 있었다.

키워드: 나노 기포, 초미세 기포, 물질전달, 상수처리, 하수처리, 모델링

학번: 2014-30862